UNIVERSIDAD AUTÓNOMA DE MADRID

DEPARTAMENTO DE BIOLOGÍA MOLECULAR

Auto-fluorescent intracellular sink – A novel inherent biomarker for drug discovery in pancreatic cancer stem cells

Irene Miranda Lorenzo

Madrid, 2013

DEPARTAMENTO DE BIOLOGÍA MOLECULAR

FACULTAD DE CIENCIAS

UNIVERSIDAD AUTÓNOMA DE MADRID

Auto-fluorescent intracellular sink – A novel inherent biomarker for drug discovery in pancreatic cancer stem cells

Irene Miranda Lorenzo

Licenciatura Ciencias Biológicas

Director de Tesis:

Prof. Christopher Heeschen, M.D. PhD

Centro Nacional de Investigaciones Oncológicas

Grupo de Células Troncales y Cáncer

Programa de Patología Molecular

Centro Nacional de Investigaciones Oncológicas (CNIO)

ACKNOWLEDGMENTS

Muchisíma gente es a la que me gustaría agradecer todo el ánimo y apoyo que me han brindado durante este tiempo.

Empezando por mi director de Tesis, Christopher Heeschen, gracias por darme la oportunidad de investigar este maravilloso proyecto.

Por otro lado, un especial agradecimiento a mis compis del labo por vuestra ayuda incondicional.

A todos,

Gracias!

SUMMARY

Pancreatic adenocarcinoma (PDAC), the fourth leading cause of cancer-related death world-wide, is a malignant neoplasm of the exocrine pancreas. It has been hypothesized that a subset of tumor cells with stem-like properties, termed cancer stem cells (CSCs), drives pancreatic tumor growth, metastasis, and chemoresistance. While multiple surface markers such as CD133 and CD44 have been successfully used to isolate and characterize CSCs, their expression are not exclusively linked to a CSC functional phenotype. Therefore, since isolating and characterizing CSCs is of paramount importance for understanding pancreatic cancer, we sought to identify new and novel markers that functionally enrich for CSCs using primary human pancreatic cancer cells. While our classic approaches, such as cell surface expression of known CSC markers or side population were either prone to alterations by the tissue culture environment or did not enrich for CSCs, we inadvertently identified a distinct population of cells characterized by a subcellular compartment exhibiting strong autofluorescence, which did exhibit defined CSC characteristics. Specifically, these autofluorescent cells were markedly enriched both in sphere culture and during chemotherapy, strongly expressed pluripotency-associated genes, and were highly invasive both *in vitro* and *in vivo*. Most importantly, they were exclusively tumorigenic *in vivo* at the single cell level and were capable of recapitulating the heterogeneity of the parental tumor. Autofluorescence was determined to be due to an accumulation of riboflavin in membrane-restricted cytoplasmic structures by means of the ATP-dependent ABCG2 transporter, which did not overlap with cells defined as the side population, but could be selectively eliminated with the ABCG2 inhibitor Fumitremorgin C. In addition, we show that autofluorescence is not restricted to PDAC, as other solid tumors similarly contain autofluorescent cells. Thus, to take advantage of this broad phenotype, we developed a low throughput screening platform, and show that autofluorescent cells are highly amendable to anti-cancer compound screening. Thus, unbiased and label-free tracking of autofluorescent cells in cancers such as PDAC represents a promising new technological advancement, which can be used not only for isolating and studying CSC, but can be additionally exploited for low throughput screening of compounds with anti-cancer activity in a clinical setting.

RESUMEN

El adenocarcinoma pancreático es una neoplasia maligna del páncreas exocrino, siendo la cuarta causa principal de muerte relacionada con cáncer en todo el mundo. Se ha planteado la hipótesis de que un subconjunto de células tumorales con propiedades troncales, denominadas células madre de cáncer, impulsan el crecimiento del tumor de páncreas, metástasis, y la quimiorresistencia. Mientras que varios marcadores de superficie tales como CD133 y CD44 se han utilizado con éxito para aislar y caracterizar este tipo de células, su expresión no está vinculada exclusivamente a un fenotipo funcional de células madre de cáncer. Por tanto, ya que el aislamiento y caracterización de este tipo de células es de vital importancia, hemos tratado de identificar marcadores novedosos que de manera funcional, enriquezan en este tipo celular utilizando células primarias de cáncer de páncreas de humanos. Los resultados premilinares de la búsqueda de un buen marcador de células madre de cáncer, tales como la expresión de marcadores de superficie o las células Side-Population (SP), observamos que podían estar sujetos a alteraciones por el cultivo de tejidos o que no enriquencían de manera especifíca en células madre. Esto nos forzó a la búsqueda de otro marcador que no fuse sensible a este tipo de alteraciones en su expresión, siendo éste nuestro principial objetivo de este trabajo. Partiendo de cultivos primarios de xenoinjertos humanos, identificamos una población de células que se caracteriza por un compartimento subcelular exhibiendo una fuerte autofluorescencia. Específicamente, estas células autofluorescentes fueron enriquecidas tanto en cultivo de esferas como durante la quimioterapia, sobre-expresan los genes de pluripotencia-asociados y mostraron ser altamente invasivas, tanto *in vitro* como *in vivo*. Además, estas celulas son exclusivamente tumorigénicas *in vivo*, siendo capaces de formar un tumor desde tan sólo una célula. Se determinó que la autofluorescencia era una acumulación de riboflavina en la estructura autofluorescente y estaba mediado por el transportador ABCG2. Debido a que se expresan en una gran parte de tumores primarios de páncreas y su expresión se mantiene constante bajo diferentes condiciones, desarrollamos una plataforma de screening donde podemos investigar el efecto de distintos compuestos anticancerígenos, así como obtener un diagnóstico clinico para medicina personalizada.

TABLE OF CONTENTS

TABLE OF CONTENTS

SUMMARY **5**
RESUMEN **7**
ABBREVIATIONS **13**
INTRODUCTION **17**
1. PANCREATIC DUCTAL ADENOCARCINOMA 18
Table I1 20
1.1 The Cancer Stem Cell Model 21
Figure I1 21
Figure I2 22
1.2 Markers for prospectively identify cancer stem cells 23
Table I2 24
1.3 Migrating Cancer Stem cells 25
Figure I3 25
1.4 Cancer Stem Cell-target Therapy 26
Figure I4 30
OBJECTIVES 31
OBJETIVOS 33
MATERIALS AND METHODS 35
1. MICE 36
1.1 Study approval 36
1.2 Xenograft 36
Figure M&M1 ..... *36*
1.3 Mice treatments 37
1.4 In vivo tumorigenicity 37
2. CELL CULTURE 37
2.1 Primary human pancreatic cancer cells 37
2.2 Sphere formation assay 38
2.3 PkH26 assay 38
2.4 Cell viability assay 38
2.5 Invasion and migration assay 39
2.6 Intracellular ATP content 39
2.7 Cell treatments 39
Table M&M1 40
3. FLOW CYTOMETRY 40
3.1 Flow cytometry analysis 40

3.2 FACS sorting.....41
3.3 Side Population.....41
3.4 Cell cycle: G0.....41
4. PROTEIN ANALYSIS.....41
4.1 Protein extraction and quantification.....41
4.2 Western Blot.....42
5. RNA ANALYSIS.....42
5.1 RNA extraction from tissue or cells.....42
5.2 RT-qPCR.....42
Table M&M2.....43
6. IMMUNOSTAINING ANALYSIS.....44
6.1 Immunofluorescence.....44
6.2 Indirect immunofluorescence analsysis.....44
7. MICROCHIOP-BASED SINGLE CELL ANALYSIS.....44
Figure M&M2.....45
8. LOW THROUGHPUT SCREENING ASSAY.....45
Table M&M3.....46
RESULTS.....47
1. ANALYSIS OF TRADITIONAL PANCREATIC CANCER STEM CELL MARKERS.....48
Figure 1.....48
Figure 2.....49
Figure 3.....50
Figure 4.....51
Figure 5.....52
Figure 6.....54
2. IDENTIFICATION OF NEW FUNCTIONAL MARKERS FOR PANCREATIC CANCER STEM CELLS.....55
Figure 7.....55
Figure 8.....56
Figure 9.....57
Figure 10.....,,,58
Figure 11.....59
3. AUTOFLUORESCENT CELLS DISPLAY FUNCTIONAL FEATURES OF CANCER STEM CELLS.....60
Figure 12.....60
Figure 13.....61
3.1 Cancer stem cell related genes.....62
Figure 14.....62
3.2 Cell divison.....63
Figure 15.....63
3.3 Tumorigenicity.....64
Figure 16.....64
Figure 17.....68

Figure 18.....69
3.4 Autofluorescent cells in other cancer types: HCC AND CRC.....70
Figure 19.....70-71
4. AUTOFLUORESCENT CELLS ARE HIGHLY INVASIVE.....72
Figure 20.....72
Figure 21.....73
Figure 22.....74
Figure 23.....75
5. AUTOFLUORESCENT PANCREATIC CANCER CELLS ARE HIGLY RESISTANT TO STANDARD THERAPY.....76
Figure 24.....76
Figure 25.....77
Figure 26.....78
Figure 27.....79
Figure 28.....80
Figure 29.....81
6. MECHANISM AND SOURCE OF THE AUTOFLUORESCENCE.....82
6.1 Mechanism.....82
Figure 30.....83
Figure 31.....84
Figure 32.....85
Figure 33.....86
Figure 34.....88
6.2 Source.....89
Figure 35.....89
Figure 36.....90
Figure 37.....91
Figure 38.....92
Figure 39.....94
7. THERAPEUTIC AND CLINICAL APPLICATION OF THE AUTOFLUORESCENT CELLS.....95
Figure 40.....96
Figure 41.....97
DISCUSSION.....**98**
Figure 42.....100
CONCLUSIONS.....**106**
CONCLUSIONES.....**108**
BIBLIOGRAFY.....**110**
APPENDIX.....**119**

ABBREVIATIONS

ABCG2	ATP-binding cassette sub-family G member 2
ABX	Abraxane
ALDH-1	Aldehyde dehydrogenases family 1
ALK-4	Activin Receptor-Like Kinase 4
ATG	Autophagy-related gene
ATP	Adenosine Tri-Phosphate
BSA	Bovine Serum Albumine
bFGF	Basic fibroblast growth factor
CK19	Cytokeratin 19
hCNT	(human) Concentrative nucleoside transporter
CRC	Colorectal Cancer
CSC	Cancer Stem Cell
CSCs	Cancer Stem Cells
CXCR4	Chemokine receptor type 4
DAPI	4',6-diamidino-2-phenylindole
DMEM/F12	Dulbecco's Modified Eagle Medium: Nutrient Mixture F-12
DNA	Deoxyribonucleic acid
DNP	2,4-Dinitrophenol
DsRED	
EDTA	Ethylenediaminetetraacetic acid
ELDA	Extreme limiting dilution analysis
hENT	(human) Equilibrative nucleoside transpoter
EpCAM	Epithelial cell adhesion molecule
5-FU	5-Fluoracil
FACS	Fluorescent-activated cell sorting
FAD	flavin adenine dinucleotide
FBS	Fetal bovine serum
FFPE	Formalin-Fixed, Paraffin-Embedded
Fluo+	Autofluorescent positive
Fluo-	Autofluorescent negative
FMN	Flavin mononucleotide

FSC	Forward Scatter
FTC	Fumitremorgin C
GAPDH	Glyceraldehyde 3-phosphate dehydrogenase
GEM	Gemcitabine
H2B	Histone 2B
HCC	Hepatocellular carcinoma
HCS-OPERA	High content screening OPERA
HPF	High power fields
HRP	Horseradish peroxidase
LC3	Microtubule-associated protein light chain 3
LTS	Low-troughput screening
mRNA	messenger ribonucleic acid
MTX	Mitoxantrone
NAD	Nicotinamide adenine dinucleotide
NADPH	Nicotinamide adenine dinucleotide phosphate
HNU mice	Athymic Nude-Foxn1nu
NSG mice	NOD scid gamma mice
PDAC	Pancreatic ductal adenocarcinoma
PaCSCs	Pancretic cancer stem cells
PBS	Phosphate buffered saline
PEN	Penicillin
PVDF	Polyvinylidene difluoride
RT-qPCR	quantitive real time polymerase chain reaction
RBF	Riboflavin
RIPA	Radioimmunoprecipitation assay
RNA	Ribonucleic acid
RPMI	Roswell Park Memorial Institute medium
SSEA-1	Stage-specific embryonic antigen-1
STREP	Streptomycin
SP	Side population
SDS-PAGE	Sodium dodecyl sulfate polyacrylamide gel electrophoresis

SDF-1	Stromal cell-derived factor 1
SHH	Sonic Hedgehog
TBS	Tris-buffered saline
TGF-ß1	Transforming growth factor beta 1

INTRODUCTION

PANCREATIC CANCER

Pancreatic cancer can be divided into two major subgroups: Adenocarcinoma, which is believed to arise from the exocrine pancreas and is the most frequent type of pancreatic cancer (95% of cases), and the endocrine tumors (also called neuroendocrine tumors), which arise from the islets cells and are very rare.
This work is focused on pancreatic ductal adenocarcinoma the most frequent and lethal type of pancreatic cancer.

Pancreatic Ductal Adenocarcinoma

Pancreatic ductal adenocarcinoma (PDAC) is the deadliest solid cancer and currently the fourth most frequent cause of cancer-related deaths (Jemal et al., 2010). In contrast to the general trend of decreasing incidences for most cancers, the incidence and death rates for PDAC continue to increase ("Cancer Facts & Figs. 2011", American Cancer Society, www.cancer.org). The highest rates of pancreatic cancer incidence are in industrialized countries, with Europe and Nordic countries having the highest incidence. Interestingly, in the United States, the incidence is higher in Native Hawaiians, Korean Americans and African Americans (Han and Von Hoff, 2013).

Only 5 to 10% of patients with pancreatic cancer have a family history of the disease and the risk of pancreatic cancer increases 40% if there is familial pancreatitis (Han and Von Hoff, 2013, Hidalgo, 2010). Apart from genetic or familial predisposition, pancreatic cancer is more common in elderly people than younger people, and only 20% of patients present with potentially curable tumors, largely due to late diagnosis as a consequence of the lack of early symptoms and poor or ineffective diagnostics. Thus, the 1- and 5-year relative survival rates for PDAC are currently 25% and 6%, respectively.

The causes of the pancreatic cancer still remain unknown. Numerous studies show an association and increased incidence in patients with diabetes, chronic pancreatitis, heavy alcohol consumption, a high-fat, high-cholesterol diet, and with infectious agents such as *H. pylori* and hepatitis B virus. Smokers have around a 3 times higher risk of developing pancreatic cancer than no-smokers (Hassan et al., 2007).

Our still incomplete understanding of the causes of PDAC combined with ineffective diagnostics, all contribute to fact that when diagnosed, the majority of PDAC patients presents with extensive metastases in secondary organs including the liver, lungs and bone marrow. PDAC's high resistance to both chemo- and radiotherapy further confounds this problem and severely limits the potential to effectively treat these patients. The only "effective" treatment modality to date for pancreatic cancer is a very invasive and complex surgical process, known as the Whipple procedure, for which only ~20% of patients with a local disease can benefit (Philip et al., 2009). Despite ever increasing research efforts, little progress has been made towards developing new therapies that significantly impact clinical endpoints, particularly in patients with non-resectable PDAC.

Since the majority of PDAC patients already present with metastatic disease in the liver and peritoneal cavity at the time of diagnosis, chemotherapeutic intervention represents the only viable treatment option. Advances in PDAC-specific therapies are summarized in **Table I1** and detailed below.

Gemcitabine: The introduction of the nucleoside-analogue gemcitabine, in 1997, improved clinical response respect to 5-Fluorouracil by reducing pain and loss (Burris et al., 1997). Nevertheless, with a 5 year survival rate of 1–4% and a median survival period of 4-6 months (Ahlgren, 1996, Jemal et al., 2004, Philip et al., 2009, Rosenberg, 1997, Rothenberg et al., 1996, Warshaw and Fernandez-del Castillo, 1992) the prognosis of patients with pancreatic cancer has remained poor.

Erlotinib: The incorporation of Erlotinib in 2007, a small-molecule inhibitor of the epidermal growth factor receptor (EGFR) in combination with Gemcitabine has not resulted in a markedly improved median survival (Moore et al., 2007).

FOLFIRINOX: The use of FOLFIRINOX (combination therapy of oxaliplatin, irinotecan, fluorouracil, and leucovorin) in patients with metastatic pancraeatic cancer has improved the overall survival 11.1 months as compared with gemcitabine, which was 6.8 months. As compared with gemcitabine, FOLFIRINOX was associated with a survival advantage but had increased toxicity, therefore, only patients with a good performance most likely could benefit from this combination therapy (Conroy et al., 2011).

Abraxane: Although a recent phase III clinical trial combining gemcitabine with abraxane (a protein-bound form of paclitaxel) showed prolonged survival with the combination of both treatments with 8.5 vs 6.7 (Han and Von Hoff, 2013).

Although tremendous efforts have been invested in improving our therapeutic arsenal for treating patients with pancreatic cancer, all patients inevitably succumb to the disease. Therefore, new approaches for targeting pancreatic cancer are still desperately needed to pave the way for the development of disease-free treatment regimens (Hermann et al., 2009, Neesse et al., 2010).

CLINICAL REGIMENS PROVEN TO INCREASE SURVIVAL FOR PATIENTS WITH ADVANCED METASTATIC PANCREATIC CANER				
Regimen	Control	Median Survival (months) Regimen	Control	Reference
Gemcitabine	5-FU	5.6	4.4	Burris, et al., 1997
Gemcitabine + Erlotinib	*GEM	6.24	5.91	Moore, et al., 2007
FOLFIRINOX**	*GEM	11.1	6.8	Conroy, et al., 2011
nab-paclitaxel + gemctibaine	*GEM	8.5	6.7	Von Hoff, et al., 2012
*GEM: gemcitabine **FOLFIRINOX: Folinic acid + 5 FU + Irinotecan + Oxaliplatin				

Table I1. Current treatments for PDAC cancer. *Adapted from (Han and Von Hoff, 2013)*

1.1 The Cancer Stem Cell Concept

During the past years, different but not necessarily exclusive models have emerged to try to explain the tumor heterogeneity and inherent differences in tumor-regenerating capacity within cancer cells: 1) the clonal model describes a population of mutant cells within the tumor that have a growth advantage and are selected for and expand during tumorigenesis, resulting in a homogenous tumor mass (Nowell, 1976), 2) the cancer stem cell (CSC) model, on the other hand, postulates a hierarchical organization of cells within the tumor such that only a small subset of "stem-like" cells is responsible for sustaining tumorigenesis and establishing the cellular heterogeneity inherent in the primary tumor (Clarke et al., 2006) **(Figure I1)**. It is important to note that the two models are not mutually exclusive, as CSCs themselves undergo clonal evolution, as shown for leukemia stem cells (Barabe et al., 2007).

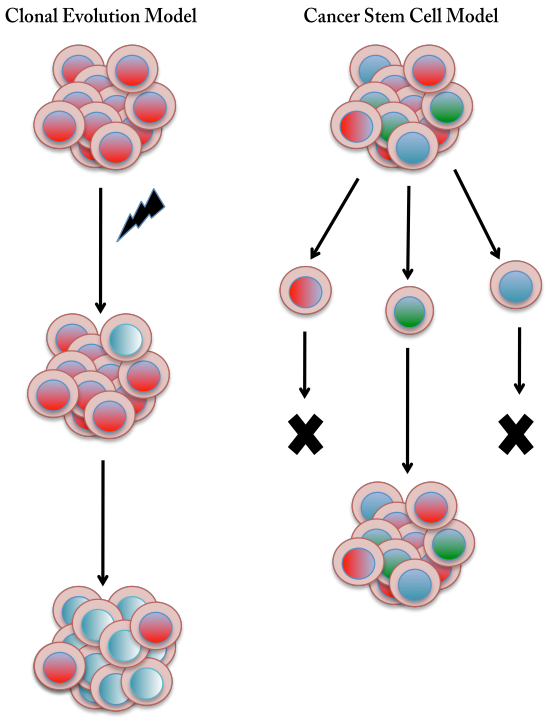

Figure I1. Sources of heterogeneity. The Clonal evolution model: genetic/epigenetic changes in cancer cells with growth advantages are selected to repopulate the tumor mass. Cancer Stem Cell Model: Tumors contained different subpopulations of tumorigenic (green) and non tumorigenic cells organized in a herarchy. Nontumorigenic cells are believed to form the bulk of the tumor. Tumorigenic cells are able to self renew and contribute to the tumorigenesis by recapitulating the tumor heterogeneity *Adapted from (Magee et al., 2012)*

According to the current definition, CSCs are defined by a cell within a tumor that is able to self-renew, is exclusively tumorigenic *in vivo*, and is capable of producing all the cancer cell lineages within a tumor (Hermann et al., 2007a, Li et al., 2007b). CSCs have also been described to bear the ability to drive metastasis (Hermann et al., 2008). The first evidence for the cancer stem cell hypothesis was generated in leukemia and myeloma (Bruce and Van Der Gaag, 1963, Park et al., 1971), but further proof has now been provided in leukemia (Bonnet and Dick, 1997) as well as several solid cancers including breast cancer (Al-Hajj et al., 2003), glioblastoma (Singh et al., 2004), colorectal (Ricci-Vitiani et al., 2007), liver (Ma et al., 2007), and pancreatic cancer (Li et al., 2007a, Hermann et al., 2007a).

CSCs are characterized by additional features, such as a distinct surface marker expression profile or the capacity for symmetric/asymmetric cell division, which allows the cancer stem cells to generate different progenies or expand itself (Wicha, 2006). Likewise, CSCs have been shown to a distinct cell cycle profile and are more resistant to standard chemotherapies compared to the their more differentiated counterparts. Thus, the CSC concept has received wide attention as it provides an explanation for therapeutic resistance and relapse based on these cells' innate stemness features including quiescence (Hermann et al., 2007a, Hermann et al., 2008). Therefore, during treatment, while more differentiated cells succumb to the effects of the chemotherapy, cancer stem cells are able to evade the effect of the chemotherapy, and upon termination of treatment, the CSC can again give rise to more differentiated progenies, recapitulating the heterogeneity of the tumor **(Figure I2)**

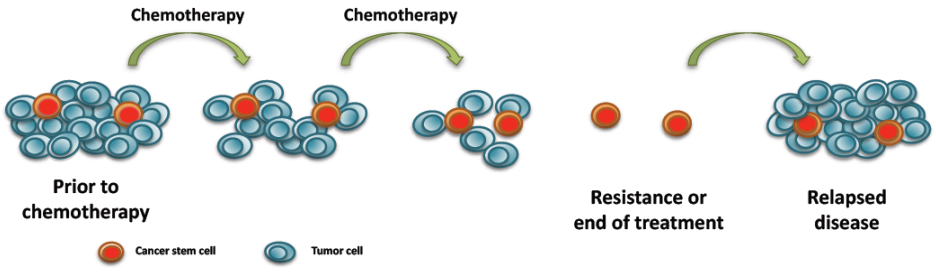

Figure I2. During the treatment, while more differentiated cells succumb to the effects of the chemotherapy, cancer stem cells are able to evade the effect of the chemotherapy recapitulating the tumor heterogeneity upon the treatment is finished.

Over the past years, many research efforts have become trying to explain " cell of origin". The accumulation of mutations in stem cells has been defined as the most suitable mechanism that gives rise tumorigenesis. Since normal stem cells have more survival during time, are prone to acquire more mutations(Fearon and Vogelstein, 1990). Based on these findings, many studies have been hypothesized that CSCs may arise from the dedifferentiation of somatic stem or progenitor cells with genetic alterations that acquire stem cell characteristics.

1.2 Markers for prospectively identifying pancreatic cancer stem cells

The first evidence for the existence of CSCs in pancreatic cancer was provided by Li et al. (Li et al., 2007b), identifying a highly tumorigenic CD44+CD24+EpCAM+ subpopulation using a xenograft model of immunocompromised mice for primary human pancreatic adenocarcinoma. This subpopulation was able to generate tumors from as few as 10^2 cells in 50% of the animals, showing a high tumorigenic capacity. However, CD44-CD24-EpCAM-, the negative population for these markers, was not capable to generate tumors until 10^4 or more cells were implanted. CD44+CD24+EpCAM+ cells displayed typical stem cell phenotypes, such as self-renewal capacity, generation of progenies and recapitulation of the parental tumor heterogeneity from which they were derived. Unfortunately, it should be noted that in this first study, CSCs were compared to their triple-negative counterparts (CD44-CD24-EpCAM-). Since EpCAM identifies epithelial cells within the tumor, it is possible that their EpCAM negative cells represented non-epithelial inflammatory stromal and vascular cells.

Using a different cell surface marker, Herman et al (Hermann et al., 2007a) showed that the expression of CD133 in freshly isolated primary human pancreatic tumors identified a population with self-renewal capacities, and most importantly, exclusive *in vivo* tumorigenicity . Importantly, CD133+ cells maintained their tumor-initiating capability during serial passaging *in vivo*. Interestingly, they also showed that the CD44+CD24+EpCAM+ subpopulation partially overlapped with the CD133+ population.

Additional markers have also been used to for the characterization of CSCs: ALDH-1

(Aldheyde Dehydrogenase-1) (Feldmann et al., 2007, Jimeno et al., 2009, Rasheed et al., 2010) has been associated with a high tumorigenic population in pancreatic cancer, although more recent data suggest an abundant expression of ALDH-1 in normal pancreas tissue (Deng et al., 2010), which may compromise the specificity of ALDH-1 as a marker for pancreatic CSCs. Indeed, ALDH-1 can be used for tumors whose normal tissue expression of ALDH-1 is limited or restricted, such as breast, lung, ovarian or colorectal tumors, or for circulating CSCs. **(Table I2)**

Pancreatic Ductal Adenocarcinoma	Markers	Reference
Tumor-initiating population	$EpCAM^+$ $CD44^+$ $CD24^+$	(Li et al., 2007a)
	CD133	(Hermann et al., 2007a)
	ALDH-1	(Feldmann et al., 2007, Jimeno et al., 2009, Rasheed et al.)
	Side Population/ABCG2	(Kabashima et al., 2009)
Migrating cancer stem cells	CD133+CXCR4+	(Hermann et al., 2007a)

Table I2. Cancer Stem cell markers for pancreatic cancer. *Adapted from (Dorado et al.)*

Taken together, the use of cell surface markers to identify CSCs have emerged as powerful tools for isolating distinct cell populations from freshly harvested primary tumors (Hermann et al., 2007b). However, none of the above listed markers appear to be capable of selectively identifying a pure population of CSCs, rather markers appear to enrich for a population containing CSC. In addition, markers such as CD133 and CD44 bear additional caveats. For example, not only can their expression levels change depending on environment conditions (e.g. xenografting and primary cell culture), but their expression is neither exclusively or reproducibly linked to a functional CSC phenotype (Wicha, 2006). In fact, the use of different surface markers has created conflicting data in some settings emphasizing our still immature knowledge of their role (Beier et al., 2007, Joo et al., 2008, Ogden et al., 2008, Wang et al., 2008). Thus, alternate detection and isolation methods based on CSC functional properties would not only avoid the use of artifact-prone surface markers but should also provide novel insights into CSC biology.

1.3 Migrating cancer stem cells and Metastasis

Metastasis remains the main cause of mortality in advanced PDAC patients. This process requires a cell to detach from the tumor followed by an invasion of the blood vessels, migration and establish secondary lesions. Not all the cancer cells that compose the tumor heterogeneity are able to drive metastasis, actually only a small subset bear this capacity. Based on the CSC concept, only CSCs are exclusive tumorigenic, therefore CSCs could have a potential role in metastasis. Herman et al. identified two distinct subsets of $CD133^+$ CSC based on the expression of the chemokine receptor CXCR4 (Hermann et al., 2007a). These authors identified a subpopulation of $CD133^+$ $CXCR4^+$ that bears a high potential migratory activity responding to the its specific ligand stromal cell derived factor 1 (SDF-1). Two different subpopulations were identified by means of expression of CXCR4. While $CD133^+$ $CXCR4^-$ were responsible for the tumor initiation, in contrast, $CD133^+CXCR4^+$ had exclusive metastatic potential. While these cells could also be detected in the portal vein of mice orthotopically transplanted with $CD133^+CXCR4^+$ cells, it remains to be demonstrated whether these cells can also be detected in the circulation of patients with advanced pancreatic cancer. **(Figure I3)**

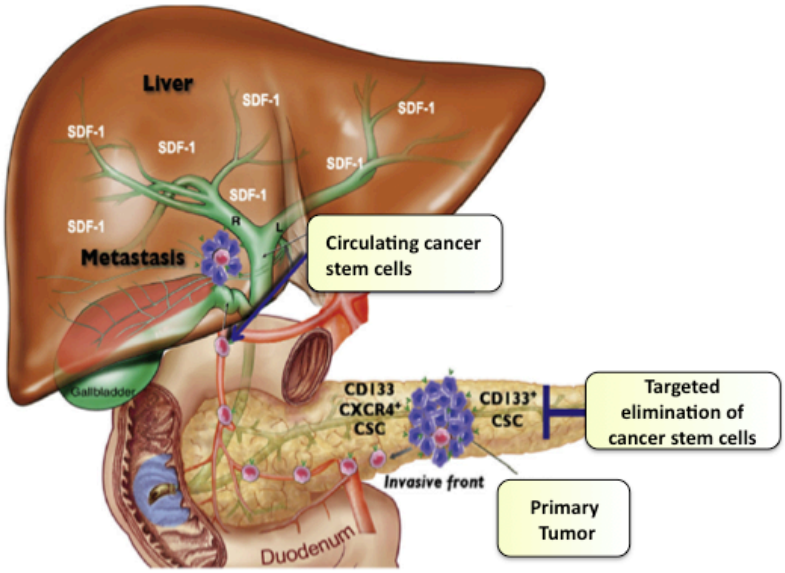

Figure I3. A subpopulation of migrating cancer stem cells, identified by CD133+CXCR4+ is responsible for metastasis. Detection of these circulating CSC could serve as prognostic and therapeutic biomarker. *Adapted from (Lonardo et al., 2010)*

Indeed, is possible that CSC acquire a migratory capacity due to the Epithelial-Mesenchymal-Transition (EMT), while maintaining their stemness features, initiate tumorigenesis. The EMT phenotype is associated with low expression of E-cadherein and *de novo* expression of vimentin. Moreover, Wellner et al. recently showed for pancreatic cancer that the EMT-activator ZEB1 represents an important promoter of metastasis by suppressing E-cadherin. (Wellner et al., 2009)

These results suggest that the metastatic process is not random. Actually, it depends of the CXCR4 and the specific ligand expression in the host organ.

1.4 Cancer stem cell-targeted therapy

Despite strong efforts trying to develop a more effective therapy for the treatment of pancreatic cancer, nowadays, represents one of the deadliest cancer related deaths (Jemal et al., 2010). Therefore, improving the overall survival as well as develop more sensitive early detection diagnostics, such as biomarkers or imaging methods, will be crucial in order to improve the prognosis of these patients. Different studies have demonstrated that CSC are highly resistant to standard chemotherapy and radiation in pancreas (Hermann et al., 2007a, Jimeno et al., 2009). Cell cycle analysis have shown that CD133+ population undergo cell cycle arrest during gemcitabine treatment but as soon the treatment was withdraw, the cells could restore the tumor heterogeneity, representing the main source of rapid disease relapse. In contrast, CD133- cells became apoptotic during the treatment. Future studies will needed to determine if the CSC remained quiescence during treatment and why did not respond to chemotherapy.

During the past years different mechanisms have been linked to resistance in cancer stem cells, such as their enhanced anti-apoptotic mechanisms (Visvader and Lindeman, 2008) or the over-expression of membrane transporters ABC family that efflux cytotoxic compounds from cells (Goodell et al., 1996), high DNA repair capacity (Al-Assar et al., 2011), and more anti-apoptotic properties (Visvader and Lindeman, 2008). Quiescence will evade the effects of cytotoxic drugs because there is no proliferation being a consequence of cellular resistance to therapy and

radiation (Wilson et al., 2008). In addition, some studies have shown the isolation of stem cells from cultured breast tumors in mamospheres based on their ability to retain the lipophilic dye PKH26 (Pece et al., 2010).

Thus, since CSC were shown to be responsible for the exclusive tumorigenicity and resistance, should represent a target for novel therapeutic approaches. There are two different approches to target CSC. One is develop therapeutic agents that specifically these cells by targeting their self-renewal machinery, and the other would be to force the differentiation of the CSC, but since this could be reversible due to the enhace plasticity, these treatments should be combined by other therapies.

Some studies suggested that CSCs expresses high levels of telomerase in a small subset of this population (Armanios and Greider, 2005, Bhagwandin and Shay, 2009, Harley, 2008, Phatak et al., 2007). Telomerase, which has been shown to be essential for tumor progression, has become a crucial marker in many cancers, therefore, telomerase inhibition has emerged as an universal tumor target. Actually, combination of standard therapy and telomerase inhibitors shown more effectiveness in prostate cancer (Marian and Shay, 2009).

Successful targeted CSC elimination may require the inhibition stem cell-associated pathways (e.g. sonic hedgehog, mTOR, notch, Nodal/Activin). Feldmann et al. described increase sonic hedgehog activity in pancreatic cancers (Feldmann et al., 2007). The Sonic Hedgehog (Shh) pathway has been shown to be critical for the embryonic development of the pancreas (Ingham and McMahon, 2001), but has played a crucial role in progression and maintenance of pancreatic cancer (Bailey et al., 2009, Morton et al., 2007). Shh inhibits the transmembrane receptor patched, which inhibits smoothened in the absence of Shh. Patched inactivation leads to an activation of Smoothened, which leads to transciption of the Gli protein family target genes. Shh has been considered to be fundamental for the maintenance of CSCs. Actually, inhibition of Shh signaling improved survival in mouse model of pancreatic cancer (Olive et al., 2009). However, Mueller et al. have shown that neither Shh inhibition alone nor in combination with chemotherapy were capable to deplete the CSC pool but cyclopamine alone significantly decreased the metstatic activity of the

treated cells as compared to gemcitabine alone (Mueller et al., 2009). Interestingly, a combine therapy with cyclopamine and gemcitabine depleted the CD133+CXCR4+ migrating population. Moreover, the authors showed that CD133+ cells in pancreatic cancers showed high expression of mTOR signaling suggesting that these pathway may play an important role in the CSC population. The mammalian Target Of Rapamycin (mTOR) is a serine/threonine kinase, which belongs to the phosphatidylinositol 3-kinase (PI3K) superfamily, and is the target of a widely branched signaling pathway that activates mTOR among other downstream effectors (Inoki et al., 2005). For pancreatic CSCs the authors demonstrate that the specific mTOR inhibitor rapamycin resulted in a significant decreased in CD133+ cells, however, it was not sufficient to completely eliminate CSCs. Only the triple combination Cyclopamine, Rapamycin and Gemcitabine (CRG) therapy could abrogate in a complete depletion of the pancreatic cancer stem cell pool (Mueller et al., 2009). Implantation of cells in nude mice that were pre-treated *ex vivo* with the triple therapy CRG, demonstrated that the *in vivo* tumorigenicity activity was abrogated. The authors also investigated the effects of the triple therapy on primary cultures derived from pancreatic cacner tissues, resulting in a complete elimination of the CSCs. Tumorigenicity and metastatic activity was significantly reduced, and long-term survival was increased using, for the first time, two relevant stem cells pathways and additional chemotherapy. Unfortunately, clinical trials with advanced PDAC patients showed no improvement in median survival. Probably, optimal therapeutic targeting of the PDA stroma may recquire specific clinical trial design. Most of the new therapies are introduced in late stages of the disease, and even though PDAC primary tumor shows high content and rich hypovascular stroma meanwhile metastases derived from PDAC tumors do not. This could be an explanation why, thus far, inhibitors of the hedgehog pathway tested in these patients did not benefit (Hidalgo and Von Hoff, 2012).

Other studies were focused on targeting Notch pathways. Fan et al. in glioblastoma indicated that inhibition of Notch pathway by use of an inhibitor of γ-secretase (GSI-18) was also capable of significantly reducing the $CD133^{+}$ $Notch^{+}$ cell population, leading to the depletion of medulloblastoma side population cells (Fan et al., 2006).

Medulloblastoma treated cells with GSI-18 lost the tumorigenicity capacity in vivo, therefore, the authors conclude that the CSCs were eradicated. These findings might be also applicable to pancreatic CSCs, as Notch 2 has also been implicated in pancreatic cancer progression (Mazur et al., 2010).

A more recent study by Lonardo et al. showed that Nodal/Activin pathway is essential for the self-renewal capacity and stemness properties of pancreatic CSCs (Lonardo et al., 2011). Nodal/Activin is strongly expressed in pancreatic CSCs, but is also expressed in pancreatic stellate cells, which are present in the stroma and serve as a CSC niche (Lonardo et al., 2012). Using primary pancreatic cancer cells, the authors showed that the CSC pool was severely compromise by SB431542, specific inhibitor of Nodal/Activin receptor Alk4, recombinant Lefty, a specific endogenous Nodal inhibitor, and with a genetic knockdown Nodal/Alk4 and Smad4 using shRNA technology. Importantly, Nodal/Activin pathway lacks activity in normal pancreas or other adult tissue making it as a possible therapeutic target. Moreover, the blocking of Alk4/7 receptor using small molecule inhibitor SB431542 and shRNA technology had a strong impact on CD133+ expression. In addition, they identified that pancreatic stellate cells also expresss Nodal/Activin, therefore, directly eliminating the paracrine source of Nodal/Activin, may provide additional therapeutic benefits. Translating these findings into *in vivo* settings SB431532 as a single therapy was not sufficient to abrogate tumorigenicity. Actually, after withdrawal of SB431532, that drives CSCs to a more differentiated state, a population of CD133+ cells was observed due to the enhance plasticity of the cells to revert to a CSC phenotype. However, when combined with gemcitabine, resulted in their irreversible and complete elimination using establish pancreatic cancer cell lines. For further evaluation by primary human pancreatic xenograft, surprisingly, tumorigenicity was not affected by this combination. It's important to remark that pancreatic tumors bear high content of stroma, therefore, the authors combined hedgehog pathway inhibitor CUR199691 (Mueller et al., 2009) to deplete the stroma together with SB321542 and gemcitabine obtaining a rapid disease stabilization.

Current therapies may be effective with the tumor bulk, but tumor relapse occurs due to the ineffectiveness against CSCs. Based on the CSC theory, targeting CSCs will

abrogate the tumor relapse, therefore, new designs for target therapies should be the focus of our efforts **(Figure I4).**

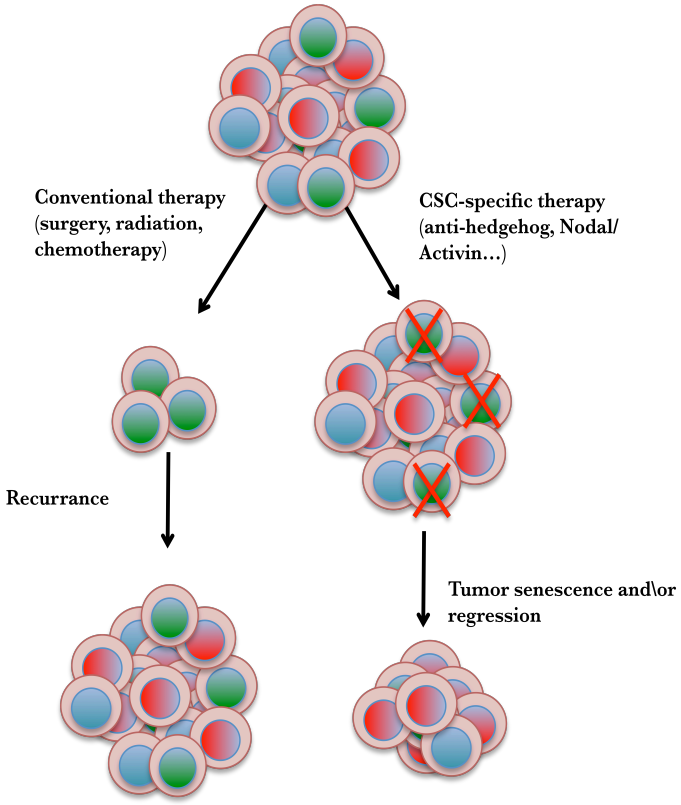

Figure I4. CSC target therapy. Tumors are heterogeneous containing CSCs, progenitor cells, stroma etc.. Conventional therapies eliminates tumor mass but does not target CSCs, resulting in a tumor relapsed. CSC target therapies, will kill or differentiate the CSCs, resulting in a loss of tumor initiating cells that will conduce to a regression. *Adapted from (Ebben et al., 2010)*

OBJECTIVES

Single surface markers such as CD133 or combination of markers such as EpCAM/CD44/CD24 have been described as means to enrich for pancreatic cancer stem cells (CSC) in fresh tumor samples bearing exclusive tumorigenicity and resistance chemotherapy (Hermann et al. 2007). However, changes in the environment conditions such as xenografting of these tumors and their subsequent cultivation, although very important models for comprehensively studying human pancreatic CSC, dramatically reduces the ability of these markers to reproducibly identify CSC. Therefore, alternative prospective isolation methods based on phenotypic properties of CSC avoiding the use of surface markers are urgently needed to further progress in our ability to reproducibly study CSC in these model systems and subsequently develop novel CSC-targeted therapies or accurate clinical diagnoses.

In the present PhD thesis project, we are aiming to:

1. Identify and functionally characterize suitable markers for identifying and isolating pancreatic CSCs
2. Validate the markers identified by demonstrating that isolated cells possess CSC phenotypes.
3. Define the functional relevance and the molecular clues of the identified CSC maker for improving our understanding of CSC
4. Determine whether CSC markers can be utilized for anti-cancer compound screening

OBJETIVOS

Marcadores de superficie tales como CD133 o combinación de marcadores, tales como EpCAM/CD44/CD24 se han descrito para enriquecer en células madre de cáncer de páncreas (CSC) en muestras de tumores frescos, teniendo una exclusiva tumorigenicidad y siendo tambien altamente resistentes a la quimioterapia (Hermann et al. 2007). Sin embargo, los cambios en las condiciones del entorno tales como los xenoinjertos de estos tumores y su cultivo posterior aunque siendo estos modelos muy importantes para el estudio de CSCs de pancreas, se ha observado que se reduce de manera drástica la capacidad de estos marcadores para identificar de una manera reproducible CSCs. Por lo tanto, se necesitan con urgencia métodos para poder aislar e identifcar las CSCs alternativos basados en las propiedades fenotípicas de CSC evitando el uso de marcadores de superficie y, posteriormente, desarrollar nuevas terapias CSC-dirigidas o diagnósticos clínicos precisos.

En el presente proyecto de tesis doctoral, nuestro objetivo es:

1. Identificar y caracterizar de manera funcional marcadores adecuados para aislar células madre cancerígenas de páncreas.

2. Validar los marcadores identificados mediante la demostración de que las células aisladas poseen fenotipos CSC

3. Definir la relevancia funcional y las claves moleculares de la maquinaria para mejorar nuestro entendimiento de las CSCs.

4. Determinar si los marcadores CSC pueden ser utilizados para la investigación de compuestos anti-cancerígenos.

MATERIALS AND METHODS

1. MICE

1.1 Study approval

Mice were housed in the CNIO's animal facility in accordance with institutional policies and federal guidelines. Animal treatments were approved by the Animal Experimental Ethics Committee of the Instituto de Salud Carlos III (Madrid, Spain). Human pancreatic tumors were obtained with written informed consent and after approval from the Ethics Committee of Instituto de Salud Carlos III (Madrid, Spain).

1.2 Xenograft

PDAC, CRC and HCC xenografts from patient derive samples were kindly obtained from Manuel Hidalgo's group (CNIO, Spain). Primary tumors were minced into small fragments and then implanted subcutaneously in 4 to 5 nude mice (NU-*Foxn1*^{nu}; Charles River, Wilmington, MA. USA) with two small tumor pieces per mouse. Once tumors reached 1cm^3, tumors were resected, minced and re-implanted in another set of female nude mice, following the protocol described in Rubio- Viqueira et al. (Rubio-Viqueira et al., 2006), and represented in **Figure M&M1.**

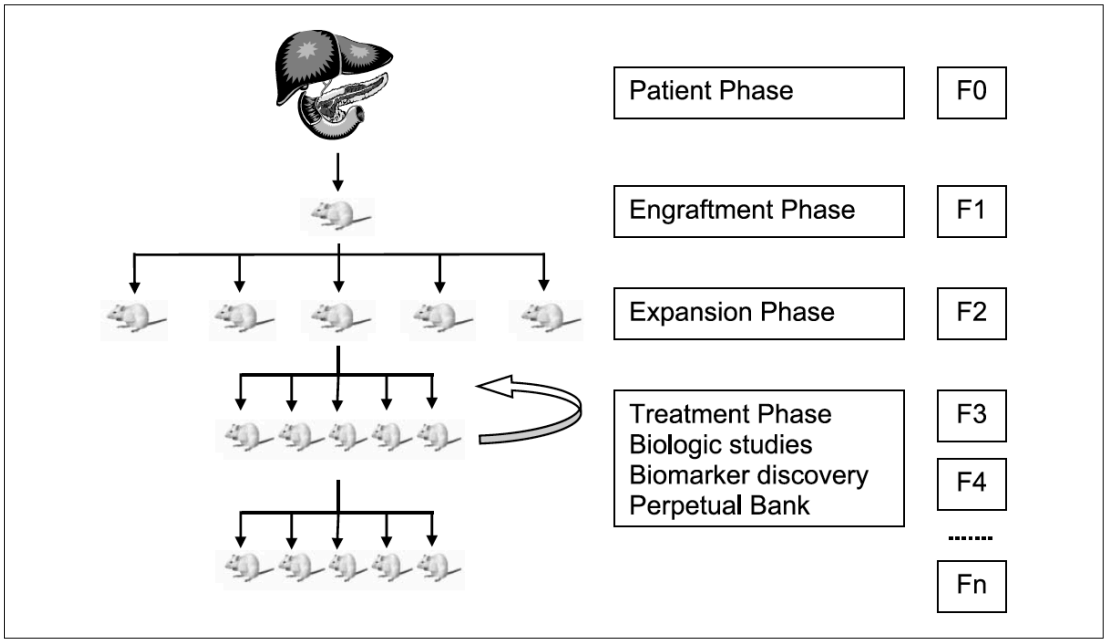

Figure M&M1. Xenograft study schema. Tumor samples are implanted in F1 generation and then expanded in a cohort of nude mice. *Adapted from Rubio-Viqueira et al., 2006.*

1.3 Mice treatments

Four to six week old female nude mice were used as recipients for primary human xenograft transplantations. Upon reaching a volume of 200mm^3, mice were assigned to the following treatment groups: Control, Abraxane (Celgene, NJ, USA) 50mg/kg twice weekly (i.v) and Gemcitabine (Eli Lilly, IN, USA) 125mg/kg twice weekly (i.p.). Mice were treated for 15 days.

1.4 In vivo tumorigenicity and metastasis assays

Primary pancreatic cells were sorted for autofluorescence as detailed below. For tumorigenicity assays, serial dilutions of single-cells resuspended in Matrigel™ (BD Bioscience, Heidelberg, Germany) were subcutaneously injected into female nude mice. For metastasis assays, 10^3 FACSorted autofluorescent positive and negative cells, with nuclear mCherry labeling directed by Histone H2B type 2-E (HIST2H2BE), were resuspended in 1X PBS and intrasplenically injected into NSG mice as previously described (Sainz et al., 2012).

2. CELL CULTURE

2.1 Primary human pancreatic cancer cells.

Human pancreatic tumors were minced, mechanically (gentleMACS Dissociator; Miltenyi, Bergisch-Gladbach, Germany) and enzymatically digested with collagenase (Stem Cell Technologies, Vancouver, BC) and subsequently cultured *in vitro* for 90 min at 37°C and after centrifugation for 5 min at 1200 rpm (Mueller et al., 2009). Cell pellets were resuspended and cultured in RPMI (Invitrogen, Alcobendas, Spain) supplemented with 10% FBS and 50 units/ml pen/strep.

2.2 Sphere formation assay

Spheres were generated by culturing ~2×10^4 pancreatic cancer cells in Ultra-Low attachment plates (Corning, USA) in suspension in serum-free DMEM/F12 supplemented with B27 (1:50, Invitrogen, Alcobendas, Spain), 20 ng/ml bFGF and 50 units/ml pen/strep for a total of 7 days, allowing spheres to reach a size of >75µm. For serial passaging, 7-day-old spheres were harvested using 40µm cell strainers, dissociated into single cells, and then re-cultured for 7 additional days as previously described (Lonardo et al.).

2.3 PKH26 assay.

Human primary pancreatic cancer cells were labeled with PKH26, a red fluorescent cell membrane labeling dye (Sigma), according to manufacturer's instructions. Every 7 days, cells were harvested and PKH26+ cells were determined using a FACS Canto II (BD) for a total of 3 weeks.

2.4 Cell viability assay

Cells were seeded in 96-well plates (Nalgen Nunc International, Penfield, NY) at a concentration of 10^3 cells per well in 100µL of complete medium. Cells were incubated for 24 hours after administration of compounds to allow sufficient adhesion. The cytotoxic activity was measured by sulforhodamine B (SRB)-based cytotoxicity assay as described previously (Limame et al., 2012). The protein absorbance of the viable cells at each concentration is expressed as the relative percentage of absorbance compared with the control well without drug exposure. Each experiment was carried out with three replicate wells for all conditions tested, and all the experiments were done in triplicate.

2.5 Invasion and migration assays

Invasion assays were performed using modified Boyden chambers filled with Matrigel™ (BioCoat®, BD Biosciences). Human primary pancreatic cancer cells were added to the Matrigel™ coated inserts, and 750µl of serum-free medium with 300ng/ml recombinant human Nodal, 100ng/ml SDF-1, 100ng/ml Shh, and 10ng/ml TGF-β was added to the lower chamber. The assay chambers were incubated for 22h at 37°C. Invaded cells were fixed in 4% PFA and stained with DAPI. The ratios of cells in the lower chamber versus total seeded cells (in percent) were calculated. The data are calculated as the mean of 10 high-power fields (HPF).

2.6 Intracellular ATP content

Intracellular ATP was analyzed using the ATP determination Kit (Invitrogen, Alcobendas, Spain). Briefly, Sorted Fluo+ and Fluo- cells were collected and resuspended at an equal concentration in PBS followed by a boiling step for 3min. Cell lysates were collected and ATP content, measured with a luminescence-based substrate, was performed using a luminometer following the manufacture's instructions.

2.7 Cell treatments

For chemoresistance studies, primary human cell lines were treated with Gemcitabine (100ng/ml) and Abraxane (10uM) for 3, 5 and 12 days. Media with each compound was replaced every 48h. For experiments using FTC, Rotenone, DNP or Oligomycin, cells were treated for 72h. For incubation with different types of media, cells were resuspended in Basal Media, which does not contain vitamins, ($DMEM^{gfp}$ antibleaching live cell visualization Evrogen, Moscow, Rusia) for 72h and recovered in basal media with a vitamin cocktail (Sigma) for 72h. (Composition in **Table M&M1**)

Table M&M1

Basal Media

DMEM^{gfp} Antibleaching live cell visualization Evrogen, Moscow, Russia

Component	Concentration, mg/L
$CaCl_2$	200
$FeSO_4x7H2O$	0,07
KCl	400
$MgSO_4$	97,67
NaCl	6400
$NaHCO_3$	3700
NaH_2PO_4	108,7
Glucose	4500
Sodium Pyruvate	110
L-Arginine HCl	84
L-Cystine	63
Glycine	30
L-Histidine HClxH_2O	42
L-Isoleucine	105
L-Leucine	105
L-Lysine HCl	146
L-Methionine	30
L-Phenylalanine	66
L-Serine	42
L-Threonine	95
L-Triptophan	16
L-Tyrosine 2Na x $2H_2O$	104
L-Valine	94

Vitamin Cocktail

Components	Molecular Weight	Concentration (mg/L)
Vitamins		
Choline chloride		100
D-Calcium pantothenate	477	100
Folic Acid	441	100
Nicotinamide		100
Pyridoxal hydrochloride		100
Riboflavin		10
Thiamine hydrochloride		100
I-Inositol		200
Inorganic Salts		
Sodium Chloride (NaCl)		8500

3. FLOW CYTOMETRY

3.1 Flow cytometry analysis

For Flow cytometry analysis, primary pancreatic cells, dissociated cells from spheres cultures or cells obtained from tumor digestions, were stained using different combinations of antibodies depending on the experiment. Autofluorescent cells were excited with a 488nm blue laser and selected as the intersection with filters 530/40 and 580/30 as shown in **Figure 2.** To characterize autofluorescent cells, the following antibodies were used: anti-CD133/1-APC (Miltenyi Biotec); EpCAM-APC, CD44-APC, SSEA-1-APC, CXCR4-APC or appropriate isotype-matched control antibodies (all from BD, Heidelberg, Germany). DAPI was used for exclusion of dead cells. For Anexin V-APC (BD) stainings, we followed the manufacter's instructions. Cells were acquired with a FACS CANTO II instrument (BD, Heidelberg, Germany). Data were analyzed with FlowJo 9.2 software (Tree Star, Ashland, OR).

3.2 FACS sorting

Primary pancreatic cells, dissociated cells from sphere cultures or cells obtained from tumor digestions were adjusted to a concentration of 10^6 cells/ml in Sorting buffer [1X PBS; 3% FBS (v/v); 3mM EDTA (v/v)]. DAPI was added to exclude dead cells at a concentration of 2mg/ml. Cells were sorted with a FACS Influx instrument (BD, Heidelberg, Germany).

3.3 Side Population

Primary PDAC cells at a concentration of 10^6 cells/ml were stained with Hoechst 33342 (5µg/ml) at 37 °C for 2h in the absence or presence of the ABCG2 transporter inhibitor Fumitremorgin C (5µg/ml; Sigma). Cells were washed and resuspended in cold 1X PBS. Propidium iodide (Sigma) was used to exclude dead cells. SP and non-SP cells were sorted using a FACS Influx sorter (BD).

3.4 Cell cycle: G0

Previously sorted autofluorescent positive and negative cells were fixed with 100% cold ethanol and placed at -20°C over night. Cells were washed with PBS twice and stained with Ki67 (BD, Heidelberg, Germany) for 30min at room temperature, followed by another wash with PBS. Cells were stained with DAPI to perform the cell cycle analysis using a FACS CANTO II (BD) instrument.

4. PROTEIN ANALYSIS

4.1 Protein extraction and quantification

Cells were harvested in RIPA buffer (Sigma) supplemented with a protease inhibitor cocktail (Roche Applied Science, Indianapolis, IN). The cell lysate was spin down at maximum speed and supernatant was collected. Protein lysates were quantified using a BCA Protein Assay Reagent kit (Pierce, Thermo Scientific).

4.2 Western Blot

50µg of protein was resolved by SDS-PAGE and transferred to PVDF membranes (Amersham Pharmacia, Piscataway, NJ). Membranes were sequentially blocked with 1X TBS containing 5% BSA (w/v), 1% chicken albumin (w/v) and 0.1% Tween20 (v/v), incubated with a 1:1000 dilution of antibodies against ABCG2 (ab24115) or GAPDH (ab8245; both Abcam, Cambridge, UK) overnight at 4ºC, washed 3 times with 1X PBS containing 0.05% Tween20 (v/v), incubated with horseradish peroxidase-conjugated goat anti-rat or goat anti-mouse antibody (Sigma), and washed again to remove unbound antibody. Bound antibody complexes were detected with SuperSignal chemiluminescent substrate (Amersham, Barcelona, Spain).

5. RNA ANALYSIS

5.1 RNA extraction from tissue or cells

Total RNAs from human primary pancreatic cancer cells or livers of NSG mice were extracted with TRIzol (Life Technologies, Madrid, Spain) according to the manufacturer's instructions.

5.2 RT-qPCR

1µg of total RNA was reverse-transcribed with SuperScript II reverse transcriptase (Life Technologies) using random hexamers. Quantitative real-time PCR was performed with an Applied Biosystems 7500 real-time thermocycler (Applied Biosystems, Alcobendas, Spain) using Fast SYBR Green (Qiagen, Barcelona, Spain) as per the manufacturer's instructions. The list of utilized primers are shown in **Table M&M2**

Table M&M2- RT-qPCR primers

Gene	Primer sense	Primer antisense
Nanog	tgaacctcagctacaaacaggtg	aactgcatgcaggactgcagag
Klf4	acccacacaggtgagaaacc	atgtgtaaggcgaggtggtc
Sox2	agaaccccaagatgcacaac	cggggccggtatttataatc
Bmil	ttctttgaccagaacagattgg	gcatcacagtcaattgctgct
Oct3/4	cttgctgcagaagtgggtggaggaa	ctgcagtgtgggtttcgggca
CXCR4	ggtggtctatgttggcgtct	tggagtgtgacagcttggag
CXCR7	gcagccagcagagctcacagt	ccatcgttctgaggcgggcaa
Nodal	agcatggttttggaggtgac	cctgcgagaggttggagtag
Activin	aaagcttcatgtgggcaaag	aatctcgaagtgcagcgtct
Alk4	ggagcgtcttgtctttggag	tgcaacaggatcgacttgag
hCNT1	ggtggcctgcctcctggatt	aagcagcaagagctagacccctct
hCNT3	cttttctggagtacacagatgct	cggcaggaccttaaatgcaaa
hENT1	ctctcagcccaccaatgaaag	ctcaacagtcacggctggaa
hENT2	tctccaactctcagcccaccaa	cctgcgatgctggacttgacct
ABCB1	tgacatttattcaaagttaaaagca	tagacactttatgcaaacatttcaa
ABCC1	ggaataccagcaaccccgactt	ttttggttttgttgagaggtgtc
ABCB5	agaactcgaaccgttggaatgc	tcatccaggattctgagctgag
ABCG1	tcagggacctttcctattcg	ttcctttcaggagggtcttgt
ABCG2	tcaagtggggcgatgctg	atcagcagagggggcagaga
B-ACTIN	gcgagcacagagcctcgcctt	catcatccatggtgagctggcgg

6. IMMUNOSTAINING ANALYSIS

6.1 Immunofluorescence

Primary pancreatic cancer cells and sphere-derived cells were seeded in 96-well culture dishes (Corning, One Riverfront Plaza, NY) and incubated at 37°C for 24h. For tracking the cytosol, mitochondria, lysosomes, and lipid droplets, Cytotracker, Mytotracker, Lysotracker (all Invitrogen) and Nile Red (Sigma), respectively, were used at dilutions of 1:20,000 for 30 min at 37°C. Following two washes with 1X PBS, and 5 min incubation with Hoechst (5µg/ml; Sigma, St. Louis, MO), cells were analyzed using an SP5 confocal microscope (Leica, Heidelberg, Germany).

6.2 Indirect immunofluorescence analysis

For histopathological analysis, FFPE blocks were serially sectioned (3 µm thick) and stained with hematoxylin and eosin (H&E). Additional serial sections were probed with antibodies against dsRed (Clontech, Saint-Germain, France), human cytokeratin 19α (abcam, Cambridge, UK), or in situ hybridization was performed using the Alu probe (Qbiogene, Bath, UK). Following incubation with primary antibodies, samples were incubated with HRP-conjugated secondary antibodies (DAKO, Barcelona, Spain) and positive cells were visualized using 3,3-diaminobenzidine tetrahydrochloride plus (DAB+) as a chromogen.

7. MICROCHIP-BASED SINGLE CELL ANALYSIS

The microchip pattern was designed with AutoCAD (Autodesk), and was manufactured using standard soft-lithography techniques (Qin et al.). This post-array is made of polydimethylsiloxane and contains ~4600 micro-wells of 80um diameter. The chip was bonded to a 24-well glass bottom plate using a plasma oven prior to cell seeding (**Figure M&M2**). For semi-automated analysis of single cells seeded in micro-wells we used a custom-developed software (CNIO MSRC). During a first low resolution fast scan, settings for generating one image per well were established. After image

acquisition, the software automatically localizes microwells containing single cells and records the presence or absence of autofluorescence and the respective well coordinates. Using this spatial information, the application interacts with the SP5 microscope (Leica) and loads high-resolution settings, scanning automatically just the areas of interest at customizable time intervals.

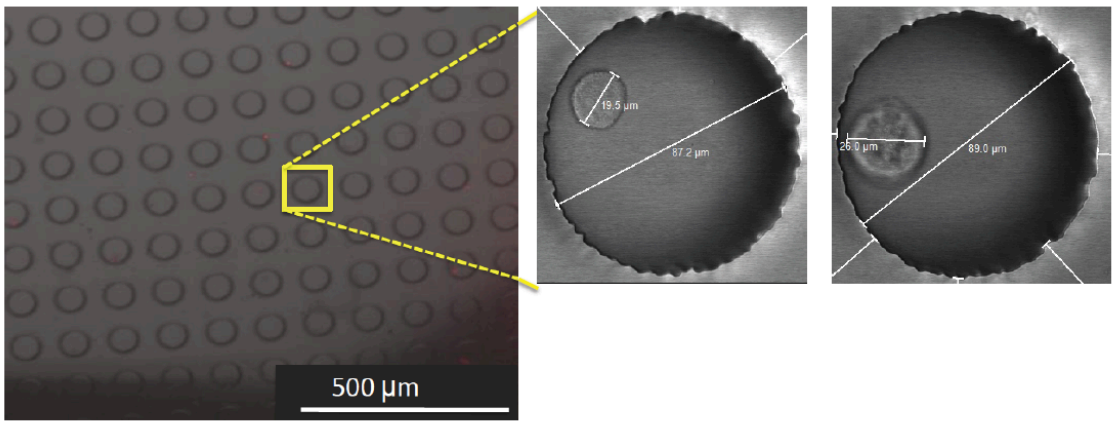

Figure M&M2 Polydimethylsiloxane post-arrays containing several thousands of microwells. Single pancreatic cancer cells were followed by time-lapse microscopy for 72h.

8. LOW THROUGHPUT SCREENING ASSAY

Singularized cells isolated from pancreatic cancer tissue or primary cultures of PDAC cells were incubated over night with 30µM riboflavin (Sigma), sorted for autofluorescence as described above, seeded in 96-well black plates with clear bottoms (Greiner bio-one GmbH, Germany) at a density of 3,000 cells/well, and cultured for 72h in complete RPMI plus 30µM Riboflavin. Allocated compounds were tested in triplicate and changes in autofluorescence and total cell number (Hoechst 33342+ cells) were determined 72h post treatment using the HCS OPERA (PerkinElmer, Waltham, MA). Drug-mediated cellular toxicity was determined using the Toxilight BioAssay kit (Lonza, Walkersville, MD) according to the manufacturer's instructions. The list of the compounds used in the LTS and concentrations are showed in **Table M&M3**

Table M&M3- List of compounds and concentrations used in LTS platform

Compound	Concentration
Gemcitabine	100ng/ml
Abraxane	10µM
SB43154	20µM
Rapamycin	100ng/ml
Cyclopamine	10µ/L
FTC	5µg/ml
Metformin	10mM
Dopamine	10µM
Irinotecan	10µg/ml
5-FU	10µg/ml
Oxaliplatin	50µg/ml
Cisplatin	10µg/ml
Docetaxel	10µg/ml

Statistical analyses. Results for continuous variables are presented as means ± standard deviation unless stated otherwise and significance was determined using the Mann-Whitney test. All analyses were performed using SPSS 17.0 (SPSS, Chicago, IL).

RESULTS

1. ANALYSIS OF TRADITIONAL PANCREATIC CANCER STEM CELL MARKERS

It has been described by Herman et al (Hermann et al., 2007b) that primary pancreatic CSCs can be enriched for *in vitro* by culturing as anchorage-independent three-dimensional colonies, also termed spheres. Spheres are enriched for cells bearing stemness features including the ability to form secondary spheres as well as more differentiated progenies. Furthermore, the enrichment and isolation of pancreatic CSCs using surrogate cell surface markers, such as the pentaspan transmembrane glycoprotein CD133, also known as Prominin-1, has been reported (Hermann et al., 2007b). In the present study, we used these two supplementary methods to functionally identify pancreatic CSCs in a total of eight previously described human pancreatic adenocarcinoma xenografts (Jones and Wagers, 2008, Rubio-Viqueira et al., 2006). Cells were freshly isolated from early passage xenografts, and cultured as low passage adherent cells or spheres. Cells were phenotyped by flow cytometry for the expression of CSCs markers, and as previously reported (Lonardo et al.), spheres were enriched in $CD133^{+}$ cells. (**Figure 1)**

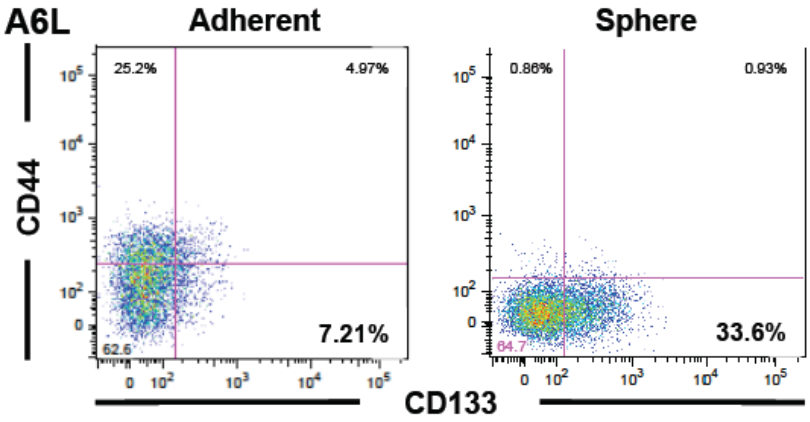

Figure 1. Flow cytometry of CD44+CD133+ cells is shown for primary PDAC A6L cells cultured as adherent cells or spheres.

Although sphere-derived cells lost expression of some CSC markers such as CD44 even after one passage *in vitro*, they were consistently more enriched for tumorigenic CSCs as compared to their adherent counterparts when injected in vivo. Using the extreme limiting dilution analysis (ELDA) algorithm for determining CSC frequency (http://bioinf.wehi.edu.au/software/elda/index.html), we observed that the frequency of tumorigenic cells was indeed strongly enhanced in spheres compared to adherent cells, but was still regularly far below 1% indicating the need for further enrichment to eventually allow for comprehensive studies of highly purified CSCs versus their differentiated progenies (**Figure 2).**

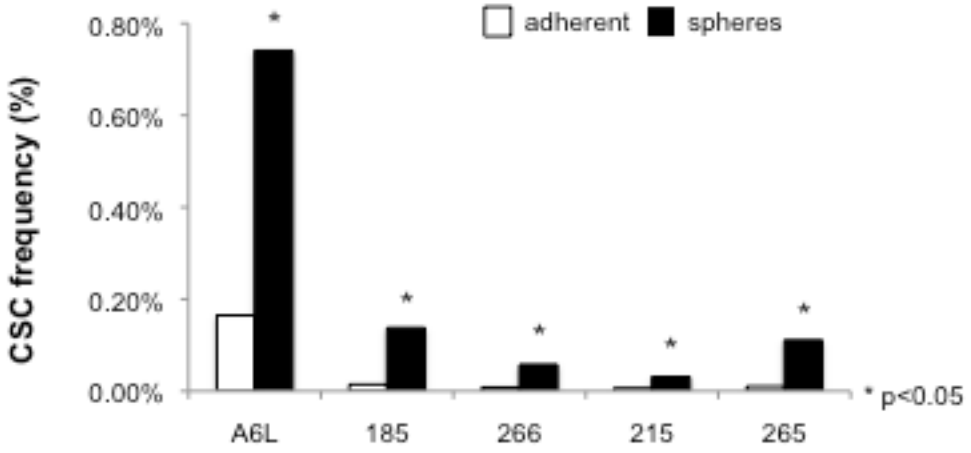

Figure 2. Cancer stem cell frequency for adherent versus sphere-derived cells was calculated using ELDA algorithm and is expressed as a percent of tumorigenic cells per total cells

In fact, even serial dilutions from EpCAM+CD133+CD44+ cultured primary A6L cells did not show a consistent enrichment in tumorigenicity, indicating a loss of specificity during progression or *in vitro* passaging **(Figure 3)**

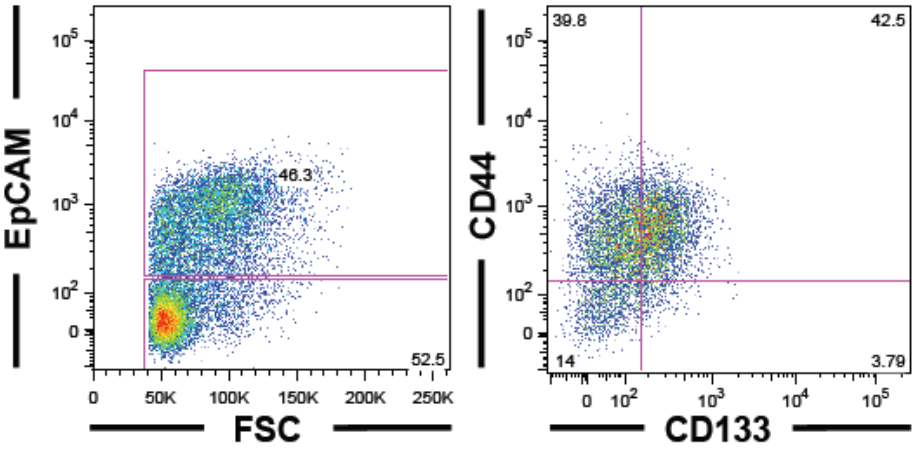

Tumor take after three months
(# tumors / # injections)

	10^4	10^3	10^2
$CD133^-$ $CD44^-$	3/6	1/6	0/6
$CD133^-$ $CD44^+$	4/6	2/6	0/6
$CD133^+$ $CD44^-$	6/6	3/6	1/6
$CD133^+$ $CD44^+$	6/6	3/6	2/6

Figure 3. $EpCAM^+$ cells from PDAC 185 tumor were sorted for CD44 and CD133 expression (upper panel). *In vivo* tumorigenicity for serial dilutions of sorted cells (bottom panel).

Therefore, although it has been previously shown that CD133 significantly enriches for CSCs in freshly resected primary human pancreatic cancer tissue (Hermann et al., 2007b) and in multiple primary human pancreatic cancer xenografts, expression levels are also subject to considerable variation, even when cultured in conditions that enrich for CSC and subsequently CD133+ cells (**Figure 4**).

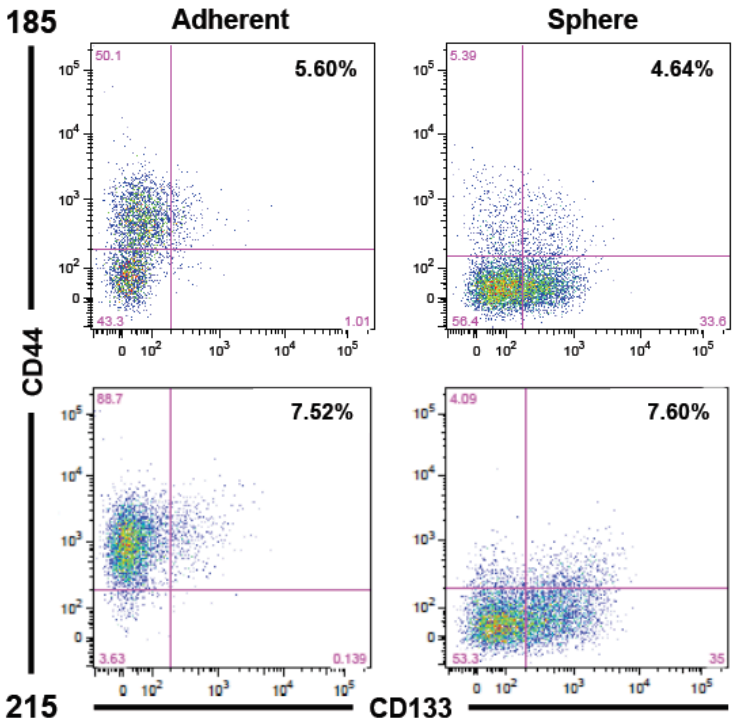

Figure 4 Flow cytometry analysis of CD44+CD133+ cells from primary PDAC 185 and 215 cells cultured as adherent cells or spheres

Likewise, other putative CSC markers like c-Met were also virtually undetectable in sphere-derived cultures established from many primary PDAC tumors **(Figure 5A)**. Taken together, this general lack of specificity during *in vitro* culture highlighted to us that although known CSC markers can identify CSC, their expression is variable, sensitive to in vitro culture conditions **(Figure 5B)** and lacks intrinsic specificity. Thus, these findings forced us to identify other means for isolating CSCs from primary cultures.

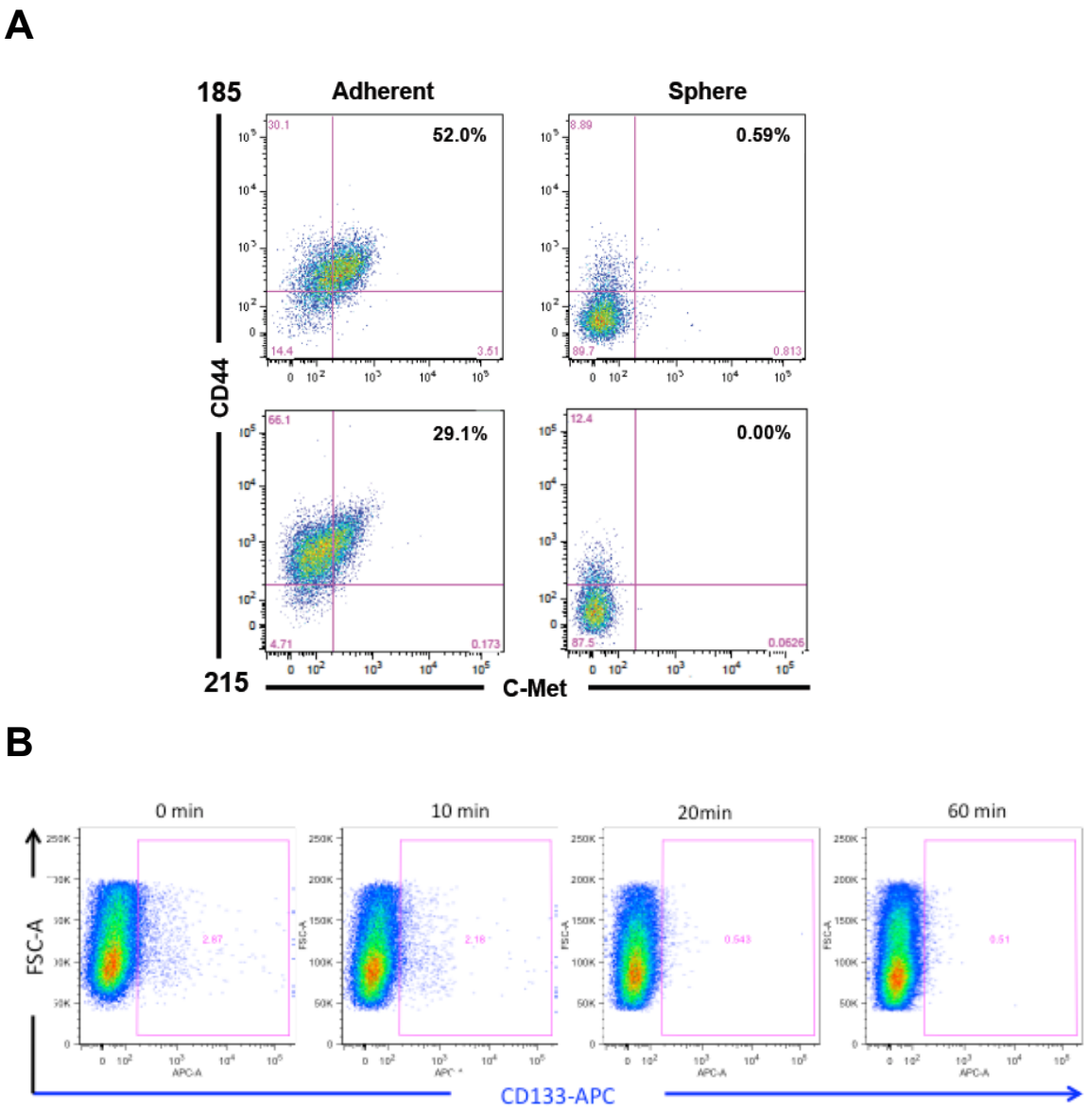

Figure 5 (A) Flow cytometry analysis for CD44+CMet+ cells from primary PDAC 215 cells cultured as adherent cells or spheres. **(B)** Flow cytometry analysis for CD133. Cells were tripsinized and then resuspended in RPMI for recovering. Cells were acquired with no recovering time after tripsinization (0min), at 10min, 20 and 60min of recovering.

Side population (SP) cells, which exclude the DNA dye Hoescht 33342 through the overexpression of the transporters ABCG2, have been shown to be enriched in cancer-initiating cells for several tumors (Hirschmann-Jax et al., 2004). Indeed, Kabashima et al described a SP in pancreatic cancer cells with stem cell-like properties but these data were exclusively obtained with establish pancreatic cancer cell lines rather than primary cultures. Surprisingly, using primary pancreatic cancer cells as the most suitable model system, we observed that while SP cells from five primary tumors have a slightly higher capacity for sphere formation, these cells are not enriched for CSCs as functionally determined using *in vivo* tumorigenicity assays (**Figure 6**).

Therefore, the culmination of these observations highlight that the identification of CSC subpopulations by means of traditional markers (i.e. cell surface markers and SP) can be non-specific, is highly variable between tumors, may change over time, and strongly depends on selected conditions such as the use of cell lines versus primary tumors; therefore, there still exists a need to identify other more specific CSC marker(s) whose expression is not susceptible to environmental factors and intrinsically specific to a CSC population.

A

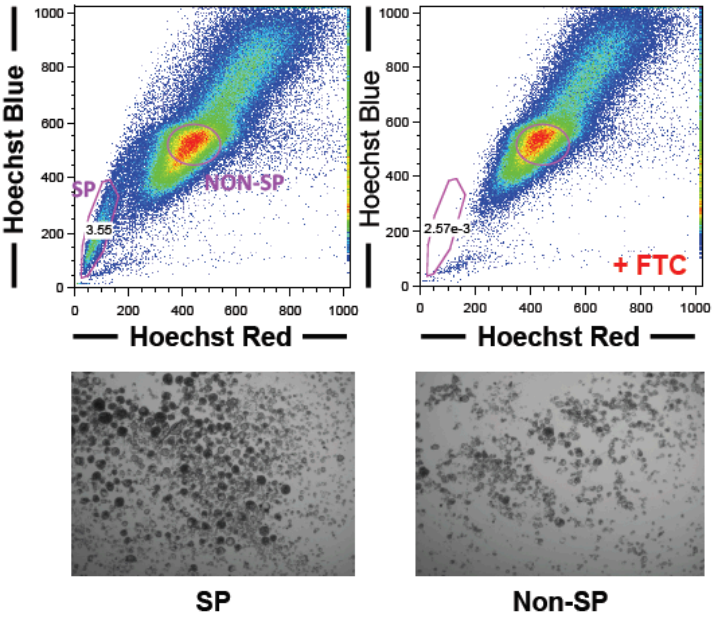

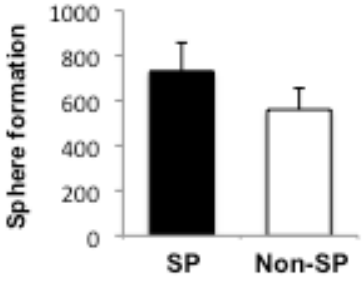

B

Tumor take after three months
(# tumors / # injections)

	10^4	10^3	10^2
SP	3/3	2/3	1/3
Non-SP	3/3	3/3	1/3

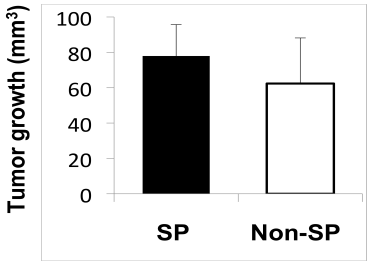

Figure 6 (A) Side population (SP) and non-side population (Non-SP) sorting strategy for primary PDAC 185 cells (un-treated or treated with FTC) (upper panel). Representative sphere formation pictures for SP and Non-SP cells (middle panel). Summary of sphere formation and tumor growth of SP-sorted cells. **(B)** *In vivo* tumorigenicity for serial dilutions of sorted cells (lower panel)

2. IDENTIFICATION OF NEW FUNCTIONAL MARKERS FOR PANCREATIC CANCER STEM CELLS

Since the aforementioned experiments highlighted sphere formation as the most powerful and reliable condition for the enrichment of CSCs from primary human pancreatic cancer cell cultures, we next studied in more detail the differences between sphere-derived cells and their adherent cell counterparts. Interestingly, during our analyses we observed a small subpopulation of autofluorescent cells with excitation and emission maximums of 490 and 532 nm, respectively, which were markedly enriched for in spheres (**Figure 7**).

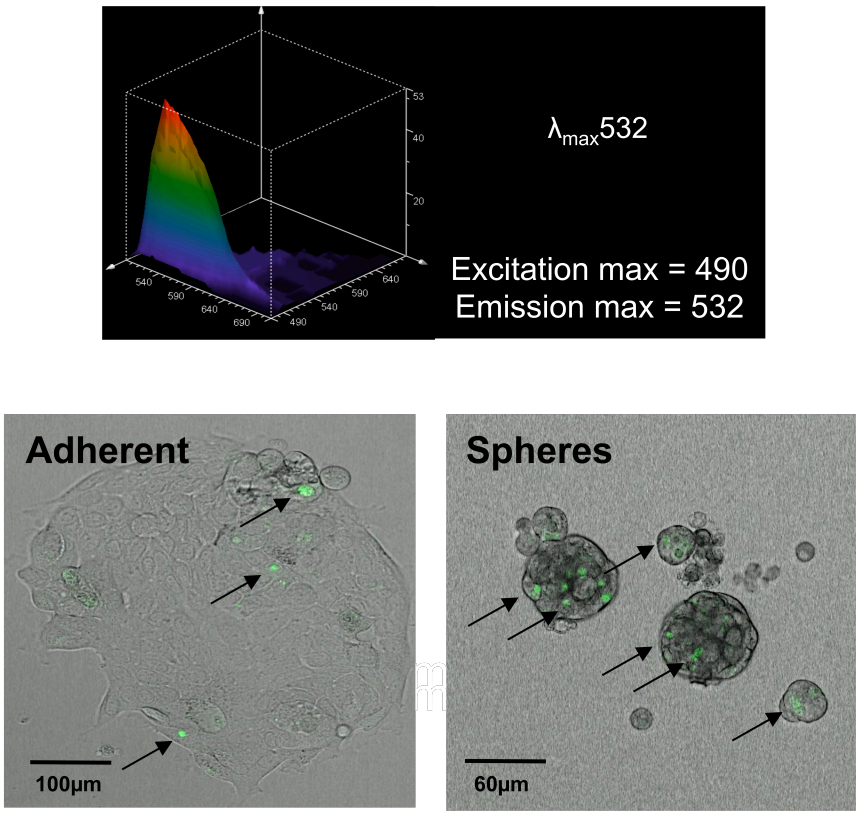

Figure 7. Spectrum of autofluorescence in primary pancreatic cancer cells (upper panel). Representative images of autofluorescent cells cultured as adherent cells or spheres (lower panel).

Moreover, autofluorescence could be tracked and quantified by flow cytometry making it a suitable marker for fluorescence-activated cell sorting (FACS) (**Figure 8**).

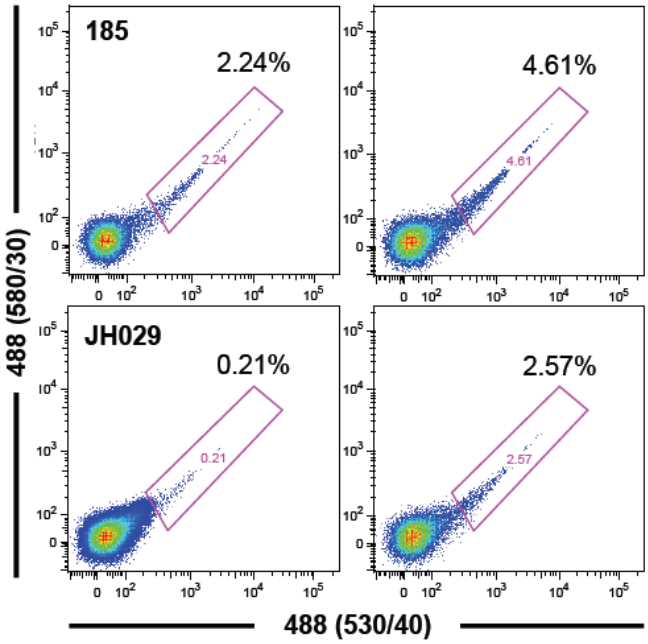

Figure 8. Flow cytometry analysis of autofluorescent content in both adherent and sphere cultures.

Importantly, this autofluorescent feature was present in a large panel of primary pancreatic cancer tumors, showed consistent, although varying enrichment in sphere conditions, and was not restricted to PDAC as it could also be detected in colorectal and hepatocellular carcinomas (HCC) (**Figure 9**).

A

Entity	Patient	Adherent	Spheres	Fold change
PDAC	185	2.24	4.61	2.15
PDAC	A6L	1.50	3.50	2.33
PDAC	286	1.46	2.61	1.7
PDAC	266	1.29	6.38	4.95
PDAC	215	0.30	0.90	3.00
PDAC	JH029	0.21	2.57	12.23
PDAC	Panc025	0.082	0.364	4.44
PDAC	B06	0.049	2.12	43.3
	Mean	0.73±0.84	2.58±2.17	9.22±14.2
CRC	CRC025	0.131	2.15	16.4
HCC	HCC-5	0.316	1.31	4.14

B

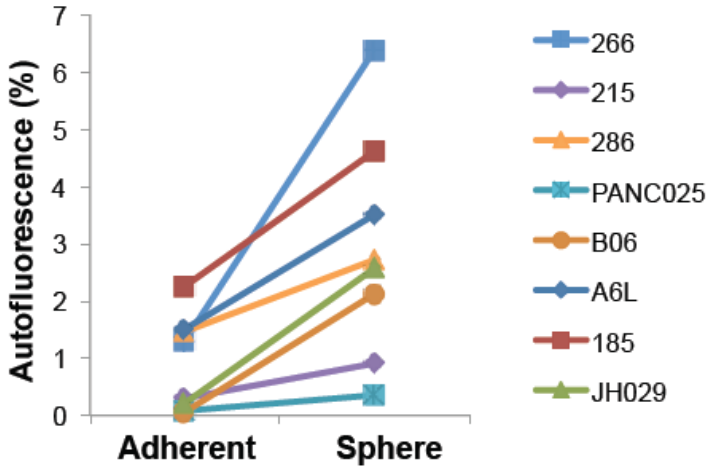

Figure 9. Autofluorescent content in adherent and sphere cultures, respectively, for different primary pancreatic and non-pancreatic tumors (upper table). Autofluorescent percentage across eight tumors cultured as adherent cells or spheres (lower panel)

Having discovered this unique autofluorescent phenotype present in a large panel of tumors, we next sought to dissect its morphological association in the cell. While the location of the autofluorescence appeared compartmentalized in some cells, we found that the autofluorescence could be equally eliminated in all regions by localized laser-induced photobleaching (**Figure 10**), indicating that 1) the autofluorescence is diffusible and rather than being crystalline in nature must be in a liquid solution and 2) the apparently separate compartments in some cells are interconnected.

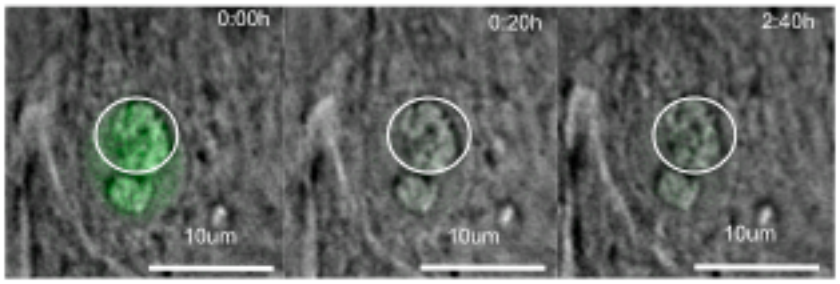

Figure 10. Sequence of images depicting fluorescence recovery after photobleaching (FRAP) in autofluorescent vesicles. Circles indicate bleached area.

Assuming that the autofluorescent was compartmentalized in an organelle-like structure we next aimed to determine if the autofluorescence was associated with other known organelles, such as lipid droplets, lysosomes or mitochondria. Interestingly, autofluorescence did not co-localize with lipid droplets or lysosomes nor was it restricted to mitochondria as demonstrated by lack of co-localization with Nile Red, LysoTracker®, and MitoTracker®, respectively (**Figure 11A**). Rather, using Cytotracker, we determined by confocal microscopy that the autofluorescence was restricted to large and distinct membrane-bound cytoplasmic organelle(s), as shown in the Z-stack image in **Figure 11B**.

A

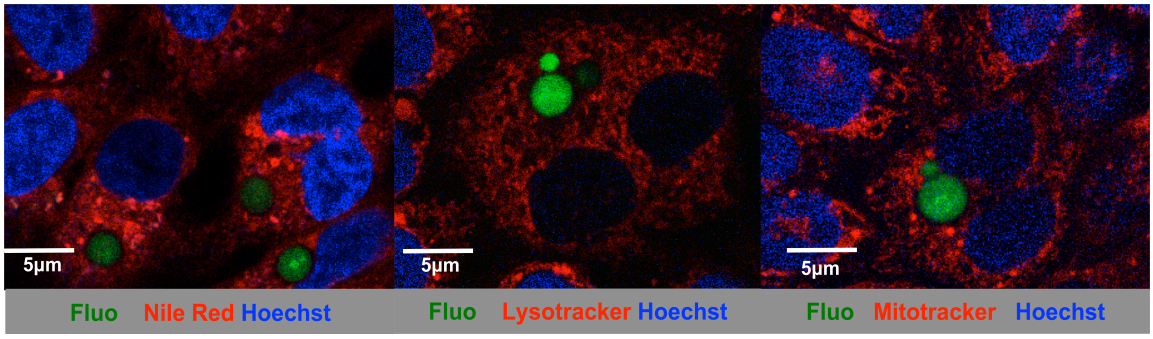

B

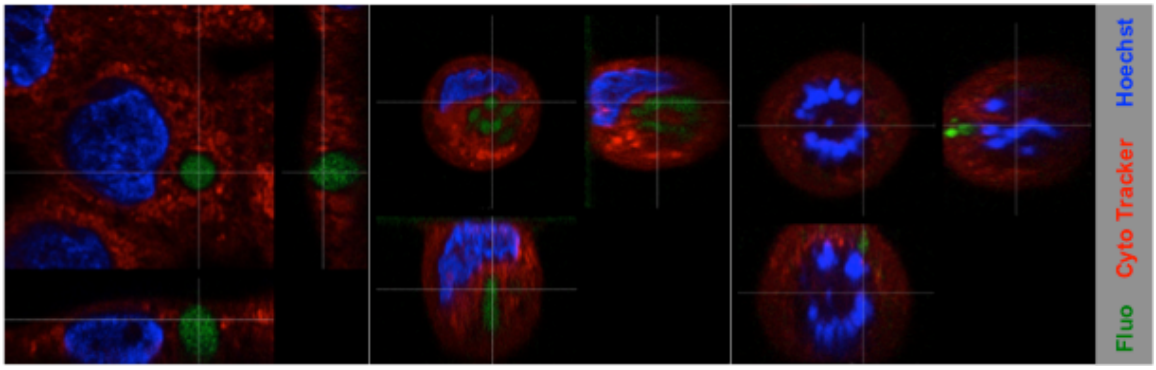

Figure 11. **(A)** Confocal images for Nile Red, LysoTracker® and MytoTracker® localization in autofluorescent cells. **(B)** Z-stack confocal images of CytoTracker®-stained cells illustrating the cytosolic localization of the autofluorescence compartment.

3. AUTOFLUORESCENT CELLS DISPLAY FUNCTIONAL FEATURES OF CANCER STEM CELLS

Having identified a unique autofluorescent sub-population of cells, we next aimed to determine whether these cells were phenotypically and functionally distinct from their autofluorescent negative counterparts, specifically whether or not these cells bear CSC features. We addressed the later by assessing the expression of established surface marker expression profile, capacity to form spheres, pluripotency-associated genes, cell division and tumorigenicity between both cell types. Interestingly, the CSC markers EpCAM, CD44, CD133 and SSEA1 were more highly expressed in autofluorescent positive cells compared to the autofluorescent negative cells, but none of the markers could completely identify the total population of the autofluorescent cells **(Figure 12)**

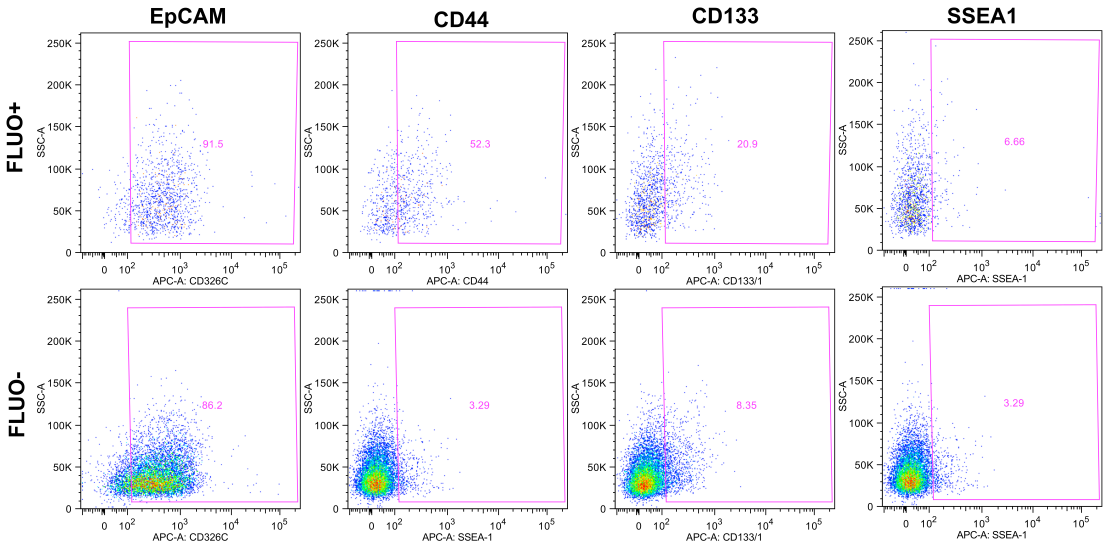

Figure 12 Flow cytometry analysis for markers EpCAM, CD44, CD133, SSEA-1 in Fluo+ and Fluo- cells.

In order to study the self-renewal, we performed serial spheres formation assays using sorted autofluorescent positive and negative cells. Our results showed that autofluorescent cells formed significantly more secondary and tertiary spheres, suggesting that these cells have an intrinsic self-renewal capacity, while the autofluorescent negative cells exhaust during multiple passages (**Figure 13**).

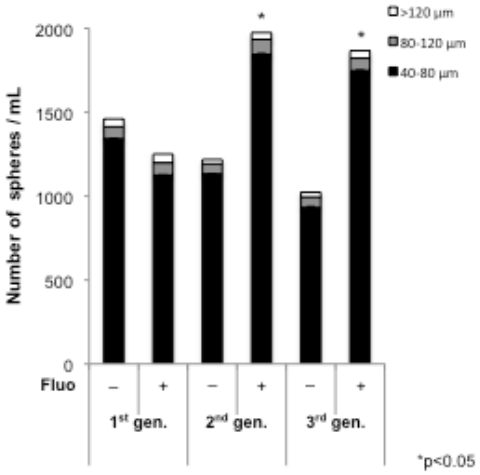

Figure 13 Sphere numbers and size (µm) for FACSorted autofluorescent positive (Fluo+) and negative (Fluo–) cells over three generations (gen)

3.1. Cancer Stem related genes

We and others have shown that like stem cells, CSCs up-regulate the expression of pluripotency-associated genes (ref). QPCR analysis for the expression of pluripotency-associated genes revealed that FACSorted autofluorescent primary PDAC cells significantly over-expressed Nanog, Klf4, Sox2, Bmi1, and Oct3/4 as compared to the non-autofluorescent population (**Figure14**). Importantly, this "stem-like" phenotype was observed for autofluorescent cells isolated from several PDAC tumors (data not shown).

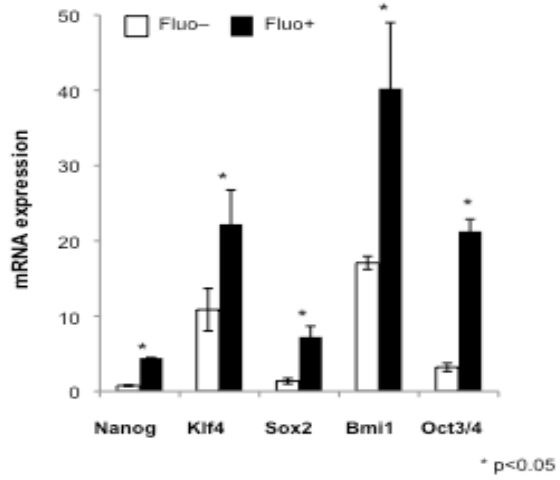

Figure 14. QPCR analysis of pluripotency-associated genes in Fluo+ and Fluo– cells. Data are normalized for ß-Actin expression

3.2. Cell division

To determine if autofluorescent negative cells could generate autofluorescent positive cells, we FACsorted primary PDAC cells for autofluorescence and followed the division of a total of 155 autofluorescent negative cells and 30 autofluorescent positive cells. The use of customized microwells allowed us to microscopically evaluate cells on a single cell level by confocal microscopy. During 72 hours of observation, non-autofluorescent cells did not give rise to autofluorescent cells irrespective if the cells underwent cell division or not. In contrast, autofluorescent cells gave rise to both autofluorescent and non-autofluorescent cells with the majority (90%) of cell divisions being asymmetric (**Figures 15**).

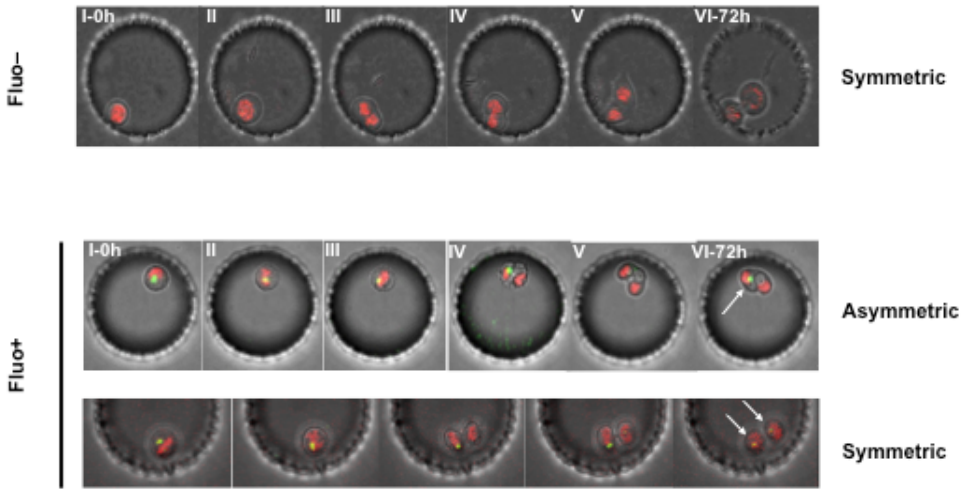

Figure 15. Representative images showing that single non-autofluorescent cells give rise to non-fluorescent cells only (upper panel). Asymmetric division of single Fluo+ cells giving rise to one Fluo+ and one Fluo– cell each (lower panel)

3.3 Tumorigenicity

The most defining feature of CSCs is their ability to form tumors *in vivo*. Using this criterion, we show that *in vivo* implantation of decreasing numbers of autofluorescent FACSorted sphere-derived PDAC revealed a clear restriction for *in vivo* tumorigenicity to autofluorescent cells (**Figure 16**).

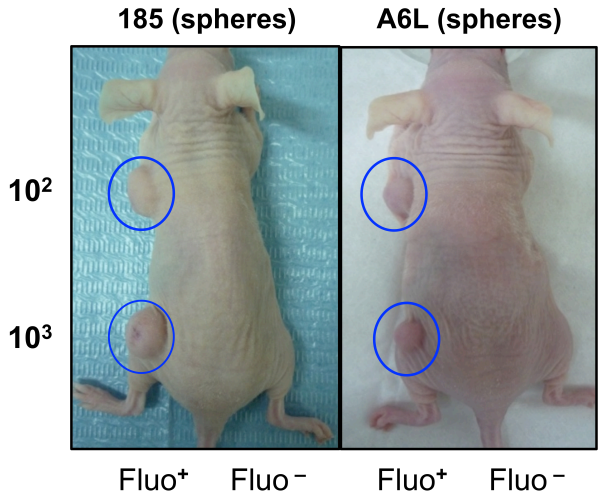

Tumor take after three months
(# tumors / # injections)

		10^3	10^2	1
A6L	Fluo–	4/5	0/5	
	Fluo+	5/5	4/5	
185	Fluo–	2/5	0/5	0/21
	Fluo+	4/5	4/5	2/21

Figure 16. Representative photos illustrating *in vivo* tumorigenicity of subcutaneously-injected FACSorted Fluo+ and Fluo– cells from 185 and A6L tumors (left panel) and summary of *in vivo* tumorigenicity (right panel).

In addition and more relevant, while we obtained no tumors in mice injected with non-fluorescent PDAC single cells, we did obtain tumors from single autofluorescent cells. Importantly, single autofluorescent cell-derived tumors recapitulated the composition of the original tumors at the level of autofluorescence, expression of cells surface markers (**Figure 17A**), and at the level of pluripotency gene expression **(Figure 17B)**.

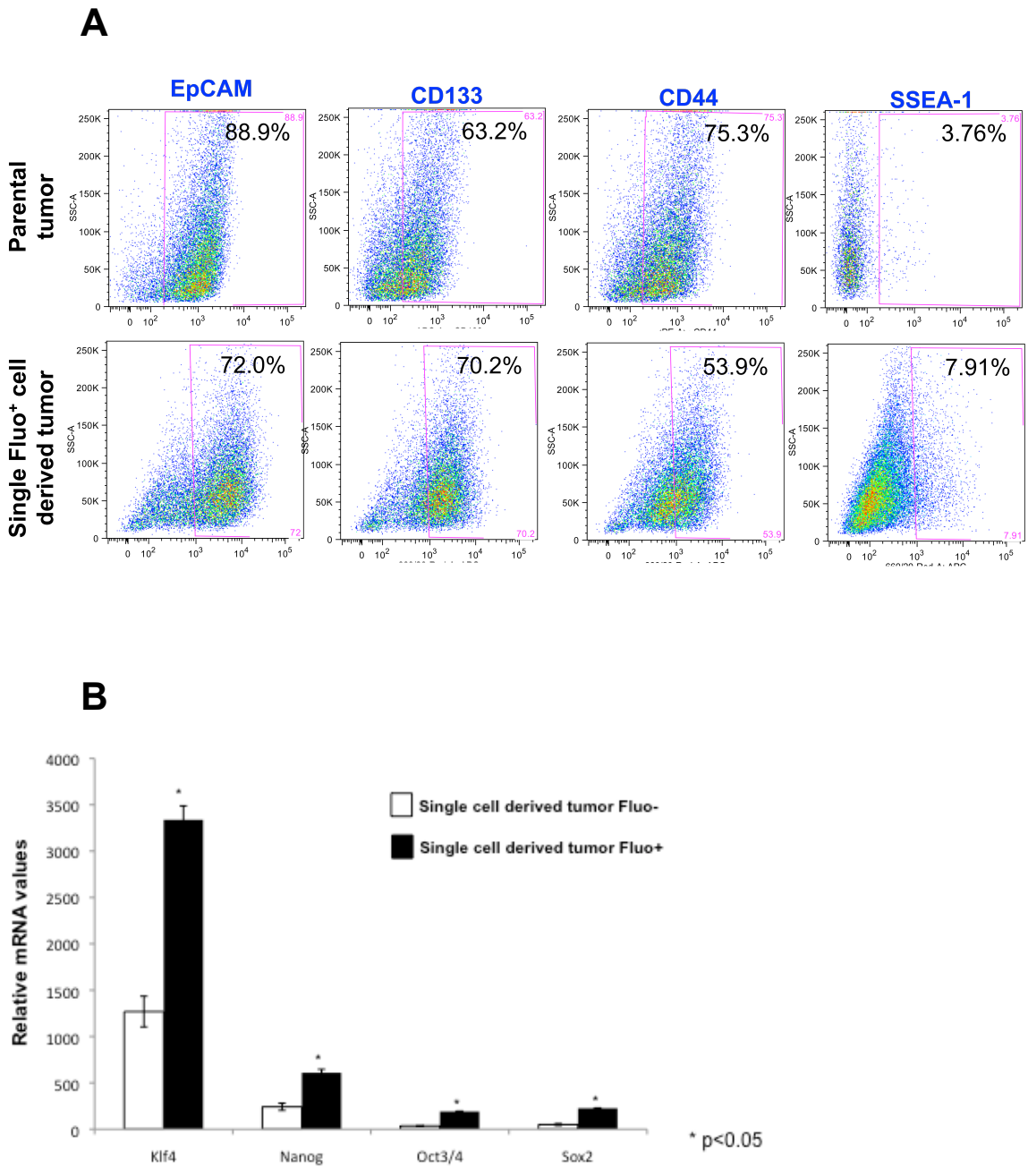

Figure 17. **(A)** Flow cytometry analysis of EpCAM+, CD133+, CD44+, and SSEA1+ cells in parental and single-cell-derived tumors. **(B)** QPCR analysis for pluripotency-associated genes in sorted Fluo+ and Fluo– cells obtained from a single cell-derived tumor. Data are normalized for ß-actin expression.

Finally, to further dissect the hierarchical and tumorigenic potential of autofluorescent cells, we performed *in vivo* tumorigenicity assays using sphere-derived cells FACSorted for both autofluorescence and the expression of the established CSC marker CD133. These analyses revealed four populations with distinct tumorigenicity. While low numbers of non-autofluorescent cells did not form any tumors irrespective of CD133 expression, tumorigenicity of autofluorescent cells could be further divided based on CD133 expression. Specifically, with low numbers of cells, autofluorescent cell tumor take was restricted to cells co-expressing CD133 (**Figure 18)**.

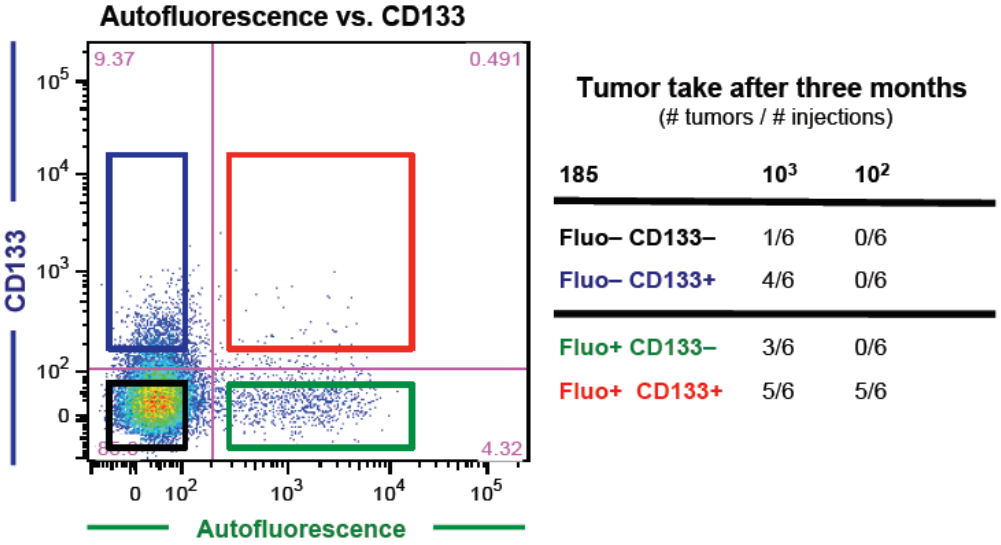

Figure 18. Gating strategy for the sorting of cells according to autofluorescence and CD133 expression (left panel) and summary of *in vivo* tumorigenicity of sorted cells (right panel)

3.4 Autofluorescent cells in other cancer types: HCC and CRC

In Table X we show that autofluorescent cells can be detected in other tumors, such as HCC and CRC, and the percentage of autofluorescent cells increases when primary cells are cultured as spheres. Since we have demonstrated the pancreatic autofluroescent cells bear stem-like features, we next investigated whether autofluorescent cells derived from other cancer types also bear the same stem-like phenotypes. As expected, QPCR analysis for the expression of pluripotency-associated genes revealed that FACSorted autofluorescent primary HCC and CRC cells significantly over-expressed Nanog, Klf4, Sox2, Bmi1, and Oct3/4 as compared to the non-autofluorescent population (**Figure 19**). Moreover, *in vivo* implantation of decreasing numbers of autofluorescent FACSorted sphere-derived HCC revealed a clear restriction for *in vivo* tumorigenicity to autofluorescent cells.

A

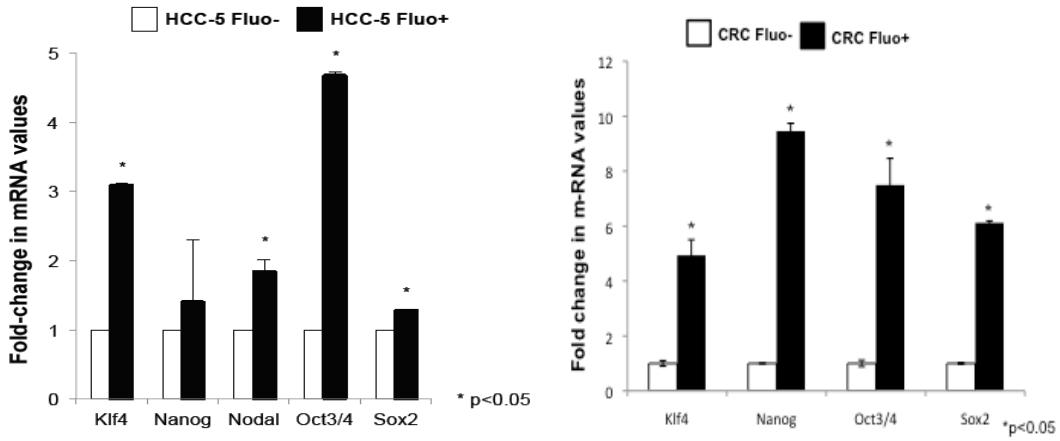

B

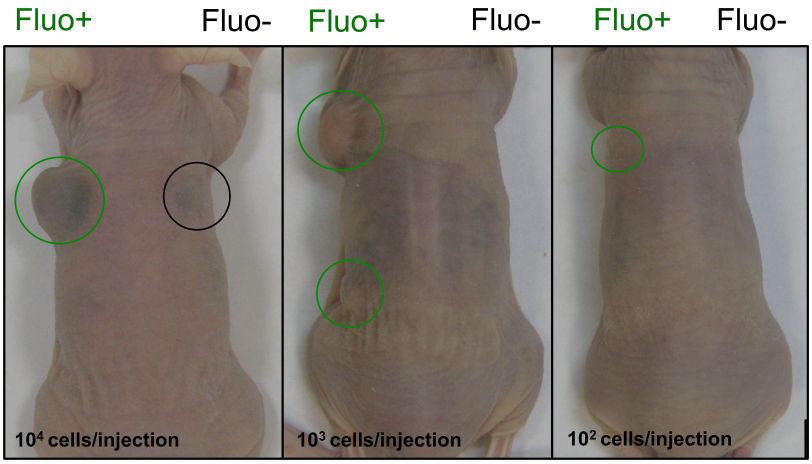

Tumor take after three months
(# tumors / # injections)

		10^4	10^3	10^2
HCC-5	**Fluo–**	1/2	0/2	0/2
	Fluo+	1/2	2/2	1/2

Figure 19. **(A)** QPCR analysis for pluripotency-associated genes in FACSorted Fluo+ and Fluo– cells derived from a primary hepatocellular carcinoma (HCC-5) (left panel) and colorectal cancer (right panel). Data are normalized for ß-actin expression. **(B)** Representative photos illustrating *in vivo* tumorigenicity of subcutaneously-injected FACSorted Fluo+ and Fluo– cells from hepatocellular carcinoma (HCC-5) (upper panel). Summary of *in vivo* tumorigenicity of the serial dilutions (lower panel)

4. AUTOFLUORESCENT CELLS ARE HIGHLY INVASIVE

Holding true to the CSC phenotype, invasion assays revealed an enhanced invasive capacity for autofluorescent cells compared to non-autofluorescent cells, even at control non-stimulatory conditions. More important, chemoattraction of invading cells by the CXCR4/7 ligand SDF-1 and the Alk4 ligand Nodal both resulted in an enhanced invasive capacity of autofluorescent cells, while non-autofluorescent cells did not show a significant increase in their invasive activity. (**Figure 20**).

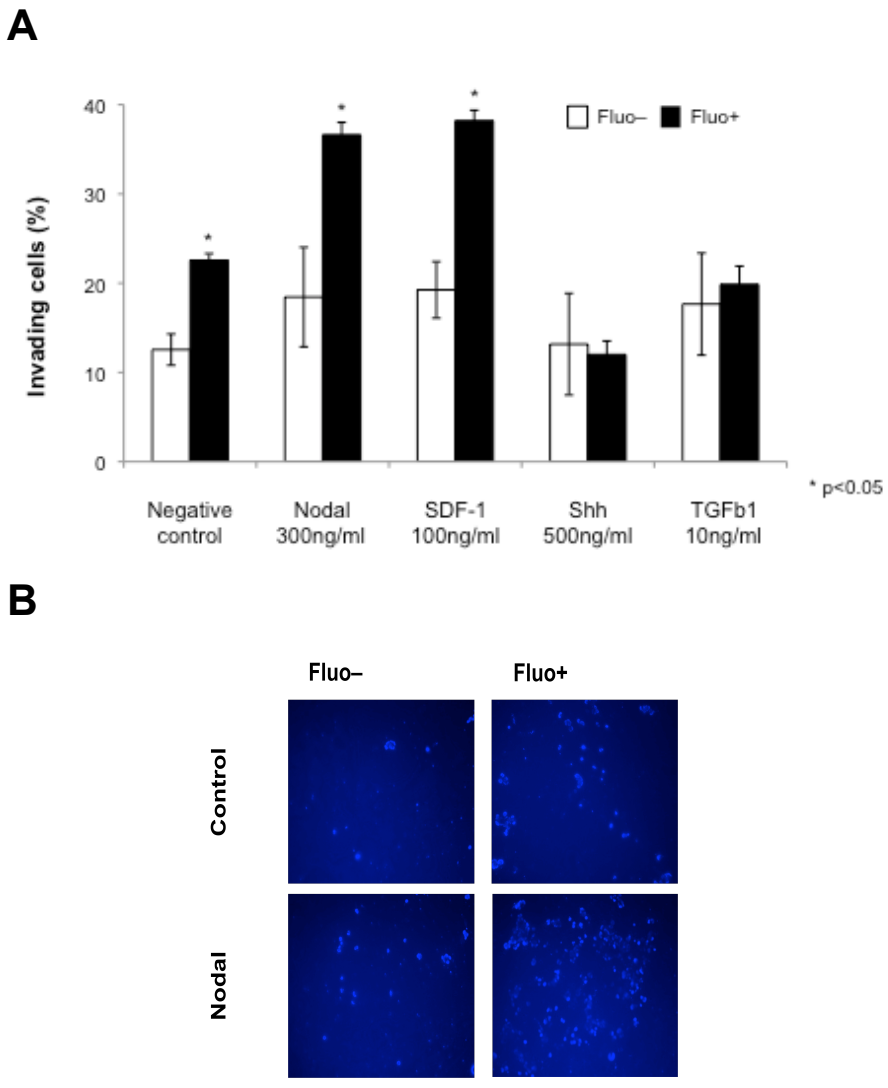

Figure 20. **(A)** Percentage of invading Fluo- and Fluo+ cells through Matrigel™ following stimulation with Nodal, SDF-1, Shh or TGFß**. (B)** Representative images of invaded cells.

Consistent with these observations, autofluorescent cells overexpressed at the RNA level Alk4 as well as their specific ligands Nodal and Activin. Flow cytometry analysis for ALK4 receptor revealed increased cell surface expression in autofluorescent positive versus negative cells. While there was no specific and detectable overexpression of CXCR4 mRNA in autofluorescent cells, CXCR7 was significantly overexpressed in these cells. More importantly, however, flow cytometry data showed over expression for CXCR4 receptor in autofluorescent positive cells, explaining in part, these cells invasive capacity towards SDF-1. **(Figure 21)**

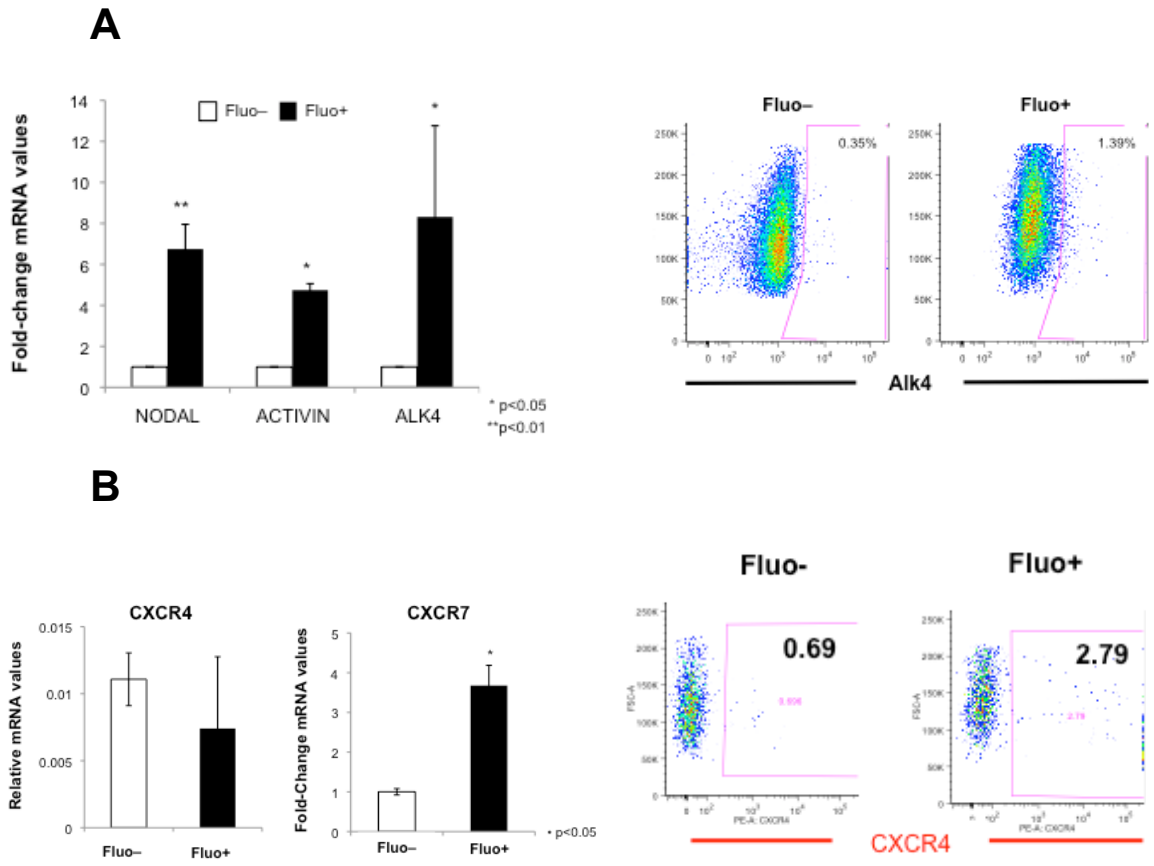

Figure 21. **(A)** QPCR analysis of Nodal, Activin, and Alk4 in sorted Fluo- and Fluo+ cells, respectively. Data are normalized for ß-actin expression (left panel). Flow cytometry analysis of Alk4 receptor expression in Fluo- and Fluo+ cells (right panel). **(B)** QPCR analysis of CXCR4 and CXCR7 in sorted Fluo- and Fluo+ cells. Data are normalized for ß-actin expression (left panel). Flow cytometry analysis of CXCR4 expression in Fluo- and Fluo+ cells (left panel).

To test the invasive capacity of autofluorescent cells in vivo, we performed intrasplenic injections with sorted cells. Intrasplenic injections of autofluorescent FACSorted cells co-expressing an H2B-mCherry reporter revealed increased and restricted cell dissemination to the liver (i.e. micro-metastases) compared to non-autofluorescent cells, as determined by RT-qPCR analysis of human GAPDH and mCherry mRNA expression in livers resected 4 months after intrasplenic injection (**Figure 22**).

A

	Splenic Tumors	Liver Micro-metastases
Fluo+	5/9	5/9
Fluo–	0/6	0/6

B

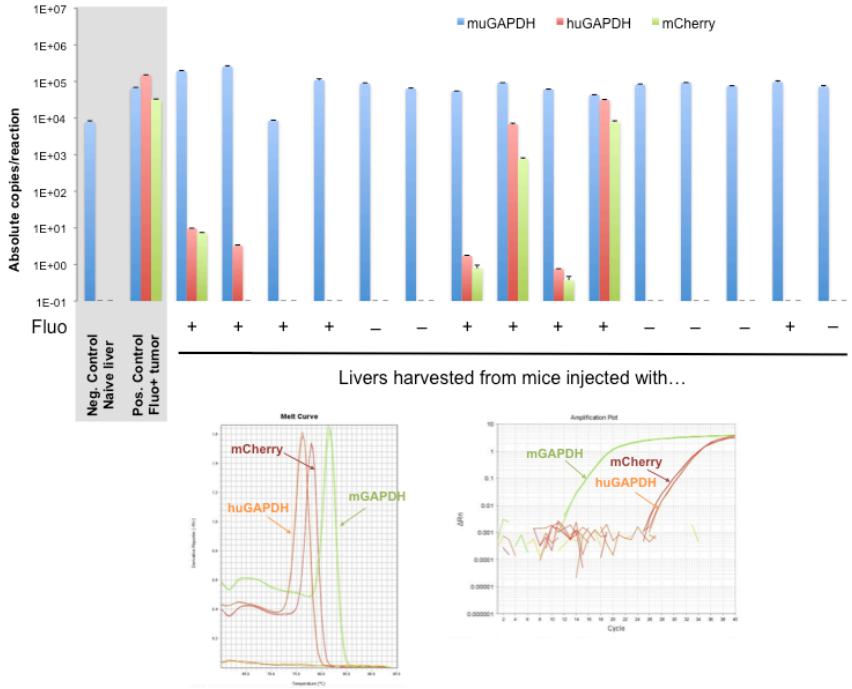

Figure 22. **(A)** Quantification of *in vivo* tumorigenicity and subsequent liver micrometastases for Fluo- and Fluo+, determined by QPCR analysis. **(B)** QPCR analysis for mGAPDH, hGAPDH, and mCherry mRNA expression in livers of NSG mice. A naïve liver served as negative control. A tumor generated from Fluo+ cells served as positive control. Data are normalized for ß-actin expression (upper panel). Representative melt curves and amplification plots for primers utilized (lower panel)

Findings were further corroborated by *ex vivo* whole tissue confocal microscopy showing mCherry+ cells and immunohistochemistry demonstrating the presence of cells positive for human-specific ALU, huCK19, and DsRed (**Figure 23**).

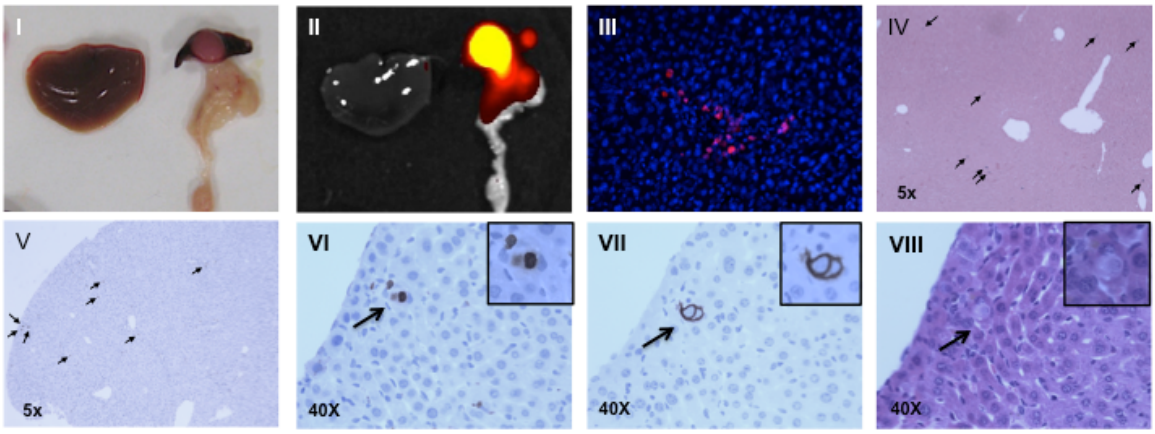

Figure 23. Representative images of pancreatic cancer cell human micrometastasis in mouse livers 4 months after intrasplenic injection of Fluo+ cells. Arrows indicate cells stained positive for indicated markers (***I***) Mouse liver, spleen, and pancreas. (***II***) IVIS for mCherry+ cells in the spleen. (***III***) *Ex vivo* whole tissue confocal image for mCherry+ cells in the liver. (***IV***) *In situ* hybridization using a human-specific ALU probe. (***V***) IHC for DsRed (***VI-VIII***) Serial sections stained for DsRed, cytokeratin19, and hematoxylin-eosin. Arrows indicate cells stained positive for indicated markers

5. AUTOFLUORESCENT PANCREATIC CANCER CELLS ARE HIGHLY RESISTANT TO STANDARD THERAPY

Based on the CSC model, CSCs are believed to be highly chemoresistant due to their inherent stem-like properties including quiescence. Indeed, treatment of primary pancreatic cancer cells with the standard chemotherapeutic agent gemcitabine or with Abraxane for five days resulted in an enrichment of autofluorescent cells (**Figure 24**).

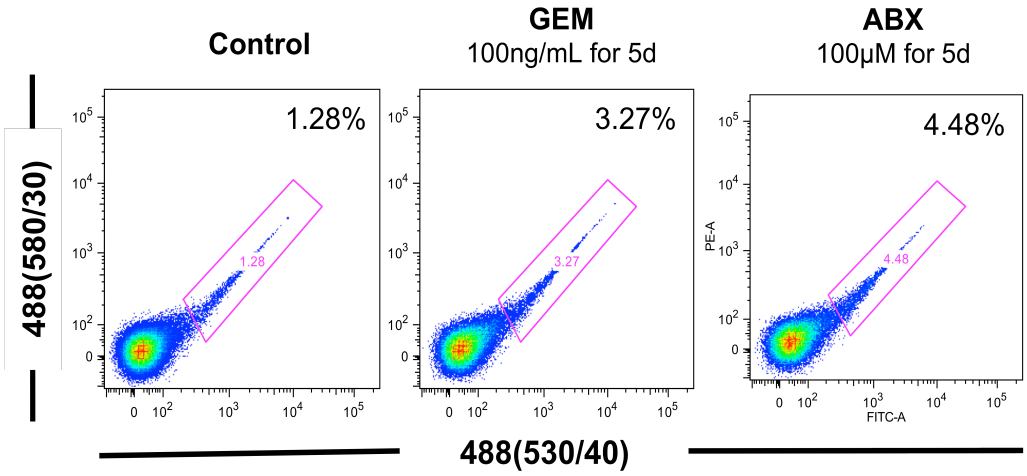

Figure 24. Flow cytometry analysis of autofluorescence in control versus gemcitabine and abraxane-treated primary PDAC cells.

When combining autofluorescence with CD133 surface expression, we noted that although CD133+Fluo- cells were more resistant to gemcitabine than CD133-Fluo- cells, autofluorescent cells, independent of CD133 expression, again represented the most resistant cell population (**Figure 25**).

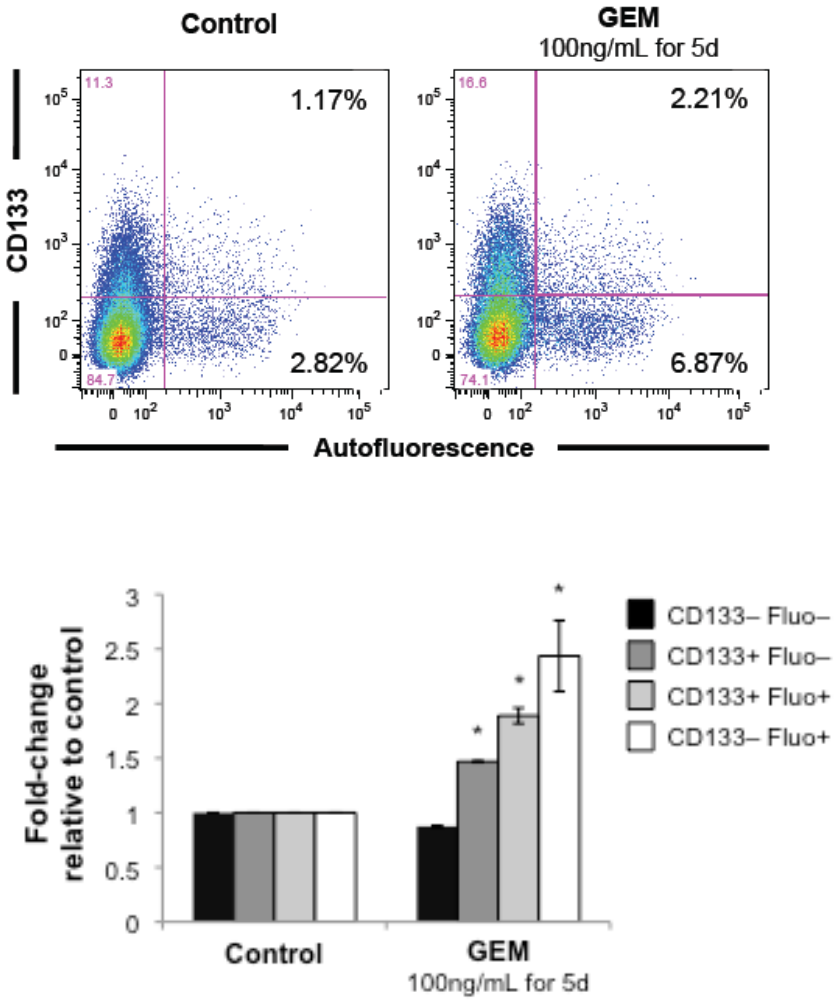

Figure 25. Representative flow cytometry plots of autofluorescence and CD133 in control cells versus cells treated with gemcitabine (upper panel) and quantification of three independent experiments (lower panel). Results are presented as fold change in the % of marker$^{+/-}$ cells in gemcitabine-treated cells compared to control-treated cells.

To further investigate this observation, longer periods of gemcitabine treatment were performed using a variety of primary cells, and while the non-autofluorescent cell population was reduced to ~40% of the total starting population after 12 days of treatment, the autofluorescent positive cells showed no reduction in absolute cell numbers, but rather a notable enrichment (**Figure 26A**). This unique CSC phenotype held true across a representative panel of seven primary tumors, in which overall chemoresistance correlated with autofluorescence (**Figure 26B**).

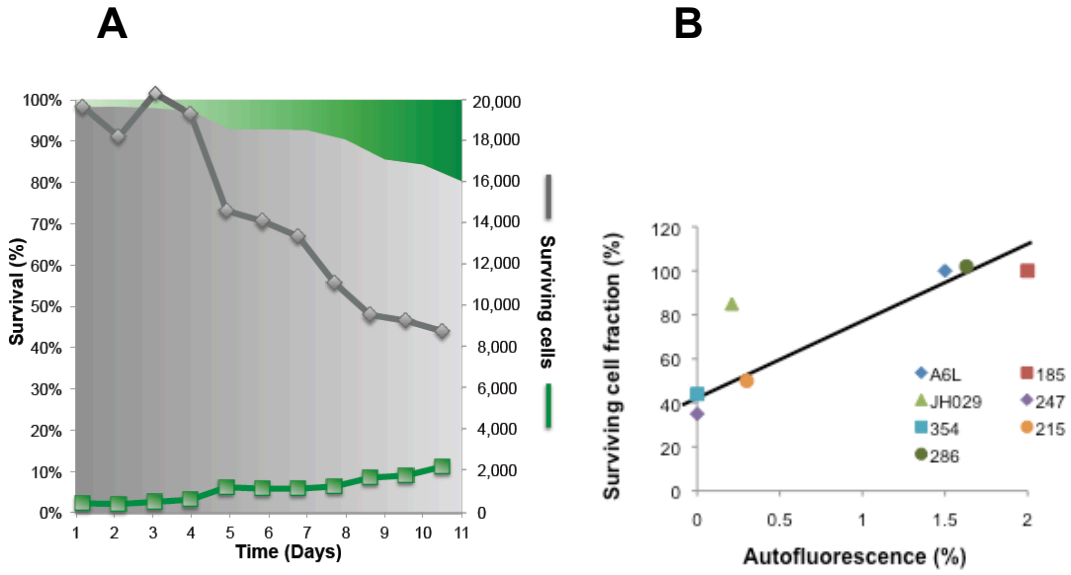

Figure 26. **(A)** Chemoresistance of autofluorescent cells during 12 days of treatment with gemcitabine. Areas indicate surviving cell fraction (%; grey=non-autofluorescent, green=autofluorescent). Lines indicate absolute number of surviving cells (grey=non-autofluorescent, green=autofluorescent). **(B)** Correlation between autofluorescence and chemoresistance for 7 primary PDAC cultures

Moreover, AnnexinV staining revealed that non-autofluorescent cells were more rapidly forced into apoptosis following 5 days of treatment with gemcitabine or abraxane as compared to autofluorescent cells (**Figure 27**).

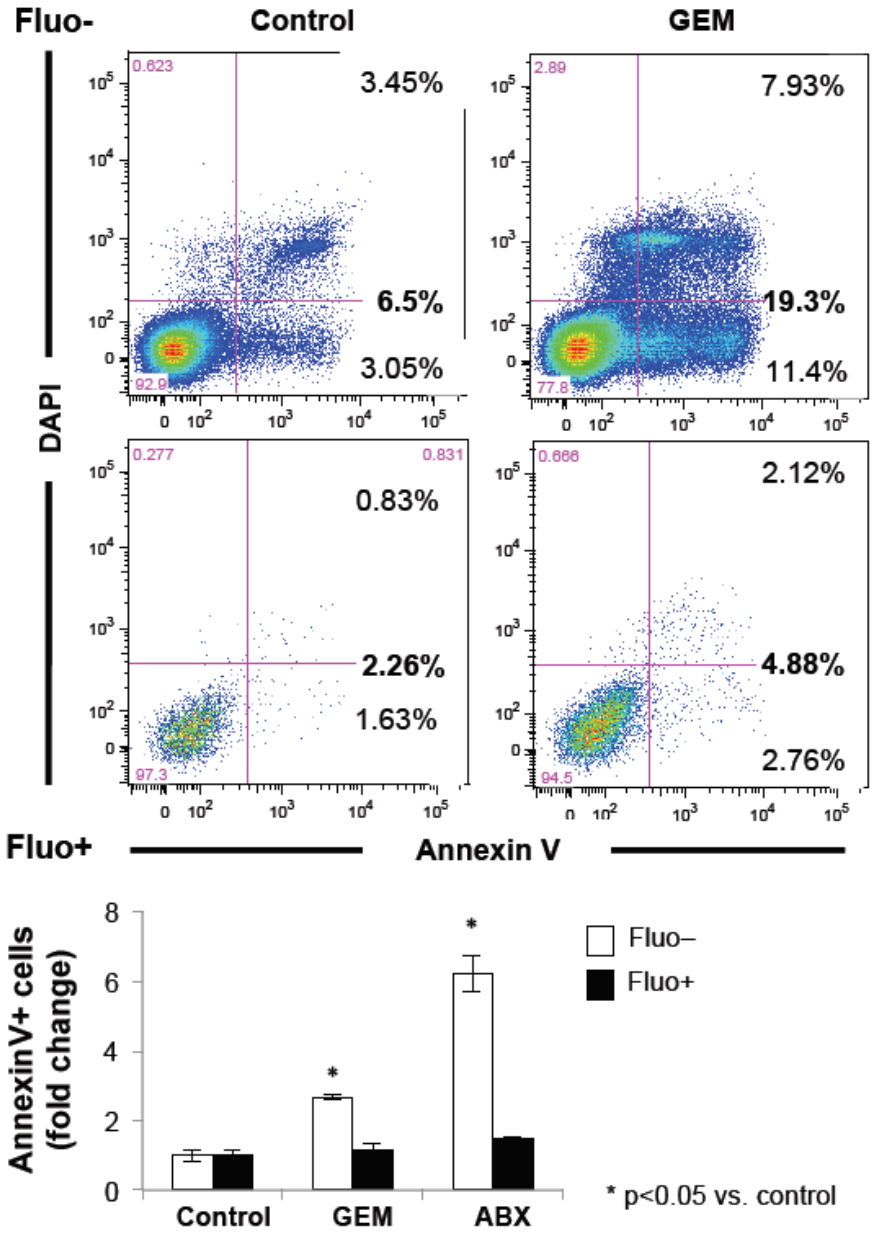

Figure 27. Flow cytometry analysis of AnnexinV staining in gemcitabine-treated cells compared to control-treated cells as a function of autofluorescent (upper panel). Quantification of three independent experiments for cells treated with gemcitabine and abraxane (lower panel).

To dissect the inherent chemoresistance of the autofluorescent cells, we first assessed quiescence by using the lipophilic fluorescent dye PKH26, which labels relatively quiescent cells (Cicalese et al., 2009). We observed significantly more PKH26 label retaining autofluorescent cells indicating that these cells are more quiescent. To rule out that the observed quiescence is an in vitro phenotype, we sorted autofluorescent positive and negative cells from freshly digested tumors to study the cell cycle state (i.e. G0 population) as a measure of quiescence. Our results showed a significant enrichment in the G0 population in autofluorescent positive cells (12.7%) isolated from fresh tumors compared to the negative population (5.15%), supporting our in vitro data and confirming that these cells are more quiescent (**Figure 28).**

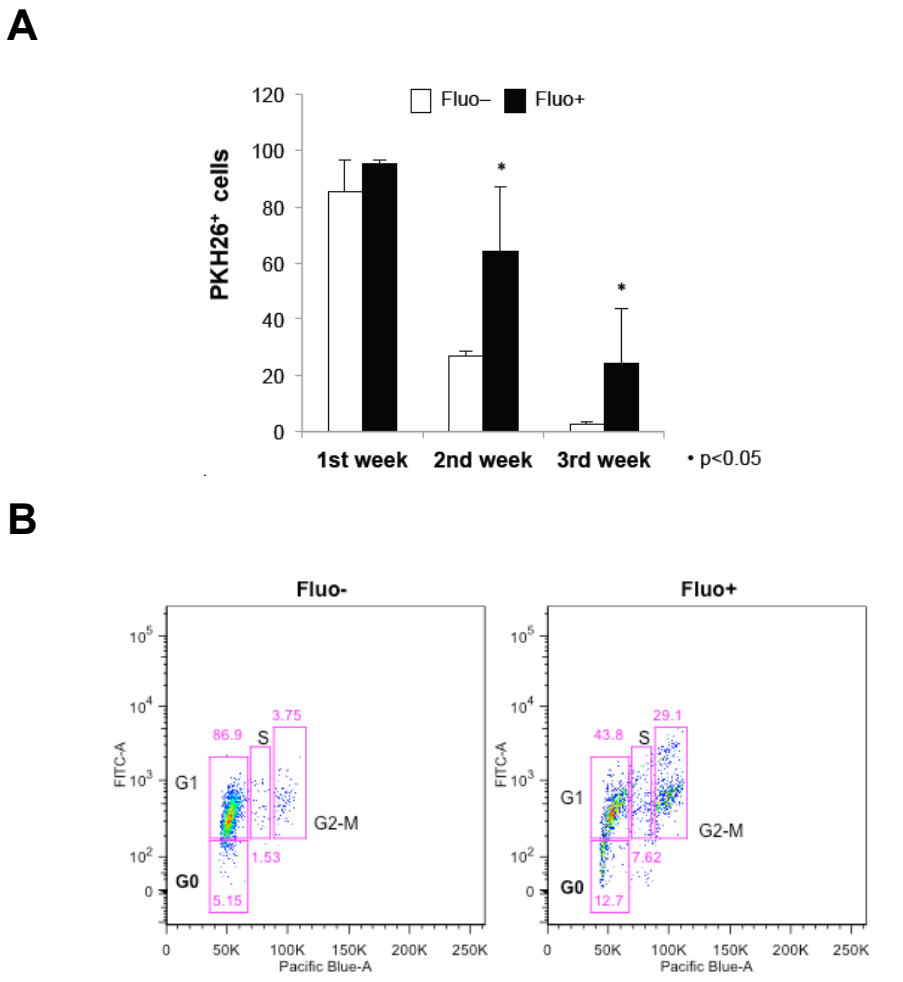

Figure 28. **(A)** Loss of PKH26 labeling in Fluo+ and Fluo– cells during 3 weeks of culture. **(B)** Flow cytometry analysis for G0 population *in vivo* sorted Fluo+ and Fluo- cells

Since chemoresistance is a dynamic process and can be explained by multiple mechanisms, we next studied the expression levels of both the human concentrative nucleoside transporter (hCNT) and human equilibrative nucleoside transporter (hENT), as gemcitabine uptake depends on both of these transporters and expression levels predict response to gemcitabine (Santini et al., 2010). QPCR analysis for hCNT1, hCNT3, hENT1, and hENT2 showed significantly lower expression in autofluorescent cells versus the non-autofluorescent population **(Figure 29)**, demonstrating that in addition to quiescence, autofluorescent cells express lower levels of the transporters necessary for gemcitabine influx.

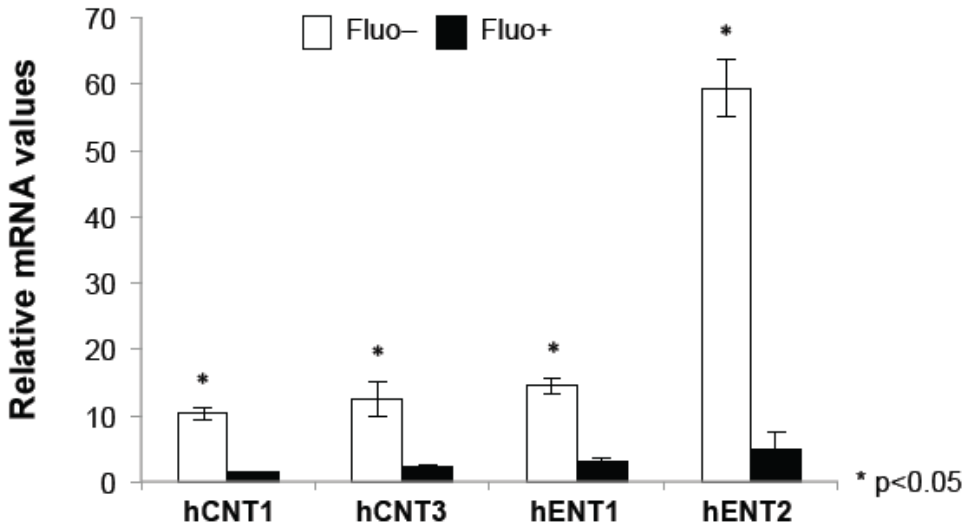

Figure 29. QPCR analysis of human concentrative nucleoside transporter (hCNT) 1 and 3 and human equilibrative nucleoside transporter (hENT) 1 and 2 in sorted Fluo+ and Fluo– cells. Data are normalized for ß-actin expression and representative of 3 independent experiments.

6. MECHANISM AND SOURCE OF THE AUTOFLUORESCENCE

6.1. Mechanism

We next explored the mechanism and the origin of the autofluorescence. We hypothesized that autofluorescence was an active transporter-dependent process. Since autofluorescent cells have more intracellular ATP (**Figure 30A**) and inhibition of ATP production by different means resulted in reproducible, but reversible loss of autofluorescence, we reasoned that the subcellular autofluorescent compartment is driven by ATP-dependent transporters. Specifically, depletion of the cellular ATP pools by uncoupling oxidative phosphorylation using 2,4-Dinitrophenol (DNP), by blocking the proton channels of the ATP synthase using the macrolid antibiotic oligomycin, and by interfering with the electron transport chain using rotenone all prevented the intravesicular accumulation of autofluorescence. Likewise, restoration of cellular energy resources by withdrawal of the inhibitors restored intravesicular autofluorescence. These findings are not only consistent with the tight coupling of ABCG2 drug transport to ATP hydrolysis but strongly point towards an ABCG2-mediated intravesicular drug accumulation mechanism driving autofluorescence (**Figure 30B and Figure 30C**),

A **B**

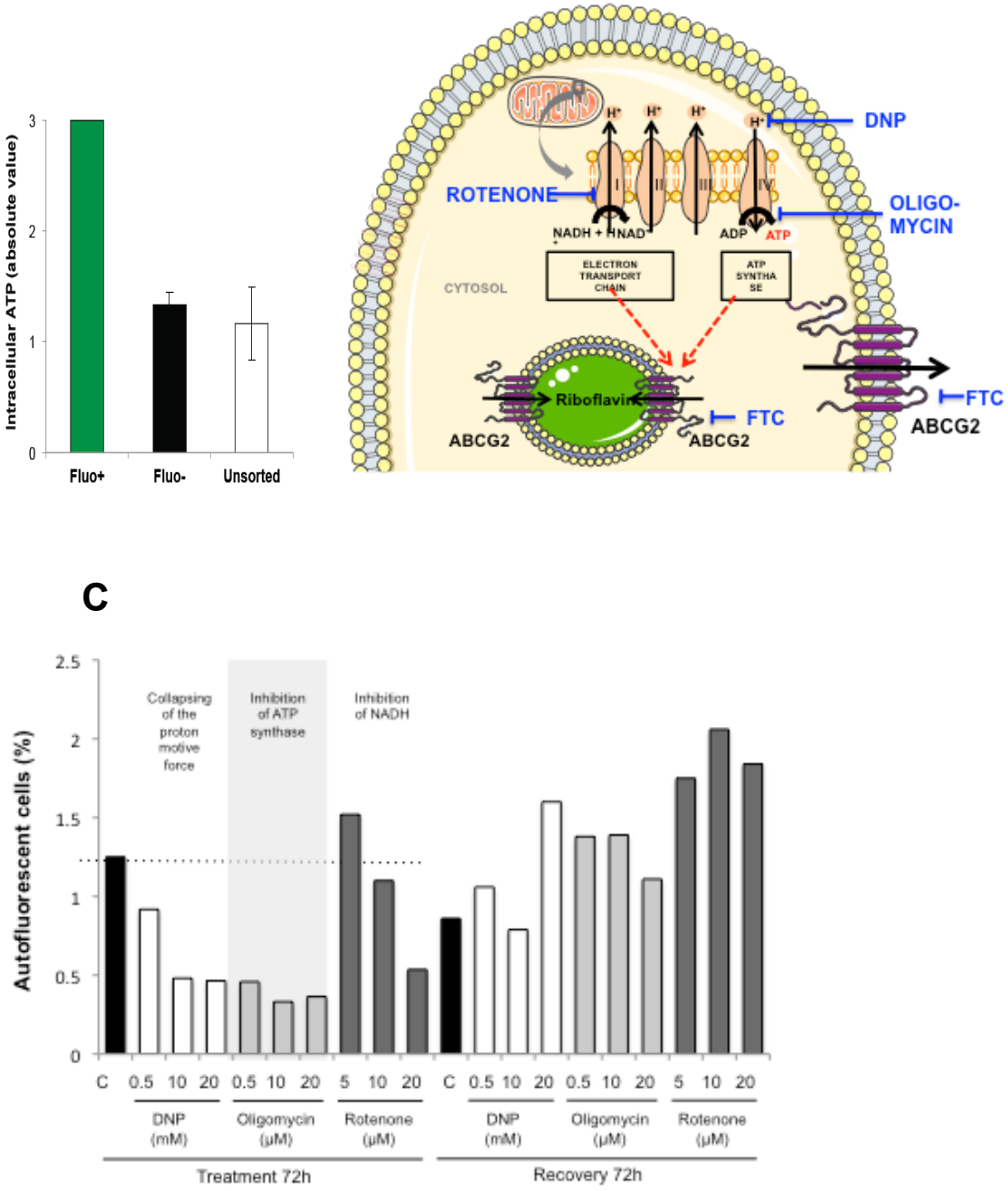

Figure 30. **(A)** Intracellular ATP content in sorted Fluo+ and Fluo– cells versus unsorted cells. **(B)** Illustration representing different mechanism of inhibition of autofluorescence: 2,4-Dinitrophenol (DNP): depletion of the cellular ATP pools by uncoupling oxidative phosphorylation; Oligomycin: macrolid antibiotic that blocks the proton channels of the ATP synthase; Rotenone: interferes with the electron transport chain. **(C)** Graph representing autofluorescent content after treatment and withdrawal of different ATP inhibitors (right panel).

Consistent with this hypothesis, autofluorescent cells overexpressed ABCG2 both at the mRNA and protein level (**Figure 31A and Figure 31B**), whereas other ATP transporters were not differentially expressed. Blocking the ABCG2 transporter with the ABCG2 inhibitor fumitremorgin C (FTC) reversibly abrogated the accumulation of autofluorescence (**Figure 31C**).

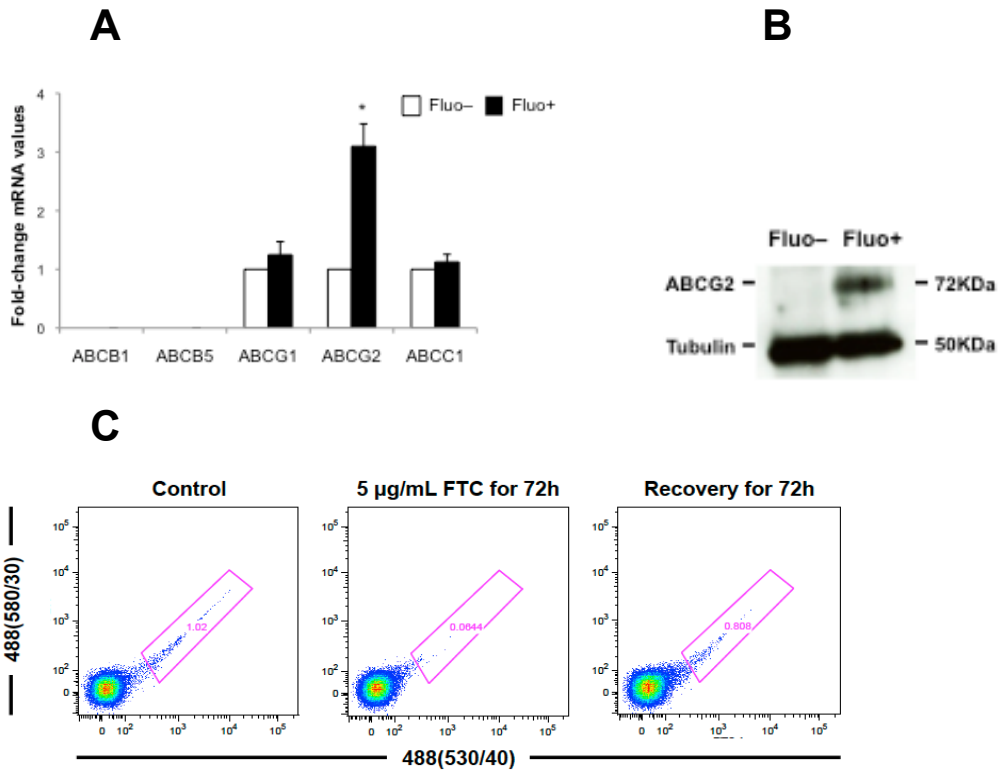

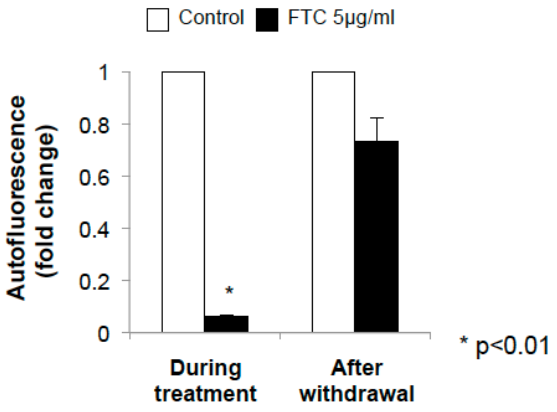

Figure 31. **(A)** QPCR analysis of ABC transporter family members in sorted Fluo+ and Fluo– cells. mRNA for ABCB1 and 5 was undetectable. Data are normalized for ß-actin expression. **(B)** Western Blot for ABCG2 transporter in sorted Fluo+ and Fluo– cells. **(C)** Flow cytometry analysis of autofluorescent content in cell during and after FTC treatment (upper panel). Quantification of three independent experiments (lower panel).

Interestingly, when primary PDAC cultures were infected with a vector expressing an ABCG2-mcherry fusion protein, we could observe that the expression of this transporter was co-localized to the membrane of the autofluorescent vesicle. Moreover, we found that the fluorescent type II topoisomerase inhibitor mitoxantrone, which is specifically expelled by the ABCG2 transporter (Bell, 1988), co-localized with the autofluorescent subcellular compartment, further confirming the expression of ABCG2 transporters in membranes of autofluorescent vesicles (**Figure 32B**). These findings are not only consistent with the tight coupling of ABCG2 drug transport to ATP hydrolysis but strongly point towards an ABCG2-mediated mechanism driving autofluorescence.

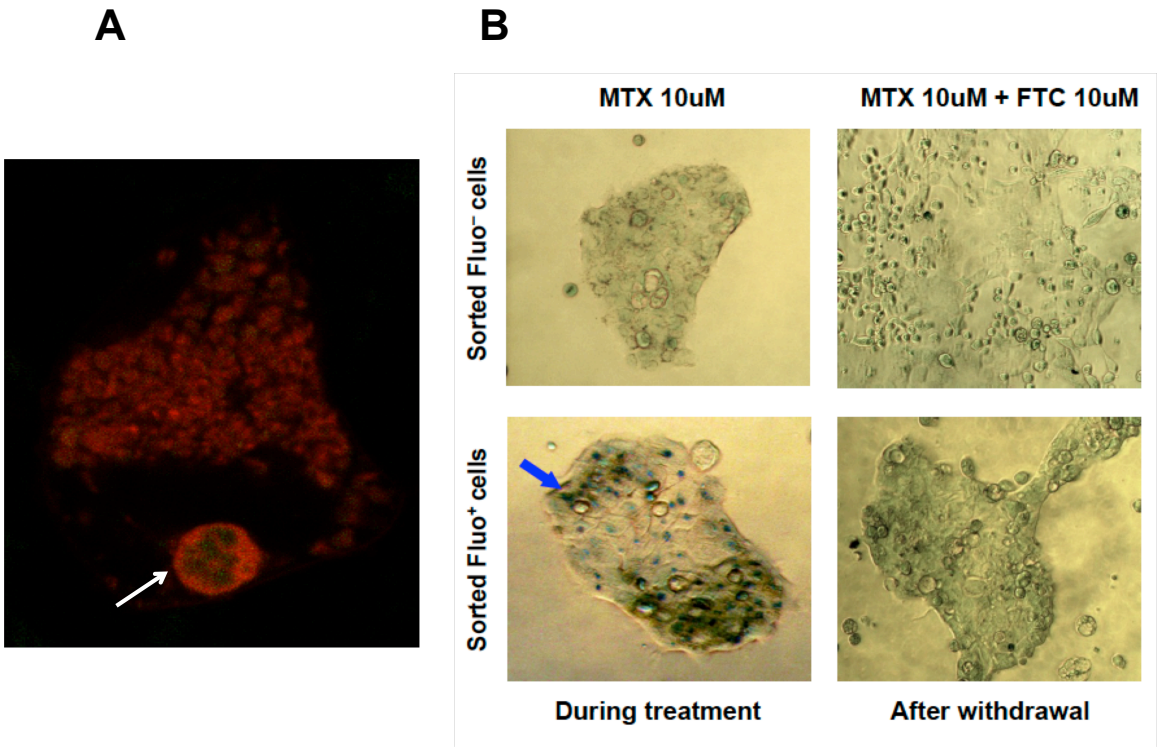

Figure 32. **(A)** Confocal image of ABCG2-mcherry plasmid transfected in a autofluorescent cell. Arrow indicates autofluorescent vesicle surrounded by ABCG2-mherry expression on the membrane. **(B)** Mitoxantrone accumulation in cytoplasmic vesicles in sorted Fluo+ and Fluo– cells, in the presence or absence of 10µM FTC

Importantly, since overexpression of ABCG2 is a defining feature of SP cells, we investigated the distribution of autofluorescent cells between SP and non-SP cells. Interestingly, autofluorescent cells were more prominent in the non-SP, indicating that autofluorescent cells are a distinct ABCG2-expressing subpopulation of cells that are phenotypically different than SP cells (**Figure 33**), which is consistent with our finding that SP-sorted cells were not enriched for tumorigenic cells (**Figure 6**).

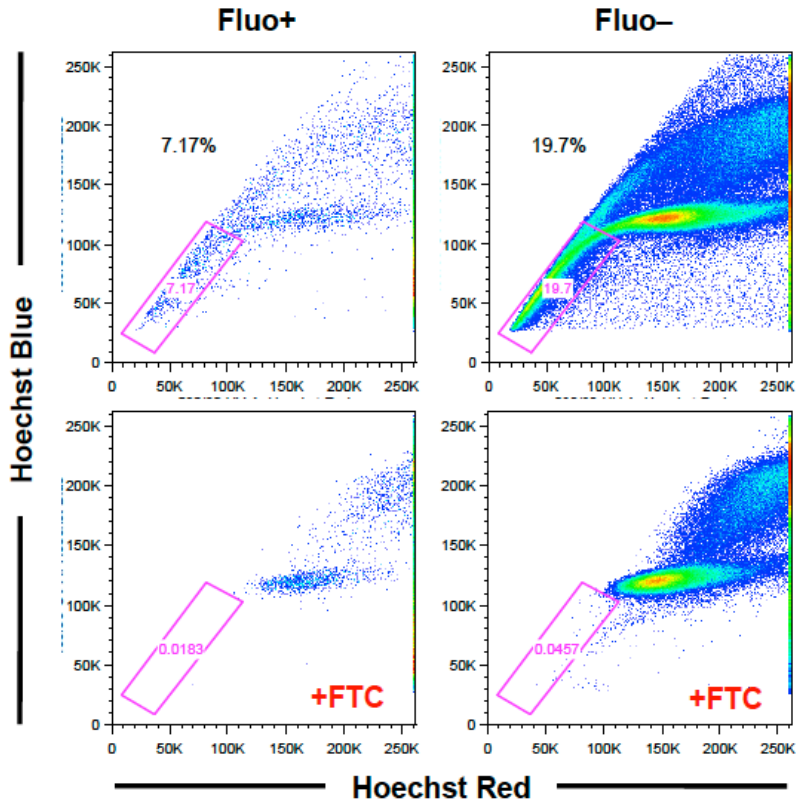

Figure 33. Side population analysis of sorted Fluo+ and Fluo– cells. ABCG2 was specifically inhibited by FTC.

Since our data demonstrate that autofluorescence is mediated by the expression of ABCG2 transporters in the membrane of the intracellular autofluorescent vesicles, we next studied whether the inhibition of ABCG2 transporters, by the specific inhibitor FTC, in the autofluorescent positive cells or the overexpression of ABCG2 in the autofluorescent negative cells would have an effect on the stem-like properties of these two cell populations. Using the expression of pluripotency-associated genes as a readout for "stemness", we show that the stemness capacity of the autofluorescent cells was not affected by FTC treatment, which resulted in complete loss of autofluorescemce. These cells maintained expression of KLF4, Nanog, Oct3/4 and Sox2, indicating that their "stemness" was not directly mediated by the ABCG2 transporters **(Figure 34A)**. Likewise, the overexpression of ABCG2 transporters in autofluorescent negative cells had no effect on the expression of stemeness genes nor did a de novo population of autofluorescence cells arise from the autofluorescent negative population following overexpression of ABCG2 and the overexpression of ABCG2 transporters in autofluorescent negative cells had any effect neither stemeness genes nor in the autofluorescence **(Figure 34B)**

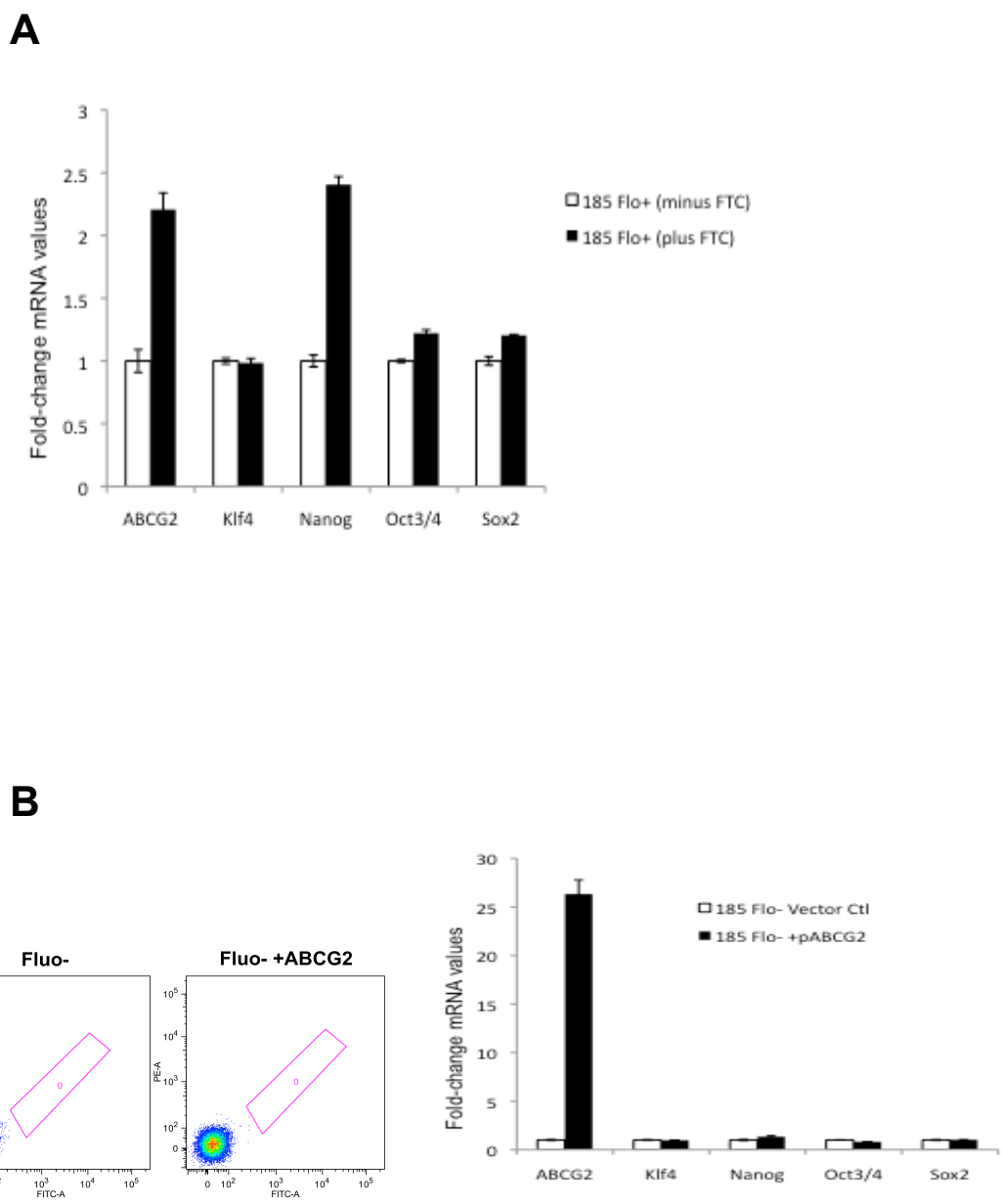

Figure 34. (A) QPCR analysis for stemnes genes in sorted Fluo+ treated with FTC. (B) Flow cytometry analysis for sorted Fluo- transfected with ABCG2 plasmid (left panel). QPCR analysis for stemenes genes in Fluo- cells.

6.2. Source

We next investigated the source of the cellular autofluorescence. Autophagy has been related to autofluorescence (White, 2012), but neither expression levels of the autophagy related-protein LC3 or autophagy-related gene ATG12 (**Figure 35A**) nor inhibition of autophagy by E64D combined with pepspatin-A or with the activator rapamycin supported this notion (**Figure 35B**).

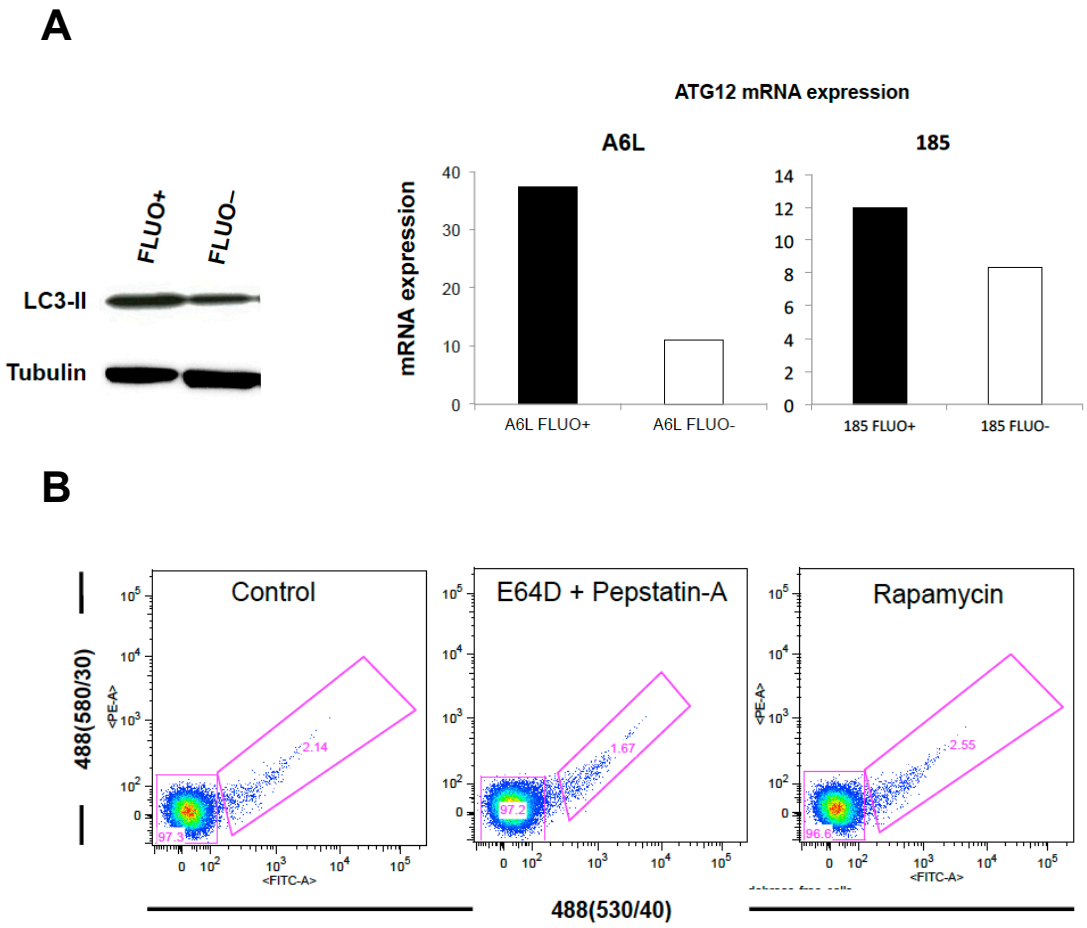

Figure 35. Side population analysis of sorted Fluo+ and Fluo– cells. ABCG2 was specifically inhibited by FTC

Therefore we reasoned that an ABCG2-transported substrate in the culture medium might be responsible for autofluorescence. Indeed culturing primary cancer cells in basal media (vitamin-free) resulted in complete loss of autofluorescence within 72 hours (**Figure 36**; media composition listed on **Table M&M1**). Importantly, while basal-media alone could not restore autofluorescence following short-term FTC treatment, basal media supplemented with a cocktail of essential vitamins quickly restored autofluorescence (**Figure 36**). Based on the spectroscopic profile (490/532nm) of the inherent cellular autofluorescence, we selected retinol (330/500nm) and riboflavin (450/520nm) as the most likely candidates as both have overlapping spectroscopic profiles, and it has been previously shown that ABCG2 is a specific transporter of riboflavin (Vitamin B2) (van Herwaarden et al., 2007). Indeed, basal media supplemented with numerous vitamins revealed that only riboflavin was capable of restoring autofluorescence (**Figure 37A and B**).

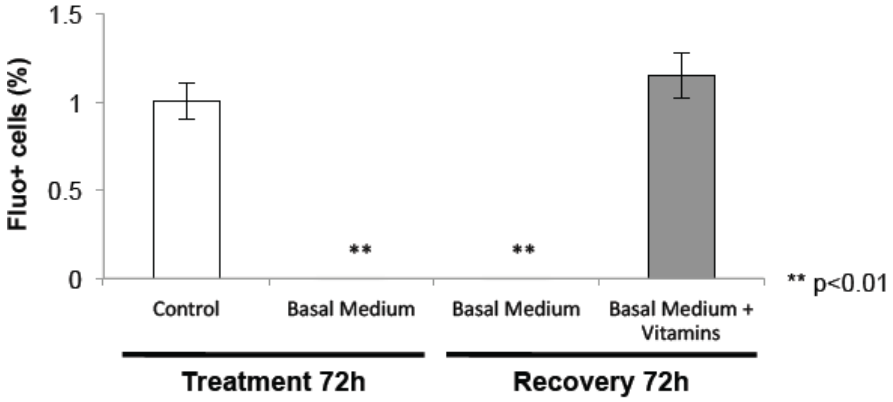

Figure 36 Loss of autofluorescence following culture of primary PDAC cells in basal medium (without vitamins), and recovery of autofluorescence 72h after continued culture in basal media or basal medium plus vitamin cocktail

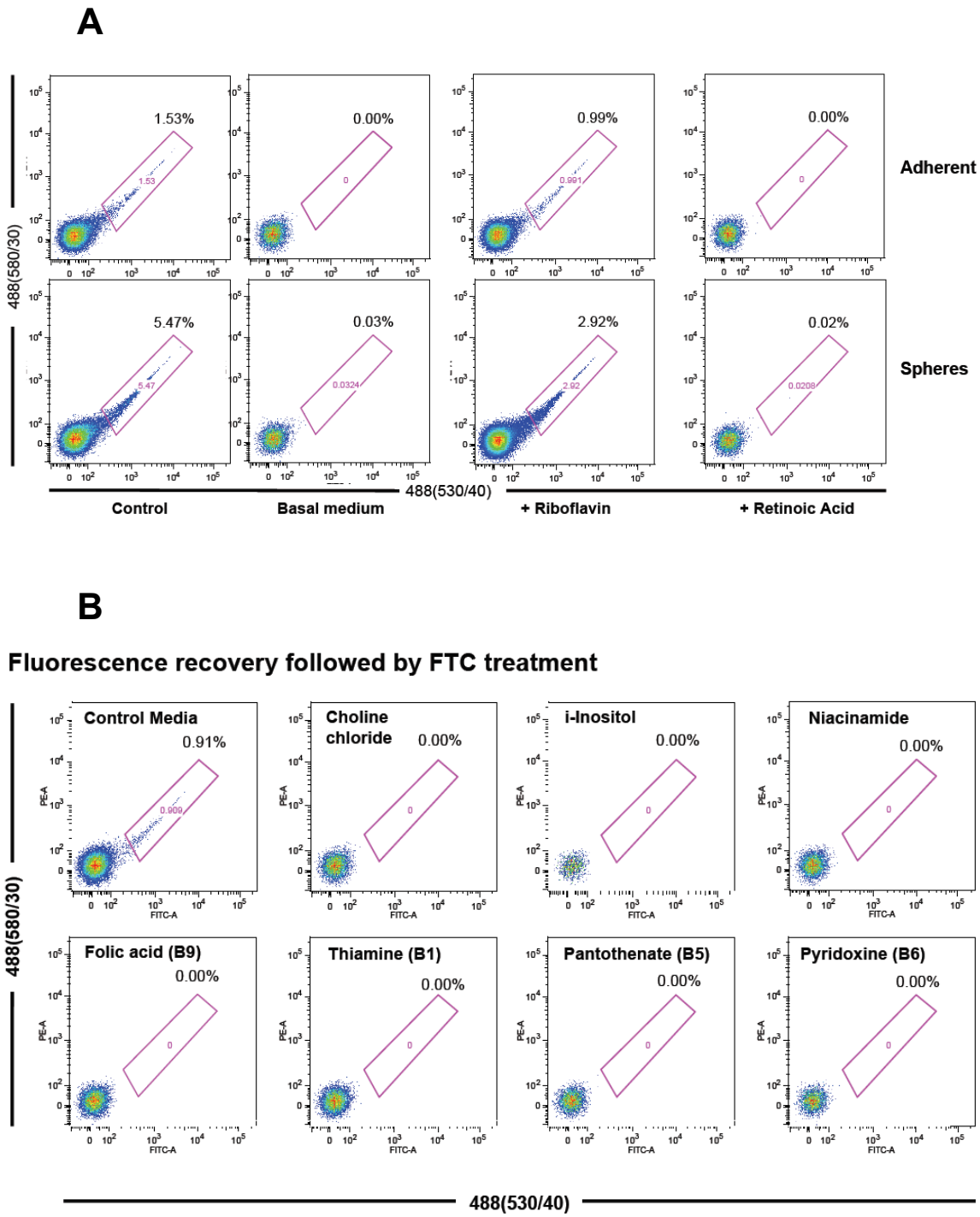

Figure 37. **(A)** Flow cytometry analysis of autofluorescence recovery in adherent cells or spheres after FTC treatment in basal medium or basal medium supplemented with riboflavin or retinoic acid (each at 1μM). **(B)** Flow cytometry analysis for the recovery of autofluorescence following the addition of different vitamins after FTC treatment.

In addition, we found a strong association between the percentage of autofluorescence and riboflavin concentration in the medium, which plateaued at 30µM (**Figure 38A**). Importantly, the enhanced number of autofluorescent cells was not related to unspecific enrichment of non-CSC as riboflavin-enriched autofluorescent FACSorted cells maintained high expression of pluripotency-associated genes (**Figure 38B**).

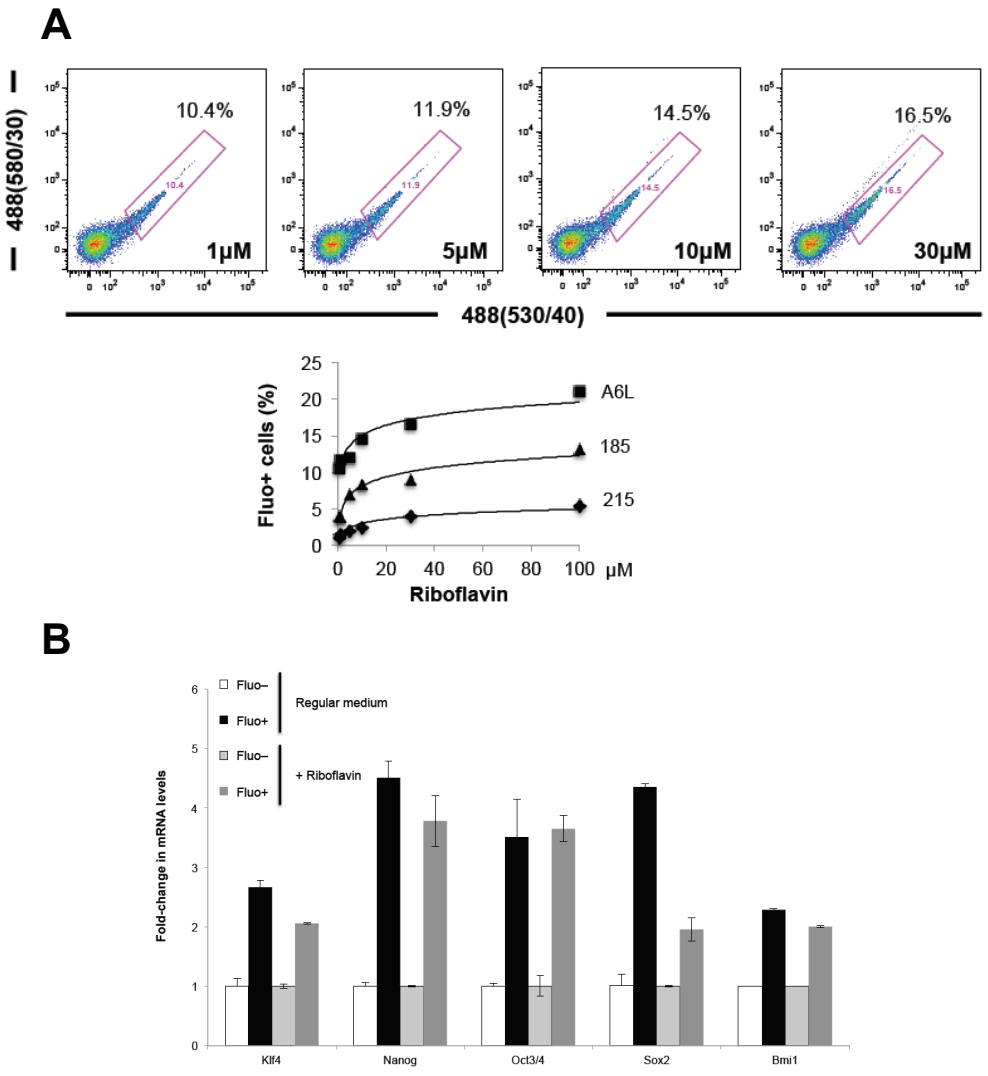

Figure 38. **(A)** Representative flow cytometry of cells exposed to increasing concentrations of riboflavin (upper panels). Increasing concentrations of riboflavin for three different primary PDAC (lower panel). **(B)** QPCR analysis for pluripotency-associated genes in sorted Fluo+ and Fluo– cells untreated or pretreated with 30µM Riboflavin for 24h. Data are normalized for ß-actin expression.

Lastly, using riboflavin we were also able to identify, isolate and validate by RT-qPCR analysis of pluripotency gene expression, autofluorescent cell populations in primary PDAC cultures (Panc025 and B023) where autofluorescence was normally low to undetectable. This was not the case for established cell lines such as Panc01 and MiaPaca2, which did not display autofluorescence under normal culture conditions nor following riboflavin treatment (**Figure 39A and Figure 39B**). Most importantly, using riboflavin not only we were also able to show enrichment in autofluorescent cells from a freshly digested tumor, these cells could be FACSorted and were equally enriched in pluripotency-associated genes (**Figure 39C)**.

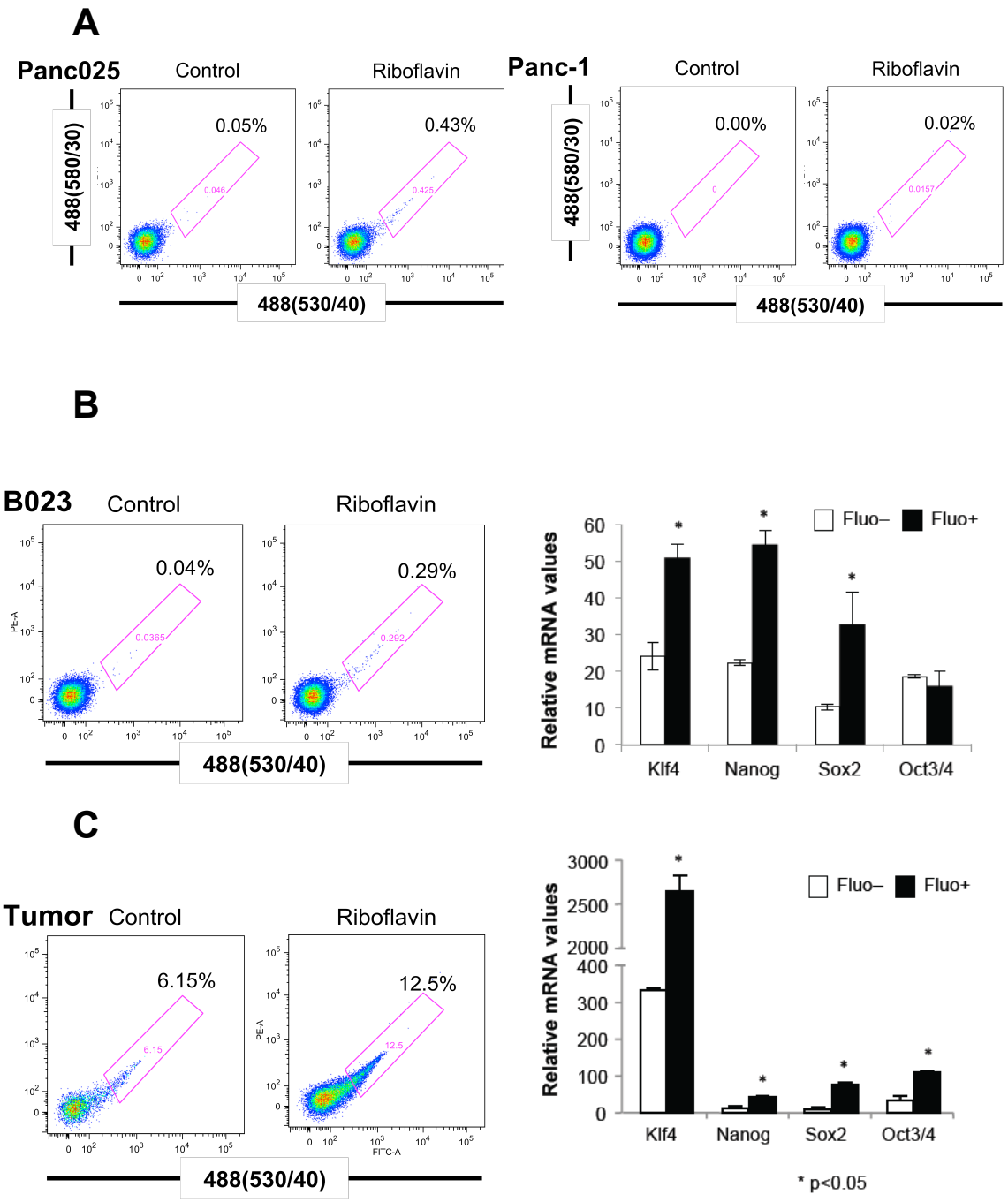

Figure 39. **(A)** Effect of 30µM riboflavin on the autofluorescence in the primary culture Panc025 and the Panc-1 cell line. **(B)** Effect of 30µM riboflavin on B023 primary culture (left panel) and QPCR analysis for pluripotency-associated genes in Fluo+ and Fluo–. **(C)** Effect of 30µM riboflavin on fresh tumor (left panel) and QPCR analysis for pluripotency-associated genes in Fluo+ and Fluo–. Data are normalized for ß-actin expression.

7. THERAPEUTIC AND CLINICAL APPLICATION OF AUTOFLUORESCENT CELLS

Since CSC are believed to be the mediating cell type behind chemoresistance, and since our data show that autofluorescent cells display a more CSC phenotype, particularly an inherent chemoresistant capacity, we sought to exploit this cell population for the purposes of anti-cancer drug screening. Specifically, we developed a low-throughput screening (LTS) platform based on the ability to sort for autofluorescent cells from any primary cell culture and/or tumor with the aid of riboflavin. As depicted in **Figure 40A**, primary pancreatic cancer cell cultures were incubated over night with riboflavin, FACSorted for autofluorescence, and subsequently seeded directly into 96-well plates in the continued presence of riboflavin to ensure maximal autofluorescence detection. Cells were then incubated with different chemotherapeutic agents for another 72h followed by assessment of autofluorescent cells and total cell numbers as well as drug-induced cytotoxicity. Changes in autofluorescence are displayed as a ratio of the total number of autofluorescent positives cells to the total number of Hoechst+ cells **(Figure 40B).**

As expected, gemcitabine alone did not reduce the ratio of autofluorescent cells while FTC, which was used as a positive control for loss of autofluorescence, reduced autofluorescence, but was not non-cytotoxic. Importantly, using a variety of compounds with putative activity against pancreatic cancer (stem cells) (Table S1), we were able to reproducibly assess their therapeutic activity against autofluorescent cells (reduction in autofluorescence and increase in cell toxicity) or non-autofluorescent cells (no reduction in autofluorescence, but increase in cell toxicity). Understanding the need to utilize low throughput screens in the clinic, particularly for the purposes of developing personalized treatment regimens for pancreatic cancer patients undergoing tumor resections in a timely fashion, we additionally show that this LTS platform can be adequately adapted to freshly digested tumors **(Figure 40B)**, yielding similarly consistent results to those obtained with cultured primary cells **(Figure 40A).**

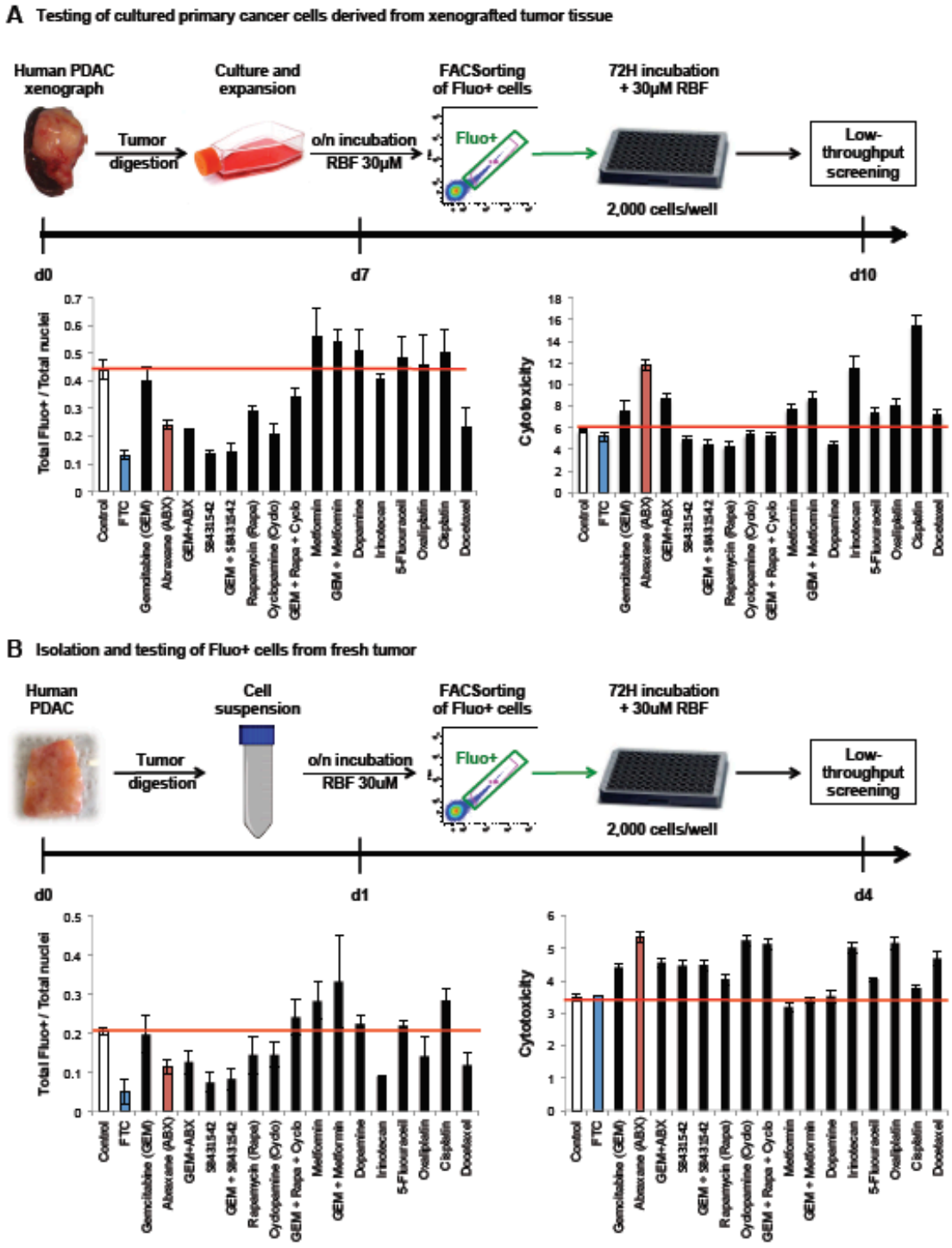

Figure 40. (A) LTS from cultured cells derived from the xenograft (B) Patient sample primary tumor

We next confirmed the efficacy of the LTS platform *in vivo*. We selected drugs that showed an effect on CSCs in vitro (i.e. inhibition of autofluorescence and increase in toxicity), as well as others that showed no effect. For patient 185, our LTS assays showed that Gemcitabine had little to no effect on autofluorescent cells while Abraxane showed a significant reduction in the number of autofluorescent cells accompanied with an increase in cyto–toxicity (**Figure XX**). To validate these finding sin vivo, we treated 185 patient-derived xenograft tumors with Abraxane and Gemcitabine and, as expected, we saw a high correlation between our in vivo findings and our LTS predictions. Specifically, Gemcitabine was not capable of reducing the autofluroescence tumor cells *in vivo,* while Abraxane had profound effect on the autofluorescent content while simultaneously reducing the size of the tumor, as showed in **Figure 41**

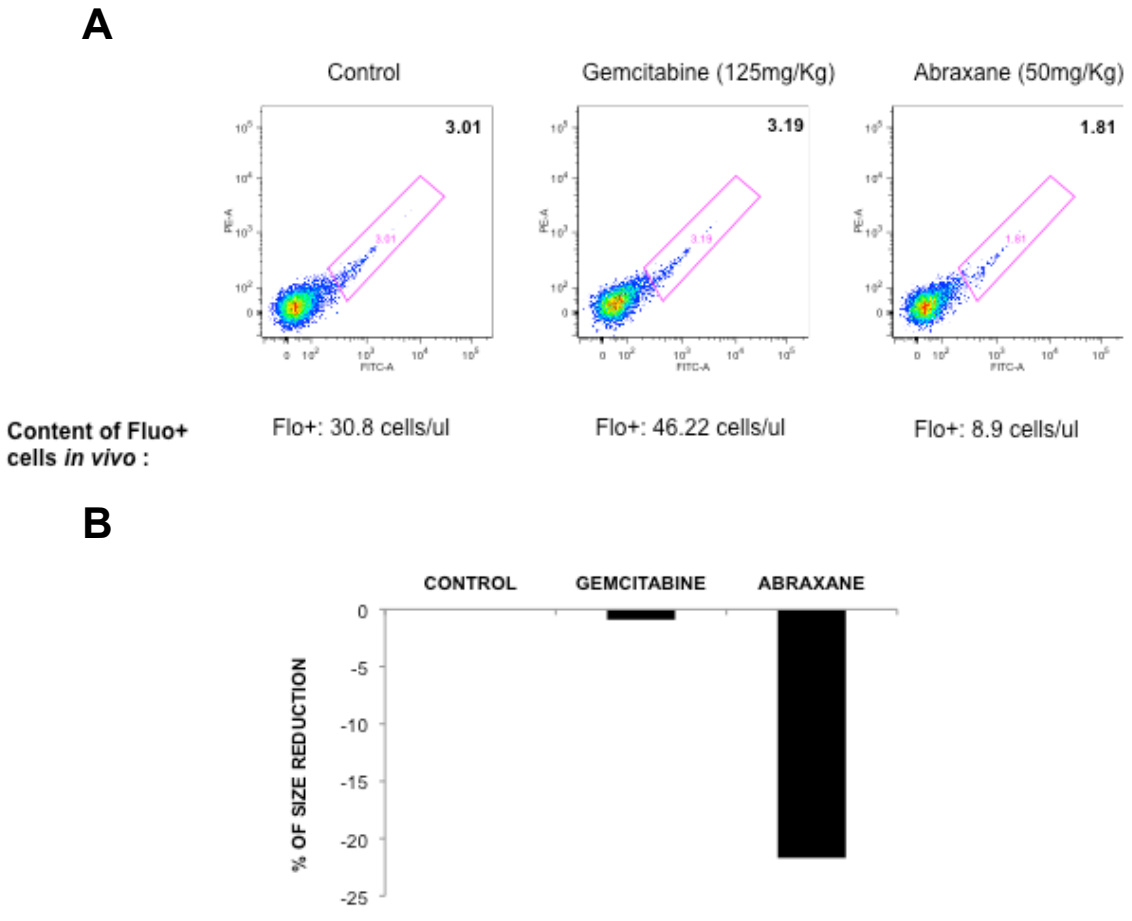

Figure 41. **(A)** Flow cytometry analysis for the content of autofluorescent cells after treatment in vivo with Gemcitabine and Abraxane. **(B)** Tumor size reduction after treatment in vivo with Gemcitabine and Abraxane.

DISCUSSION

In light of the still devastating prognosis for PDAC patients, the identification of PaCSCs with exclusive tumorigenicity in 2007 created an entirely new research field spurring renewed hope for the development of novel stem cell-specific targeted therapies. Since then, the field of PaCSCs has markedly evolved; however, comprehensive investigations of the regulatory machinery of CSCs still lacks unbiased and standardized techniques for isolating highly enriched CSCs. Although SP methodology has been widely employed as a tool to enrich CSCs, results from studies in other cancer cells question the identification of CSCs based on their efflux-capacity (Burkert et al., 2008). Consistently, we also did not find enrichment of pancreatic CSCs in SP cells, but describe here, for the first time, the presence of a distinct autofluorescent compartment in a subset of pancreatic cancer cells. These cells bear striking CSC characteristics independent of their surface marker expression profile. Autofluorescent cells overexpress pluripotency-associated genes, bear self-renewal capacity, are highly metastatic and, most importantly, demonstrate exclusive *in vivo* tumorigenicity. Intriguingly, the subcellular autofluorescent compartment represents a sink for ABCG2-dependent riboflavin accumulation, a feature that not only allows for consistent identification of CSC across numerous tumors, but one we have subsequently exploited in order to isolate these cells from primary cultures or fresh tumors for anti-cancer drug screening assays.

Our initial screening for new functional CSC biomarkers suitable for *in vivo* and *in vitro* enrichment of tumorigenic cells did not reveal striking results. Most surface markers are altered in response to different microenvironments such as xenografting or cell culture (**Figure 5**, and while functional enrichment of SP cells resulted in slightly enhanced sphere formation capacity, this method did not translate into enhanced *in vivo* tumorigenicity (**Figure 6**). Although counterintuitive, it should be noted that previous studies i) did not univocally test the CSC features of SP cells, ii) used established pancreatic cancer cell lines (Zhang et al., 2010, Zhou et al., 2008), in which enhanced chemoresistance, although not a uniformly defining feature of CSCs, was used as the main readout, and iii) failed to test SP *in vivo* tumorigenicity (Van den Broeck et al., 2012). Importantly, it seems

that the SP does not necessarily overlap with the ABCG2+ population since autofluorescent cells markedly overexpress ABCG2, but are not enriched in SP cells (**Figure 33**).

However, we were still able to identify a population of self-renewing and highly tumorigenic pancreatic CSCs based on their ability to concentrate the fluorescent vitamin riboflavin. Indeed, this feature allowed for the reliable identification and isolation of PaCSCs from the large pool of non-tumorigenic cancer cells independent of the expression of CD133 or other surface markers. These autofluorescent cells were enriched for pluripotency-associated genes and demonstrated indefinite self-renewal capacity. Interestingly, we found that autofluorescent cells were not prone to alteretions as surface markers are sensitive to. Comparing expressions of CD133 vs autofluorescent cells in primary cultures after tripsinization, results showed that CD133 was altered during the recovering time compromising the reproducibility. Meanwhile, autofluorescent cells remained stable, allowing us to reproduce our studies in different model systems (Figure xx).

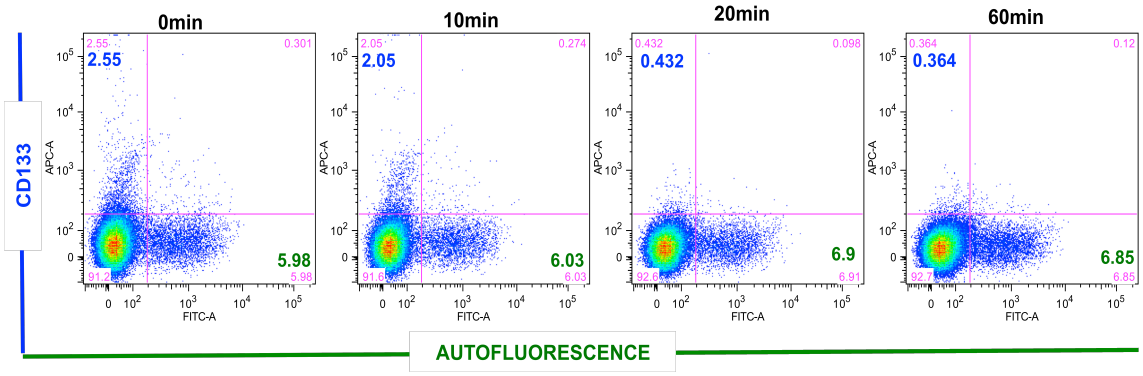

Figure 42. Flow cytometry analysis for CD133 and autofluorescence. Cells were tripsinized and then resuspended in RPMI. Cells were acquire with no recovering time after tripsinization (0min), at 10min, 20 and 60min of recovering.

Importantly, clonal spheres as well as *in vivo* tumors derived from a single autofluorescent cell contained a mixed population of autofluorescent and non-autofluorescent cells, demonstrating that distinct cell populations do not arise as the result of the co-existence of independent genetic subclones within the tumor tissue, but rather are the result of multi-lineage differentiation processes during tumor growth, with autofluorescent cells representing the cell of origin. Therefore, with monitoring of single cell cultures as well as using single transplanted cells as the most stringent *in vivo* evaluation (**Figures 16 and 17**), our data do not support the notion that the CSC pool can be replenished by non-CSCs (Iliopoulos et al., 2011).

Present understanding of other normal and cancer tissues indicates that stem cells or early progenitor populations are rarely defined by only one marker, but rather by a combination of multiple molecular markers (Hermann et al., 2010). Notably, none of the previously established CSC markers (including CD133 and CD44) was exclusively restricted to the autofluorescent population as non-autofluorescent cells also expressed these markers. Importantly, the stemness character of cancer cells might well be an elusive property that cannot be captured by invariable molecular (surface) markers, but may actually bear more unstable molecular configurations changing with time and as a result of the environmental context (Hill, 2006, Campbell and Polyak, 2007, Dontu et al., 2003). Differences between tumorigenic cancer stem cells and their non-tumorigenic progenies may not be as clear-cut as in normal tissues, in which a stringent unidirectional hierarchy and strict balanced asymmetric division preserves tissue integrity. Therefore, as cancer cells are genetically altered and unstable, surface markers may not represent the most suitable approach for capturing the functional features of CSCs as tumors might contain a spectrum of "intermediate" cancer cells with more or less aberrant differentiation states. Consequently, stemness in a given subpopulation or in single cancer cells may more likely represent a highly variable property rather than a strict committed on or off state with obligatory expression of defined surface markers. Indeed, while we do observe "switching" of established CSC markers after transferring cells into different environmental conditions (e.g. from anchorage dependent sphere culture to adherent culture), our single cell experiments show

that autofluorescent cells are a highly tractable entity *in vivo*, which is capable of producing non-autofluorescent cells, but not vice versa.

What is the source of autofluorescence? First, we looked at autophagy as an evolutionarily conserved degradation process that targets long-lived proteins, organelles, and other cytoplasmic components for degradation via the lysosomal pathway. The autophagy pathway is complementary to the action of the ubiquitin-proteasome pathway, which typically degrades short-lived proteins. Activation of the autophagy pathway is required for multiple cellular roles, including survival during starvation, the clearance of intracellular components, development, and immunity, but is also critical for the survival of cancer cells within the nutrient poor and hypoxic environment of solid tumors. Importantly, autophagy has been associated with autofluorescence due to massive lipid accumulation in some cancers (White, 2012). Therefore, we initially attributed the observed autofluorescence to a metabolically distinct population of cancer cells with high activity for autophagy. However, the fluorescence was neither associated with liposomal structures as evidenced by lysotrackers, nor were the autophagy inhibitors namely and E64D with Pepstatin A capable of reversing or abrogating the autofluorescence. Hence, using and enhancer of the autophagy, rapamycin, we didn't observe any effect of autofluorescent cells (**Figure 35)**. Moreover, we did not find enhanced expression of autophagy-related protein 3 (LC3), a ubiquitous 45 kDa member of the ATG3 family of proteins with critical function in autophagy, nor in ATG12 in autofluorescent cells as compared to non-autofluorescent cells. Finally, serum starvation, which would induce droplet triglycerides to be hydrolyzed for generating free fatty acids and subsequent oxidization to provide energy, did not revert the autofluorescence phenomenon (data not shown). Therefore, our data do not support a relevant association between the autofluorescence phenomenon and autophagy for primary human pancreatic CSCs.

Since our data did not support a relevant association between autofluorescence and autophagy we next pursued our observation that autofluorescent cells overexpress the multidrug transporter ABCG2 (also known as BCRP, breast cancer resistance protein), which has broad substrate specificity and

actively extrudes a wide variety of drugs, carcinogens, and dietary toxins from cells (van Herwaarden and Schinkel, 2006). Importantly, ABCG2 is strongly induced in the mammary gland during lactation (Jonker et al., 2002, van Herwaarden and Schinkel, 2006) and responsible for pumping riboflavin (vitamin B_2) into milk (van Herwaarden et al., 2007). In a similar fashion, ABCG2 confers mitoxantrone resistance in several cancers and mediates a marked intravesicular concentration of an unknown endogenous green fluorescent compound (Ifergan et al., 2005), which was later identified as riboflavin (Ifergan et al., 2009). The marked intravesicular concentration of riboflavin in ABCG2-overexpressing cancer cells tightly correlated with the extent of ABCG2 overexpression and its differential localization to the vesicular membrane and not to the plasma membrane was functionally demonstrated by intravesicular accumulation of mitoxantrone. Intriguingly, we demonstrate here that the molecular basis for the autofluorescence in pancreatic CSCs is also related to the concentration of riboflavin. This was demonstrated by culturing the cells in the absence of riboflavin, which led to the loss of autofluorescence or by blocking the ABCG2 transporters using FTC. Following addition of riboflavin or withdrawal of FTC, the autofluorescence reappeared, indicating an active ABCG2-dependent process (**Figures 36 and 37).**

Importantly, autofluorescent cells were not enriched in the side population suggesting that the subcellular autofluorescent compartment does not correlate with the expression of this transporter on the cell membrane. By its apical localization in normal epithelia of intestine, kidney, and placenta and in the hepatocyte bile canalicular membrane, ABCG2 can reduce the systemic and tissue uptake of its substrates and mediate their extrusion from the body. It thus protects the body from harmful xenotoxins (van Herwaarden et al., 2003, Jonker et al., 2002). However, in the setting of cancer with loss of polarity, transporting toxins out of the cancer cells will not result in their extrusion from the tumor tissue. Therefore, a more efficient mechanism for cancer cells to avoid exposure to chemotoxins may represent the active transportation of the toxins into the identified membrane-covered compartments that serve as a sink. While distinct, but extracellular vesicle have been reported in other tumor entities such as breast cancer that are capable of

concentrating large amounts of chemotoxins and depend on ABCG2 (Ifergan et al., 2005), we found that the autofluorescent compartment in pancreatic CSCs also strongly enriches for the chemotoxin mitoxantrone in an ABCG2-dependent fashion, but is located in the cytoplasma as demonstrated by 3-D confocal analyses.

Several previous studies have linked autofluorescence to cell cycle and/or cellular metabolic activity, such as the intracellular NAD/NADPH status or mitochondrial flavin content (Schuchmann et al., 2001, Reyes et al., 2006). In the mitochondria, riboflavin and its forms flavin mononucleotide (FMN) and flavin dinucleotide (FAD) are essential for one-carbon metabolism and have been related to carcinogenesis because of its involvement in the synthesis of purines and pyrimidines for subsequent DNA synthesis, and in the synthesis of methionine for DNA methylation. While our data are not in disagreement with this notion, we found that the distinct and striking autofluorescence did not co-localize with mitochondria. Whether the accumulation of riboflavin in the identified sink actually alters available riboflavin concentrations for its cellular functions is not clear and deserves future investigation.

The avatar mice is the model that is closest to the clinic, bearing the advantage that there is no clonal selection and all cellular heterogeneity that form the tumor is transplanted. This model provide a therapeutic approach where different molecules can be tested to check efficacy for personalized medicine, but bear the caveat that the complete process takes around 3 to 6 months, being quite a long period for patients where the overall survival is quite poor. Based on this model, we were able to apply the identified autofluorescent feature of cancer stem cells in a low-throughput drug screening effort using primary cultured cells and freshly digested pancreatic cancer tissue (**Figure 40**) and obtaining the efficacy results *in vitro* around in 1 week after surgery. These results were further validated *in vivo,* obtaining similar results as previously observed with the LTS.

While digested tumors are inherently difficult to analyze due to massive contamination with stroma cells and debris, here we show that sorting of autofluorescent cells out of a freshly digested tumor following overnight incubation with riboflavin is feasible. Subsequently the isolated autofluorescent CSCs could be

tested for their sensitivity to a variety of compounds with potential activity against pancreatic cancer (stem) cells. Intriguingly, in these studies we not only confirm that the combination of the Alk4,5,7 inhibitor SB43154 is highly active against autofluorescent CSCs (Lonardo et al.), but also observed that autofluorescent cells of this particular patient were quite sensitive to abraxane. Interestingly, no additional treatment effect was observed for the combination of gemcitabine and abraxane, which may imply that abraxane monotherapy represent the most effective chemotherapy for this patient. While validation of our assay using a larger set of pancreatic tumors is necessary before this LTS platform proves amendable to a clinical setting, the preliminary screens presented herein provide proof-of-principle that autofluorescent cells are highly adaptable to anti-cancer drug screening and their utility should be further investigated.

Taken together, our data show that a subpopulation of pancreatic cancer cells have an identifiable cellular phenotype, which strongly correlates with stemness and tumorigenic capacity and can be isolated without the use of molecular markers. This distinct inherent property therefore represents a new and novel biomarker that can be utilized to identify and purify CSCs in lieu of conventional surface markers. Transcriptome analysis confirmed the stem cell features of these cells and *in vivo* experiments unequivocally demonstrated their exclusive tumorigenicity down to a single cell. Further exploiting these properties may be more suitable to capture the dynamic complexity of CSCs and allow the identification of new therapeutic targets. Indeed, establishing autofluorescence as a primary readout in LTS for customized compound libraries demonstrates the translational relevance of our findings.

CONCLUSIONS

We have accumulated compelling evidence establishing auto-fluorescence as a powerful biomarker for the identification of pancreatic cancer stem cells. Therefore, we conclude:

Autofluroescence satifies all the CSC requirements:

1. Autofluorescent cells enriched in stemness-associated genes as compare to their negative counterparts.
2. Autofluorescent cells showed self renewal properties in vitro as showed with the sphere formation capacity assay
3. Autofluorescent cells presented asymmetric division, therefore they can give rise different lineages of cells
4. Autofluorescent cells are highly tumorigenic, as we showed with our in vivo experiments and based on the Limited dilution assay.
5. From one single-cell derived tumor, autofluorecent cells were able to recapitulate the tumor heterogeneity.
6. Invasion capacities is well satisfied by autofluorescent cells compare to the negative counterparts that did not have the capacity to even form tumors.
7. Autofluorescent cells were more resistant to standard chemotherapy Gemcitabine, as well described using Abraxane. Autofluorescent cells showed different mechanisms to evade the action of the therapy (low nucleoside transporters expression and more quiescence)

We have defined the autofluroescence mechanism:

8. Autofluorescence is an accumulation of riboflavin inside the vesicles
9. The autofluorescence is mediated by ABCG2 transporters, but is not equivalent to SP.

Clinical and therapeutical application of the autofluroescent cells:

10. Because autofluorescent cells are trackable and are not sensitive to the microenviroment, they can be used to develop a LTS for personalized medicine and diagnosis.

CONCLUSIONES

Hemos acumulado pruebas convincentes de que la auto-fluorescencia es un potente marcador biológico para la identificación de las células madre de cáncer de páncreas. Por lo tanto, llegamos a la conclusión:

Las células autofluorescentes satisfacen todos los requisitos de CSCs:

1. Las células autofluorescentes enriquecen en genes asociados con pluripotencia en comparación con las autofluorescentes negativas.

2. Las células autofluorescentes mostraron propiedades de auto-renovación *in vitro* tal y como demostramos con el ensayo de la capacidad de formación de esferas.

3. Las células autofluorescentes presentan división asimétrica, por lo que pueden dar lugar a diferentes linajes, siendo esta una propiedad de células madre.

4. Las células autofluorescentes son altamente tumorigénicas, como hemos demostrado en experimentos *in vivo* y tambien en el ensayo de dilución limitada.

5. De tumores derivados de una sola célula, hemos demostrado que las células autofluorecentes fueron capaces de recapitular la heterogeneidad del tumor.

6. Las celulas autofluorescentes mostratoron un fenotipo más invasivo comparandolo con las no fluorescentes que no tenían incluso capacidad de formar tumores en esas condiciones.

7. Las células autofluorescentes eran más resistentes a la quimioterapia estándar con Gemcitabina, asi como con Abraxane. Las células autofluorescentes mostraron diferentes mecanismos para evadir la acción de la terapia (baja expresión de transportadores de nucleósidos y siendo mas quiescentes)

El mecanismo de autofluroescencia se ha sido descrito:

8. La Autofluorescencia es una acumulación de riboflavina en el interior de las vesículas

9. La autofluorescencia es mediada por la expresion de los transportadores ABCG2, pero no es equivalente a SP.

Aplicación clínica y terapéutica de las células autofluroescentes:

10. Dado que las células autofluorescentes se pueden rastrear y no son sensibles al microambiente, pueden ser utilizadas para desarrollar un LTS para medicina personalizada y diagnóstico.

BIBLIOGRAPHY

BIBLIOGRAPHY

AHLGREN, J. D. (1996) Chemotherapy for pancreatic carcinoma. *Cancer,* 78**,** 654-63.

AL-ASSAR, O., MANTONI, T., LUNARDI, S., KINGHAM, G., HELLEDAY, T. & BRUNNER, T. B. (2011) Breast cancer stem-like cells show dominant homologous recombination due to a larger S-G2 fraction. *Cancer Biol Ther,* 11**,** 1028-35.

AL-HAJJ, M., WICHA, M. S., BENITO-HERNANDEZ, A., MORRISON, S. & CLARKE, M. F. (2003) Prospective identification of tumorigenic breast cancer cells. *Proc Natl Acad Sci USA,* 100**,** 3983-8.

ARMANIOS, M. & GREIDER, C. W. (2005) Telomerase and cancer stem cells. *Cold Spring Harb Symp Quant Biol,* 70**,** 205-8.

BAILEY, J. M., MOHR, A. M. & HOLLINGSWORTH, M. A. (2009) Sonic hedgehog paracrine signaling regulates metastasis and lymphangiogenesis in pancreatic cancer. *Oncogene,* 28**,** 3513-25.

BARABE, F., KENNEDY, J. A., HOPE, K. J. & DICK, J. E. (2007) Modeling the initiation and progression of human acute leukemia in mice. *Science,* 316**,** 600-4.

BEIER, D., HAU, P., PROESCHOLDT, M., LOHMEIER, A., WISCHHUSEN, J., OEFNER, P. J., AIGNER, L., BRAWANSKI, A., BOGDAHN, U. & BEIER, C. P. (2007) CD133(+) and CD133(-) glioblastoma-derived cancer stem cells show differential growth characteristics and molecular profiles. *Cancer Res,* 67**,** 4010-5.

BELL, D. H. (1988) Characterization of the fluorescence of the antitumor agent, mitoxantrone. *Biochim Biophys Acta,* 949**,** 132-7.

BHAGWANDIN, V. J. & SHAY, J. W. (2009) Pancreatic cancer stem cells: fact or fiction? *Biochim Biophys Acta,* 1792**,** 248-59.

BONNET, D. & DICK, J. E. (1997) Human acute myeloid leukemia is organized as a hierarchy that originates from a primitive hematopoietic cell. *Nat Med,* 3**,** 730-7.

BRUCE, W. R. & VAN DER GAAG, H. (1963) A Quantitative Assay for the Number of Murine Lymphoma Cells Capable of Proliferation in Vivo. *Nature,* 199**,** 79-80.

BURKERT, J., OTTO, W. R. & WRIGHT, N. A. (2008) Side populations of gastrointestinal cancers are not enriched in stem cells. *J Pathol,* 214**,** 564-73.

BURRIS, H. A., 3RD, MOORE, M. J., ANDERSEN, J., GREEN, M. R., ROTHENBERG, M. L., MODIANO, M. R., CRIPPS, M. C., PORTENOY, R. K., STORNIOLO, A. M., TARASSOFF, P., NELSON, R., DORR, F. A., STEPHENS, C. D. & VON HOFF, D. D. (1997) Improvements in survival and clinical benefit with gemcitabine as first-line therapy for patients with advanced pancreas cancer: a randomized trial. *J Clin Oncol,* 15**,** 2403-13.

CAMPBELL, L. L. & POLYAK, K. (2007) Breast tumor heterogeneity: cancer stem cells or clonal evolution? *Cell Cycle,* 6**,** 2332-8.

CICALESE, A., BONIZZI, G., PASI, C. E., FARETTA, M., RONZONI, S., GIULINI, B., BRISKEN, C., MINUCCI, S., DI FIORE, P. P. & PELICCI, P. G. (2009) The tumor suppressor p53 regulates polarity of self-renewing divisions in mammary stem cells. *Cell,* 138**,** 1083-95.

CLARKE, M. F., DICK, J. E., DIRKS, P. B., EAVES, C. J., JAMIESON, C. H., JONES, D. L., VISVADER, J., WEISSMAN, I. L. & WAHL, G. M. (2006) Cancer Stem

Cells--Perspectives on Current Status and Future Directions: AACR Workshop on Cancer Stem Cells. *Cancer Res,* 66**,** 9339-44.
CONROY, T., DESSEIGNE, F., YCHOU, M., BOUCHE, O., GUIMBAUD, R., BECOUARN, Y., ADENIS, A., RAOUL, J. L., GOURGOU-BOURGADE, S., DE LA FOUCHARDIERE, C., BENNOUNA, J., BACHET, J. B., KHEMISSA-AKOUZ, F., PERE-VERGE, D., DELBALDO, C., ASSENAT, E., CHAUFFERT, B., MICHEL, P., MONTOTO-GRILLOT, C. & DUCREUX, M. (2011) FOLFIRINOX versus gemcitabine for metastatic pancreatic cancer. *N Engl J Med,* 364**,** 1817-25.
DENG, S., YANG, X., LASSUS, H., LIANG, S., KAUR, S., YE, Q., LI, C., WANG, L. P., ROBY, K. F., ORSULIC, S., CONNOLLY, D. C., ZHANG, Y., MONTONE, K., BUTZOW, R., COUKOS, G. & ZHANG, L. (2010) Distinct expression levels and patterns of stem cell marker, aldehyde dehydrogenase isoform 1 (ALDH1), in human epithelial cancers. *PLoS One,* 5**,** e10277.
DONTU, G., AL-HAJJ, M., ABDALLAH, W. M., CLARKE, M. F. & WICHA, M. S. (2003) Stem cells in normal breast development and breast cancer. *Cell Prolif,* 36 Suppl 1**,** 59-72.
DORADO, J., LONARDO, E., MIRANDA-LORENZO, I. & HEESCHEN, C. Pancreatic cancer stem cells: new insights and perspectives. *J Gastroenterol,* 46**,** 966-73.
EBBEN, J. D., TREISMAN, D. M., ZORNIAK, M., KUTTY, R. G., CLARK, P. A. & KUO, J. S. (2010) The cancer stem cell paradigm: a new understanding of tumor development and treatment. *Expert Opin Ther Targets,* 14**,** 621-32.
FAN, X., MATSUI, W., KHAKI, L., STEARNS, D., CHUN, J., LI, Y. M. & EBERHART, C. G. (2006) Notch pathway inhibition depletes stem-like cells and blocks engraftment in embryonal brain tumors. *Cancer Res,* 66**,** 7445-52.
FEARON, E. R. & VOGELSTEIN, B. (1990) A genetic model for colorectal tumorigenesis. *Cell,* 61**,** 759-67.
FELDMANN, G., DHARA, S., FENDRICH, V., BEDJA, D., BEATY, R., MULLENDORE, M., KARIKARI, C., ALVAREZ, H., IACOBUZIO-DONAHUE, C., JIMENO, A., GABRIELSON, K. L., MATSUI, W. & MAITRA, A. (2007) Blockade of hedgehog signaling inhibits pancreatic cancer invasion and metastases: a new paradigm for combination therapy in solid cancers. *Cancer Res,* 67**,** 2187-96.
GOODELL, M. A., BROSE, K., PARADIS, G., CONNER, A. S. & MULLIGAN, R. C. (1996) Isolation and functional properties of murine hematopoietic stem cells that are replicating in vivo. *J Exp Med,* 183**,** 1797-806.
HAN, H. & VON HOFF, D. D. (2013) SnapShot: pancreatic cancer. *Cancer Cell,* 23**,** 424-424 e1.
HARLEY, C. B. (2008) Telomerase and cancer therapeutics. *Nat Rev Cancer,* 8**,** 167-79.
HASSAN, M. M., BONDY, M. L., WOLFF, R. A., ABBRUZZESE, J. L., VAUTHEY, J. N., PISTERS, P. W., EVANS, D. B., KHAN, R., CHOU, T. H., LENZI, R., JIAO, L. & LI, D. (2007) Risk factors for pancreatic cancer: case-control study. *Am J Gastroenterol,* 102**,** 2696-707.
HERMANN, P., HUBER, S., HERRLER, T., AICHER, A., ELLWART, J., GUBA, M., BRUNS, C. & HEESCHEN, C. (2007a) Distinct Populations of Cancer Stem

Cells Determine Tumor Growth and Metastatic Activity in Human Pancreatic Cancer. *Cell Stem Cell,* 1**,** 313-323.
HERMANN, P. C., BHASKAR, S., CIOFFI, M. & HEESCHEN, C. (2010) Cancer stem cells in solid tumors. *Semin Cancer Biol,* 20**,** 77-84.
HERMANN, P. C., HUBER, S. L. & HEESCHEN, C. (2008) Metastatic cancer stem cells: a new target for anti-cancer therapy? *Cell Cycle,* 7**,** 188-93.
HERMANN, P. C., HUBER, S. L., HERRLER, T., AICHER, A., ELLWART, J. W., GUBA, M., BRUNS, C. J. & HEESCHEN, C. (2007b) Distinct populations of cancer stem cells determine tumor growth and metastatic activity in human pancreatic cancer. *Cell Stem Cell,* 1**,** 313-23.
HERMANN, P. C., MUELLER, M. T. & HEESCHEN, C. (2009) Pancreatic cancer stem cells--insights and perspectives. *Expert Opin Biol Ther,* 9**,** 1271-8.
HIDALGO, M. (2010) Pancreatic cancer. *N Engl J Med,* 362**,** 1605-17.
HIDALGO, M. & VON HOFF, D. D. (2012) Translational therapeutic opportunities in ductal adenocarcinoma of the pancreas. *Clin Cancer Res,* 18**,** 4249-56.
HILL, R. P. (2006) Identifying cancer stem cells in solid tumors: case not proven. *Cancer Res,* 66**,** 1891-5; discussion 1890.
HIRSCHMANN-JAX, C., FOSTER, A. E., WULF, G. G., NUCHTERN, J. G., JAX, T. W., GOBEL, U., GOODELL, M. A. & BRENNER, M. K. (2004) A distinct "side population" of cells with high drug efflux capacity in human tumor cells. *Proc Natl Acad Sci U S A,* 101**,** 14228-33.
IFERGAN, I., GOLER-BARON, V. & ASSARAF, Y. G. (2009) Riboflavin concentration within ABCG2-rich extracellular vesicles is a novel marker for multidrug resistance in malignant cells. *Biochem Biophys Res Commun,* 380**,** 5-10.
IFERGAN, I., SCHEFFER, G. L. & ASSARAF, Y. G. (2005) Novel extracellular vesicles mediate an ABCG2-dependent anticancer drug sequestration and resistance. *Cancer Res,* 65**,** 10952-8.
ILIOPOULOS, D., HIRSCH, H. A., WANG, G. & STRUHL, K. (2011) Inducible formation of breast cancer stem cells and their dynamic equilibrium with non-stem cancer cells via IL6 secretion. *Proc Natl Acad Sci U S A,* 108**,** 1397-402.
INGHAM, P. W. & MCMAHON, A. P. (2001) Hedgehog signaling in animal development: paradigms and principles. *Genes Dev,* 15**,** 3059-87.
INOKI, K., CORRADETTI, M. N. & GUAN, K. L. (2005) Dysregulation of the TSC-mTOR pathway in human disease. *Nat Genet,* 37**,** 19-24.
JEMAL, A., SIEGEL, R., XU, J. & WARD, E. (2010) Cancer statistics, 2010. *CA Cancer J Clin,* 60**,** 277-300.
JEMAL, A., TIWARI, R. C., MURRAY, T., GHAFOOR, A., SAMUELS, A., WARD, E., FEUER, E. J. & THUN, M. J. (2004) Cancer statistics, 2004. *CA Cancer J Clin,* 54**,** 8-29.
JIMENO, A., FELDMANN, G., SUAREZ-GAUTHIER, A., RASHEED, Z., SOLOMON, A., ZOU, G. M., RUBIO-VIQUEIRA, B., GARCIA-GARCIA, E., LOPEZ-RIOS, F., MATSUI, W., MAITRA, A. & HIDALGO, M. (2009) A direct pancreatic cancer xenograft model as a platform for cancer stem cell therapeutic development. *Mol Cancer Ther,* 8**,** 310-4.

JONES, D. & WAGERS, A. (2008) No place like home: anatomy and function of the stem cell niche. *Nat Rev Mol Cell Biol,* 9**,** 11-21.

JONKER, J. W., BUITELAAR, M., WAGENAAR, E., VAN DER VALK, M. A., SCHEFFER, G. L., SCHEPER, R. J., PLOSCH, T., KUIPERS, F., ELFERINK, R. P., ROSING, H., BEIJNEN, J. H. & SCHINKEL, A. H. (2002) The breast cancer resistance protein protects against a major chlorophyll-derived dietary phototoxin and protoporphyria. *Proc Natl Acad Sci U S A,* 99**,** 15649-54.

JOO, K. M., KIM, S. Y., JIN, X., SONG, S. Y., KONG, D. S., LEE, J. I., JEON, J. W., KIM, M. H., KANG, B. G., JUNG, Y., JIN, J., HONG, S. C., PARK, W. Y., LEE, D. S., KIM, H. & NAM, D. H. (2008) Clinical and biological implications of CD133-positive and CD133-negative cells in glioblastomas. *Lab Invest,* 88**,** 808-15.

KABASHIMA, A., HIGUCHI, H., TAKAISHI, H., MATSUZAKI, Y., SUZUKI, S., IZUMIYA, M., IIZUKA, H., SAKAI, G., HOZAWA, S., AZUMA, T. & HIBI, T. (2009) Side population of pancreatic cancer cells predominates in TGF-beta-mediated epithelial to mesenchymal transition and invasion. *Int J Cancer,* 124**,** 2771-9.

LI, C., HEIDT, D., DALERBA, P., BURANT, C., ZHANG, L., ADSAY, V., WICHA, M., CLARKE, M. & SIMEONE, D. (2007a) Identification of Pancreatic Cancer Stem Cells. *Cancer Research,* 67**,** 1030-1037.

LI, C., HEIDT, D. G., DALERBA, P., BURANT, C. F., ZHANG, L., ADSAY, V., WICHA, M., CLARKE, M. F. & SIMEONE, D. M. (2007b) Identification of pancreatic cancer stem cells. *Cancer Res,* 67**,** 1030-7.

LIMAME, R., WOUTERS, A., PAUWELS, B., FRANSEN, E., PEETERS, M., LARDON, F., DE WEVER, O. & PAUWELS, P. (2012) Comparative analysis of dynamic cell viability, migration and invasion assessments by novel real-time technology and classic endpoint assays. *PLoS One,* 7**,** e46536.

LONARDO, E., FRIAS-ALDEGUER, J., HERMANN, P. C. & HEESCHEN, C. (2012) Pancreatic stellate cells form a niche for cancer stem cells and promote their self-renewal and invasiveness. *Cell Cycle,* 11**,** 1282-90.

LONARDO, E., HERMANN, P. C. & HEESCHEN, C. (2010) Pancreatic cancer stem cells - update and future perspectives. *Mol Oncol,* 4**,** 431-42.

LONARDO, E., HERMANN, P. C., MUELLER, M. T., HUBER, S., BALIC, A., MIRANDA-LORENZO, I., ZAGORAC, S., ALCALA, S., RODRIGUEZ-ARABAOLAZA, I., RAMIREZ, J. C., TORRES-RUIZ, R., GARCIA, E., HIDALGO, M., CEBRIAN, D. A., HEUCHEL, R., LOHR, M., BERGER, F., BARTENSTEIN, P., AICHER, A. & HEESCHEN, C. (2011) Nodal/Activin signaling drives self-renewal and tumorigenicity of pancreatic cancer stem cells and provides a target for combined drug therapy. *Cell Stem Cell,* 9**,** 433-46.

MA, S., CHAN, K., HU, L., LEE, T., WO, J., NG, I., ZHENG, B. & GUAN, X. (2007) Identification and Characterization of Tumorigenic Liver Cancer Stem/Progenitor Cells. *Gastroenterology,* 132**,** 2542-2556.

MAGEE, J. A., PISKOUNOVA, E. & MORRISON, S. J. (2012) Cancer stem cells: impact, heterogeneity, and uncertainty. *Cancer Cell,* 21**,** 283-96.

MARIAN, C. O. & SHAY, J. W. (2009) Prostate tumor-initiating cells: a new target for telomerase inhibition therapy? *Biochim Biophys Acta,* 1792**,** 289-96.

MAZUR, P. K., GRUNER, B. M., NAKHAI, H., SIPOS, B., ZIMBER-STROBL, U., STROBL, L. J., RADTKE, F., SCHMID, R. M. & SIVEKE, J. T. (2010) Identification of epidermal Pdx1 expression discloses different roles of Notch1 and Notch2 in murine Kras(G12D)-induced skin carcinogenesis in vivo. *PLoS One,* 5**,** e13578.

MOORE, M. J., GOLDSTEIN, D., HAMM, J., FIGER, A., HECHT, J. R., GALLINGER, S., AU, H. J., MURAWA, P., WALDE, D., WOLFF, R. A., CAMPOS, D., LIM, R., DING, K., CLARK, G., VOSKOGLOU-NOMIKOS, T., PTASYNSKI, M. & PARULEKAR, W. (2007) Erlotinib plus gemcitabine compared with gemcitabine alone in patients with advanced pancreatic cancer: a phase III trial of the National Cancer Institute of Canada Clinical Trials Group. *J Clin Oncol,* 25**,** 1960-6.

MORTON, J. P., MONGEAU, M. E., KLIMSTRA, D. S., MORRIS, J. P., LEE, Y. C., KAWAGUCHI, Y., WRIGHT, C. V., HEBROK, M. & LEWIS, B. C. (2007) Sonic hedgehog acts at multiple stages during pancreatic tumorigenesis. *Proc Natl Acad Sci U S A,* 104**,** 5103-8.

MUELLER, M. T., HERMANN, P. C., WITTHAUER, J., RUBIO-VIQUEIRA, B., LEICHT, S. F., HUBER, S., ELLWART, J. W., MUSTAFA, M., BARTENSTEIN, P., D'HAESE, J. G., SCHOENBERG, M. H., BERGER, F., HIDALGO, M. & HEESCHEN, C. (2009) Combined Targeted Treatment to Eliminate Tumorigenic Cancer Stem Cells in Human Pancreatic Cancer. *Gastroenterology*.

NEESSE, A., MICHL, P., FRESE, K. K., FEIG, C., COOK, N., JACOBETZ, M. A., LOLKEMA, M. P., BUCHHOLZ, M., OLIVE, K. P., GRESS, T. M. & TUVESON, D. A. (2010) Stromal biology and therapy in pancreatic cancer. *Gut.*

NOWELL, P. C. (1976) The clonal evolution of tumor cell populations. *Science,* 194**,** 23-8.

OGDEN, A. T., WAZIRI, A. E., LOCHHEAD, R. A., FUSCO, D., LOPEZ, K., ELLIS, J. A., KANG, J., ASSANAH, M., MCKHANN, G. M., SISTI, M. B., MCCORMICK, P. C., CANOLL, P. & BRUCE, J. N. (2008) Identification of A2B5+CD133- tumor-initiating cells in adult human gliomas. *Neurosurgery,* 62**,** 505-14; discussion 514-5.

OLIVE, K. P., JACOBETZ, M. A., DAVIDSON, C. J., GOPINATHAN, A., MCINTYRE, D., HONESS, D., MADHU, B., GOLDGRABEN, M. A., CALDWELL, M. E., ALLARD, D., FRESE, K. K., DENICOLA, G., FEIG, C., COMBS, C., WINTER, S. P., IRELAND-ZECCHINI, H., REICHELT, S., HOWAT, W. J., CHANG, A., DHARA, M., WANG, L., RUCKERT, F., GRUTZMANN, R., PILARSKY, C., IZERADJENE, K., HINGORANI, S. R., HUANG, P., DAVIES, S. E., PLUNKETT, W., EGORIN, M., HRUBAN, R. H., WHITEBREAD, N., MCGOVERN, K., ADAMS, J., IACOBUZIO-DONAHUE, C., GRIFFITHS, J. & TUVESON, D. A. (2009) Inhibition of Hedgehog signaling enhances delivery of chemotherapy in a mouse model of pancreatic cancer. *Science,* 324**,** 1457-61.

PARK, C. H., BERGSAGEL, D. E. & MCCULLOCH, E. A. (1971) Mouse myeloma tumor stem cells: a primary cell culture assay. *J Natl Cancer Inst,* 46**,** 411-22.

PECE, S., TOSONI, D., CONFALONIERI, S., MAZZAROL, G., VECCHI, M., RONZONI, S., BERNARD, L., VIALE, G., PELICCI, P. G. & DI FIORE, P. P. (2010) Biological and molecular heterogeneity of breast cancers correlates with their cancer stem cell content. *Cell,* 140**,** 62-73.

PHATAK, P., COOKSON, J. C., DAI, F., SMITH, V., GARTENHAUS, R. B., STEVENS, M. F. & BURGER, A. M. (2007) Telomere uncapping by the G-quadruplex ligand RHPS4 inhibits clonogenic tumour cell growth in vitro and in vivo consistent with a cancer stem cell targeting mechanism. *Br J Cancer,* 96**,** 1223-33.

PHILIP, P. A., MOONEY, M., JAFFE, D., ECKHARDT, G., MOORE, M., MEROPOL, N., EMENS, L., O'REILLY, E., KORC, M., ELLIS, L., BENEDETTI, J., ROTHENBERG, M., WILLETT, C., TEMPERO, M., LOWY, A., ABBRUZZESE, J., SIMEONE, D., HINGORANI, S., BERLIN, J. & TEPPER, J. (2009) Consensus report of the national cancer institute clinical trials planning meeting on pancreas cancer treatment. *J Clin Oncol,* 27**,** 5660-9.

QIN, D., XIA, Y. & WHITESIDES, G. M. (2010) Soft lithography for micro- and nanoscale patterning. *Nat Protoc,* 5**,** 491-502.

RASHEED, Z. A., YANG, J., WANG, Q., KOWALSKI, J., FREED, I., MURTER, C., HONG, S. M., KOORSTRA, J. B., RAJESHKUMAR, N. V., HE, X., GOGGINS, M., IACOBUZIO-DONAHUE, C., BERMAN, D. M., LAHERU, D., JIMENO, A., HIDALGO, M., MAITRA, A. & MATSUI, W. (2010) Prognostic Significance of Tumorigenic Cells With Mesenchymal Features in Pancreatic Adenocarcinoma. *J Natl Cancer Inst*.

REYES, J. M., FERMANIAN, S., YANG, F., ZHOU, S. Y., HERRETES, S., MURPHY, D. B., ELISSEEFF, J. H. & CHUCK, R. S. (2006) Metabolic changes in mesenchymal stem cells in osteogenic medium measured by autofluorescence spectroscopy. *Stem Cells,* 24**,** 1213-7.

RICCI-VITIANI, L., LOMBARDI, D., PILOZZI, E., BIFFONI, M., TODARO, M., PESCHLE, C. & DE MARIA, R. (2007) Identification and expansion of human colon-cancer-initiating cells. *Nature,* 445**,** 111-115.

ROSENBERG, L. (1997) Treatment of pancreatic cancer. Promises and problems of tamoxifen, somatostatin analogs, and gemcitabine. *Int J Pancreatol,* 22**,** 81-93.

ROTHENBERG, M. L., MOORE, M. J., CRIPPS, M. C., ANDERSEN, J. S., PORTENOY, R. K., BURRIS, H. A., 3RD, GREEN, M. R., TARASSOFF, P. G., BROWN, T. D., CASPER, E. S., STORNIOLO, A. M. & VON HOFF, D. D. (1996) A phase II trial of gemcitabine in patients with 5-FU-refractory pancreas cancer. *Ann Oncol,* 7**,** 347-53.

RUBIO-VIQUEIRA, B., JIMENO, A., CUSATIS, G., ZHANG, X., IACOBUZIO-DONAHUE, C., KARIKARI, C., SHI, C., DANENBERG, K., DANENBERG, P. V., KURAMOCHI, H., TANAKA, K., SINGH, S., SALIMI-MOOSAVI, H., BOURAOUD, N., AMADOR, M. L., ALTIOK, S., KULESZA, P., YEO, C., MESSERSMITH, W., ESHLEMAN, J., HRUBAN, R. H., MAITRA, A. & HIDALGO, M. (2006) An in vivo platform for translational drug development in pancreatic cancer. *Clin Cancer Res,* 12**,** 4652-61.

SAINZ, B., JR., BARRETTO, N., MARTIN, D. N., HIRAGA, N., IMAMURA, M., HUSSAIN, S., MARSH, K. A., YU, X., CHAYAMA, K., ALREFAI, W. A. &

UPRICHARD, S. L. (2012) Identification of the Niemann-Pick C1-like 1 cholesterol absorption receptor as a new hepatitis C virus entry factor. *Nat Med,* 18**,** 281-5.

SANTINI, D., VINCENZI, B., FRATTO, M. E., PERRONE, G., LAI, R., CATALANO, V., CASS, C., RUFFINI, P. A., SPOTO, C., MURETTO, P., RIZZO, S., MUDA, A. O., MACKEY, J. R., RUSSO, A., TONINI, G. & GRAZIANO, F. (2010) Prognostic role of human equilibrative transporter 1 (hENT1) in patients with resected gastric cancer. *J Cell Physiol,* 223**,** 384-8.

SCHUCHMANN, S., KOVACS, R., KANN, O., HEINEMANN, U. & BUCHHEIM, K. (2001) Monitoring NAD(P)H autofluorescence to assess mitochondrial metabolic functions in rat hippocampal-entorhinal cortex slices. *Brain Res Brain Res Protoc,* 7**,** 267-76.

SINGH, S. K., HAWKINS, C., CLARKE, I. D., SQUIRE, J. A., BAYANI, J., HIDE, T., HENKELMAN, R. M., CUSIMANO, M. D. & DIRKS, P. B. (2004) Identification of human brain tumour initiating cells. *Nature,* 432**,** 396-401.

VAN DEN BROECK, A., GREMEAUX, L., TOPAL, B. & VANKELECOM, H. (2012) Human pancreatic adenocarcinoma contains a side population resistant to gemcitabine. *BMC Cancer,* 12**,** 354.

VAN HERWAARDEN, A. E., JONKER, J. W., WAGENAAR, E., BRINKHUIS, R. F., SCHELLENS, J. H., BEIJNEN, J. H. & SCHINKEL, A. H. (2003) The breast cancer resistance protein (Bcrp1/Abcg2) restricts exposure to the dietary carcinogen 2-amino-1-methyl-6-phenylimidazo[4,5-b]pyridine. *Cancer Res,* 63**,** 6447-52.

VAN HERWAARDEN, A. E. & SCHINKEL, A. H. (2006) The function of breast cancer resistance protein in epithelial barriers, stem cells and milk secretion of drugs and xenotoxins. *Trends Pharmacol Sci,* 27**,** 10-6.

VAN HERWAARDEN, A. E., WAGENAAR, E., MERINO, G., JONKER, J. W., ROSING, H., BEIJNEN, J. H. & SCHINKEL, A. H. (2007) Multidrug transporter ABCG2/breast cancer resistance protein secretes riboflavin (vitamin B2) into milk. *Mol Cell Biol,* 27**,** 1247-53.

VISVADER, J. E. & LINDEMAN, G. J. (2008) Cancer stem cells in solid tumours: accumulating evidence and unresolved questions. *Nat Rev Cancer,* 8**,** 755-68.

WANG, J., SAKARIASSEN, P. O., TSINKALOVSKY, O., IMMERVOLL, H., BOE, S. O., SVENDSEN, A., PRESTEGARDEN, L., ROSLAND, G., THORSEN, F., STUHR, L., MOLVEN, A., BJERKVIG, R. & ENGER, P. O. (2008) CD133 negative glioma cells form tumors in nude rats and give rise to CD133 positive cells. *Int J Cancer,* 122**,** 761-8.

WARSHAW, A. L. & FERNANDEZ-DEL CASTILLO, C. (1992) Pancreatic carcinoma. *N Engl J Med,* 326**,** 455-65.

WELLNER, U., SCHUBERT, J., BURK, U. C., SCHMALHOFER, O., ZHU, F., SONNTAG, A., WALDVOGEL, B., VANNIER, C., DARLING, D., ZUR HAUSEN, A., BRUNTON, V. G., MORTON, J., SANSOM, O., SCHULER, J., STEMMLER, M. P., HERZBERGER, C., HOPT, U., KECK, T., BRABLETZ, S. & BRABLETZ, T. (2009) The EMT-activator ZEB1 promotes tumorigenicity by repressing stemness-inhibiting microRNAs. *Nat Cell Biol,* 11**,** 1487-95.

WHITE, E. (2012) Deconvoluting the context-dependent role for autophagy in cancer. *Nat Rev Cancer,* 12**,** 401-10.
WICHA, M. S. (2006) Cancer stem cells: an old idea--a paradigm shift. *Cancer Research,* 66**,** 1883-90; discussion 1895-6.
WILSON, A., LAURENTI, E., OSER, G., VAN DER WATH, R. C., BLANCO-BOSE, W., JAWORSKI, M., OFFNER, S., DUNANT, C. F., ESHKIND, L., BOCKAMP, E., LIO, P., MACDONALD, H. R. & TRUMPP, A. (2008) Hematopoietic stem cells reversibly switch from dormancy to self-renewal during homeostasis and repair. *Cell,* 135**,** 1118-29.
ZHANG, S. N., HUANG, F. T., HUANG, Y. J., ZHONG, W. & YU, Z. (2010) Characterization of a cancer stem cell-like side population derived from human pancreatic adenocarcinoma cells. *Tumori,* 96**,** 985-92.
ZHOU, J., WANG, C. Y., LIU, T., WU, B., ZHOU, F., XIONG, J. X., WU, H. S., TAO, J., ZHAO, G., YANG, M. & GOU, S. M. (2008) Persistence of side population cells with high drug efflux capacity in pancreatic cancer. *World J Gastroenterol,* 14**,** 925-30.

APPENDIX